

NIOSH

EPA 600/7-80-183

EPA

United States
Department of Health
and Human Services

Public Health Service
Centers for Disease Control
National Institute for Occupational Safety and Health

499-F-2

United States
Environmental Protection
Agency

Office of Environmental
Engineering and Technology
Washington, DC 20460

EPA-600/7-80-183
December 1980

Research and Development

Ummu
TJ
163.2
.A33
U53
no. 600/7-
80-123

Theoretical Investigation of Inlet Characteristics for Personal Aerosol Samplers

Interagency Energy/Environment R&D Program Report

THE UNIVERSITY
OF MICHIGAN
JUN 16 1981
ENGINEERING
LIBRARY



THE UNIVERSITY OF MICHIGAN
LIBRARIES
JUN 15 1981
DEPOSITED BY THE
UNITED STATES OF AMERICA

THEORETICAL INVESTIGATION OF INLET CHARACTERISTICS
FOR PERSONAL AEROSOL SAMPLERS

Narayanan Rajendran
IIT Research Institute
Chicago, Illinois 60616

Contract No. 210-78-0092

U.S. DEPARTMENT OF HEALTH AND HUMAN SERVICES
Public Health Service
Centers for Disease Control
National Institute for Occupational Safety and Health
Cincinnati, Ohio 45226

May 1981

DISCLAIMER

Mention of company names or products does not constitute endorsement by the National Institute for Occupational Safety and Health.

**NIOSH Project Officer: Jerome Smith
Principal Investigator: Narayanan Rajendran**

ABSTRACT

To keep the working environment as healthful as possible the permissible exposure to dust particles has to be decreased. Lower permissible exposure makes the representativeness of the sample more important and methods to estimate the sampling errors are necessary. A theoretical model and a computer program system has been developed to estimate such errors.

The computer program can handle various inlet geometries such as circular tube and parallel plates. Samplers whose face is not perpendicular to the ambient flow are simulated by a line sink. The model accounts for inertial and sedimentation effects on particle motion.

The results obtained by use of the computer program system agree very well with the experimental data reported in the literature.

CONTENTS

Abstract.	iii
List of Figures	v
List of Tables.	vii
Introduction.	1
Literature Survey	3
Theoretical Model	12
Method of Solution.	33
Results and Discussion.	50
References.	75
Appendixes	
A. Derivation of Boundary Condition at Section II.	78
B. Stream Function for Uniform Sink Strength Distribution.	80
C. Stream Function for Triangular Sink Strength Distribution.	82
D. Computer Program Listing.	84
E. Computer Program System User Manual	110
Glossary.	125

FIGURES

1. Comparison of theoretical and experimental effects of anisokinetic sampling.	6
2. Comparison of experimental and theoretical data taken from various authors.	8
3. Flowfield in the case of sampling a stationary fluid into a tube	9
4. Particle trajectories at $U/U_0 = 25$, $K = 0.3$	10
5. Modeling strategy	13
6. Coordinate system for solving Equation (14)	15
7. Nomenclature of flow region for two parallel plates	17
8. Nomenclature of flow boundary for circular tube	20
9. Line sink distribution along face plane of the sampler.	22
10. Triangular source/sink strength distribution.	24
11. Coordinate system for electrostatic force calculation	30
12. Rectangular mesh geometry	34
13. Unequal grid size	36
14. Various inlet geometries.	37
15. Flow field boundary and grid point layout	45
16. Boundary conditions for circular inlet.	46
17. C/C_0 vs. Stokes's number $U/U_0 = 1.2$ thin-walled circular tube	51
18. C/C_0 vs. Stokes's number $U/U_0 = 2.0$ thin-walled circular tube, $\alpha = 90^\circ$	52
19. Sampling bias for thin-walled circular tube facing the stream, velocity ratio = 0.75	53
20. Sampling bias for thin-walled circular tube facing the stream, velocity ratio = 0.375.	54
21. Sampling bias for thin-walled circular tube facing the stream, velocity ratio = 0.1875	55
22. Sampling bias for thin-walled circular tube facing the stream, velocity ratio = 0.0938	56
23. Trajectory of particles, $U = 0.375$, $\alpha = 90^\circ$, $K = 0.01$	57
24. Trajectory of particles, $U = 0.375$, $\alpha = 90^\circ$, $K = 0.3$	58
25. Trajectory of particles, $U = 0.375$, $\alpha = 90^\circ$, $K = 3.0$	59
26. Trajectory of particles, $U = 0.375$, $\alpha = 60^\circ$, $K = 0.01$	60
27. Trajectory of particles, $U = 0.375$, $\alpha = 0^\circ$, $K = 0.01$	61
28. C/C_0 vs. orientation angle for $U = 0.375$ and lip depth of 0.2.	63
29. C/C_0 vs. Stoke's number for $\alpha = 90^\circ$, square inlet, ZLIP = 0.	64
30. C/C_0 vs. Stoke's number for $\alpha = 90^\circ$, square inlet, ZLIP = 0.	65

31.	Stokes number vs. C/C_0 for $U = 0.375$, square inlet, ZLIP = 0.	66
32.	C/C_0 vs. α for $U = 0.375$, square inlet, ZLIP = 0.	67
33.	Effect of bias on the distribution, $\alpha = 90^\circ$, square inlet, ZLIP = 0	68
34.	C/C_0 vs. U/U_0 for square inlet facing the stream.	70
35.	C/C_0 vs. K for various thicknesses of wall with circular inlet facing the stream, $U/U_0 = 0.375$	71
36.	Comparison of theoretical results with experimental data of S. Badzioch (1959), circular tube facing the stream.	72
37.	Parameter description for inlet geometry and orientation	110

TABLES

1. Permissible radii of tubes (cm) for sampling aerosols in calm conditions	11
2. Typical values of Stokes number K , Peclet number Pe , Froude number Fr for unit density spheres	31
3. Parameter description and physical significance	47

INTRODUCTION

Almost all methods of aerosol characterization begin with aerosol sampling-- the capture and transport of aerosols to a characterizing instrument of some kind. The most important aspect of sampling is the representativeness of the sample. Representativeness exists when both the sample and the aerosol from which it was drawn are identical with respect to concentration, particle size distribution, and chemical composition.

As early as 1911, Brady and Touzalin¹ predicted and experimentally verified the possibility of obtaining nonrepresentative samples of particulate matter by a sampler. Since then, the experimental data of numerous investigators have confirmed the importance of sampling procedures. Few, however, have made attempts to establish a theoretical basis for estimating sampling error.

To keep the working environment as safe as possible the permissible exposure to particles is made less and less. Lower permissible exposure makes the representativeness of the sample more important, and methods to estimate the sampling errors are necessary.

The quality of air in an industrial environment is evaluated by use of sampling methods. The recent emphasis on personal sampling has produced a trend to wear small battery operated samplers. The usual approach is to attach a filter in a two or three piece cassette to the workers breathing zone and connecting the cassette to a belt mounted, battery operated pump with an appropriate length of tubing. Personal respirable dust samplers consist of a cyclone fitted to the sampling head that may be attached to the worker's clothing near his breathing zone. The cyclone is designed to closely approximate the AEC-ACGIH respirable dust curves. Some of the other commonly used samplers are horizontal elutriator, open faced filter, closed face filter, etc. The inlet geometries of the above mentioned samplers vary widely, from a square inlet in a cyclone to a circular inlet in a closed face filter.

The goal of this research program is to develop a computer program system for predicting the sampling errors for various inlet geometries encountered in personal sampling.

The program involves the following tasks:

- Task 1: Literature Survey
- Task 2: Theoretical Simulation of Fluid Flow
- Task 3: Theoretical Simulation of Particle Motion

Fluid flow simulation required the modelling of the following:

- (a) Sampling procedures and conditions for obtaining the best results differ markedly for sampling from flowing and stationary environments. Hence, a model for the environment from which the sample is drawn is very important for meaningful results.
- (b) The disturbance created by introducing a sampling inlet into the above known environment establishes a new pattern of fluid flow in the vicinity of the sampler inlet. The velocity of suction of the sample further changes the fluid dynamics of the sampling. Hence, a model for the fluid flow in and around the sampling inlet has to be developed.

To estimate the performance of the sampler inlet, the effect of flow field on particle transport has to be studied. Transport of particles depends on the fluid flow, as well as such factors as particle size, density, and shape. So a model that would enable us to calculate the transport of aerosols into the probe has to be developed. This would complete the model for effectively predicting the errors that occur during the sampling.

LITERATURE SURVEY

"Literature Search" was initiated upon commencement of this project with the help of IITRI's Computer Search Center. The following data bases were searched for pertinent works in "Inlet Characteristics of Aerosol Samplers."

- (1) NTIS 1964-1978
- (2) APTIC (Air Pollution Abstracts) 1966-1978
- (3) Compendex (Engineering Index) 1970-1978
- (4) CAC (Chemical Abstracts) 1969-1978

A total of 354 citations were obtained from the computer search. Both theoretical and experimental works that are directly connected to the program were reviewed. Two substantially different types of aerosols are sampled in practice--flowing and stationary aerosols.

(a) Sampling from flowing aerosols is encountered in the study of ducted aerosols and atmospheric aerosols in the presence of wind. Lappel and Shepperd² were the first to present a theoretical approach and proposed an equation for assessing the order of magnitude of anisokinetic errors. DallaValle³ suggested the use of experimentally determined velocity contours as a possible means for determining the errors.

There was a growing interest in this problem in the fifties and only the two methods proposed by Watson⁴ and Badzioch^{5,6} appear to be practical. The above methods allow the determination of deviations in measured concentration of particulates. Watson⁴ gave the following equation for estimating the deviation.

$$\frac{C}{C_0} = \frac{U_0}{\bar{U}} \left[1 + f(K) \left(\frac{\bar{U}}{U_0}^{\frac{1}{2}} - 1 \right) \right] \quad (1)$$

where

$f(K)$ = unknown function of K and is evaluated by experimental data

C = measured concentration of particles (#/cc)

C_0 = actual concentration of particles (#/cc)

U_0 = stream velocity (cm/sec)

\bar{U} = the mean air velocity at the sampling orifice

K = dimensionless inertial parameter called Stokes number

Badzioch investigated the efficiency of collection of gas-borne particles by an aspirated sampling nozzle. The efficiency was shown theoretically to depend on (a) the ratio of the velocity of aspiration into the sampling nozzle to the velocity of the undisturbed gas stream, and (b) the ratio of a length representing the distance of disturbance upstream of the nozzle to the "range" of a particle. The "range" is defined as the distance a particle would travel, before coming to rest, if projected into still gas with a velocity equal to that of the gas stream. In the range of conditions investigated experimentally, which included nozzles of 0.65 to 1.90 cm diameter aspirating from turbulent gas streams, it is found that the length representing the upstream disturbance is a function of the diameter of the nozzle.

He gave the following expression for estimation of sampling error:

$$\frac{C}{C_0} = \alpha \frac{U_0}{\bar{U}} + (1-\alpha) \quad (2)$$

where

$$\alpha = [1 - \exp(-D/\lambda)] / (D/\lambda)$$

$$\lambda = KL = \text{range of a particle}$$

D = assumed distance from the plane of nozzle exit at which the streamlines start either diverging or converging and is a function of L. The value of D was deduced from experiments.

Both of the above models are semi-empirical, using experimentally derived parameters to bridge gaps in theoretical deductions.

Levin was the first to consider the inertial lag of particles with the particles flowing into a point sink in the field of uniform wind. His theoretical results are valid if

$$\frac{\bar{U}}{U_0} < 64K \quad (3)$$

is fulfilled, where \bar{U} is the suction velocity of the sample (cm/sec), U_0 is free stream velocity, and K is the Stokes number ($U_0 \tau / L$). According to Levin, if particle sedimentation is ignored, the aspiration coefficient due to inertia $A_i = C/C_0$, where C is the measured concentration ($\#/cm^3$) and C_0 is the actual concentration ($\#/cm^3$), is determined as follows:

$$A_i = 1 - 3.2 \frac{U_0}{\bar{U}} K + 0.44 \frac{U_0}{\bar{U}} K^2 \quad (4)$$

Where \bar{U}/U_0 values from 4.0 to 8.0 the experimental results were in good agreement with Equation 4.

In the late fifties and early sixties there were a number of experimental studies on the effect of probe shape on the sampling accuracy and directional dependence of samplers^{8,9}.

Vitols^{10,11} calculated, by means of a computer, the flow field for an aspirated nozzle for various values of \bar{U}/U_0 ignoring the turbulence and viscosity of the fluid. Particle trajectories were computed for different values of the Stokes number, K. Gravitational force on the particles was not considered. The graphs A_i vs. \bar{U}/U_0 were obtained using the Stokes number as the parameter. A typical curve is shown in Figure 1. The lowest value of K used was large. For large values of K, the particle trajectories are nearly straight. Their motion is nearly independent of the flow lines and $A_i = U_0/\bar{U}$ because the efficiency of capture of the particles is 100% for large K values. These theoretical error estimates compared well with the experimental data of Badzioch which have a very large scatter in values of A_i . According to Davies,^{12,13} when the wind velocity $U_0 < \bar{U}/5$, the aspiration coefficient can be estimated from the sampling criteria for stationary systems. Whenever this condition is not met, the aspiration coefficient can be calculated by using Levin's⁷ solution for A_i . Because Levin's solution is based on a point sink that draws particles from a uniform stream, it is applicable only to sampling tubes of small radii. According to Davies, the maximum diameter, D, of the tube is:

$$\frac{D}{2} = \frac{\left(\frac{F}{4\pi U_0} \right)^{1/2}}{5} \quad (5)$$

where F is the rate of suction of the sampler.

For larger sampling tubes Davies gave an empirical relation based on the experimental data and A_i is determined as follows:

$$A_i = \frac{C}{C_0} = 1 + \left(\frac{U_0}{U - 1} \right) f(K) \quad (6)$$

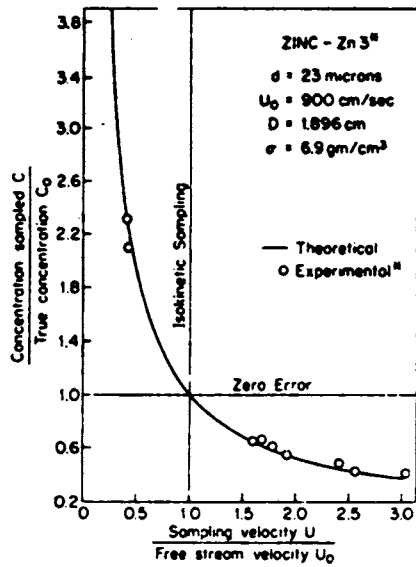
where K is the particle Stokes number and

$$f(K) = 1 - \frac{1}{1 + 2K} \quad (7)$$

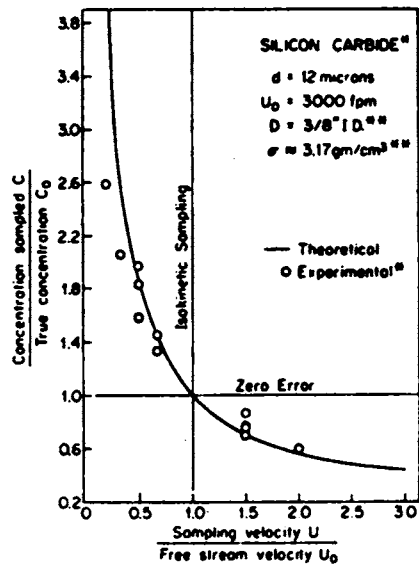
Belyave and Levin¹⁴ showed that the observed aspiration coefficient A_e could not be identified with purely inertial aspiration A_i that had been the main subject of the earlier studies (1-13). Taking into account the rebound of the particle and its deposition in the sampling tube, A_e will be a function of A_i , A_d (the coefficient characterizing the particle concentration decrease in a sample caused by deposition in the inlet channel) and A_r (the coefficient which depends on the particle rebound from the front edge of the sampling nozzle and their subsequent aspiration into it).

All three coefficients, A_i , A_d , and A_r , strongly depend on nozzle shape. Since the character of this dependence for A_r and A_d has yet to be established, A_r and A_d were assumed to be united and gave an empirical relation for A_i as follows:

$$A_i = 1 + \left(\frac{U_0}{U} - 1 \right) \beta \quad (8)$$



Zinc Sphere, $K = 10.5$



Silicon Carbide, $K = 4.5$

Figure 1. Comparison of theoretical and experimental effects of anisokinetic sampling (from reference [10]).

where β is a non-dimensional function, $\beta \rightarrow 0$ as $K \rightarrow 0$, and $\beta \rightarrow 1$ as $K \rightarrow \infty$. All the previous works concluded that β is a function of K only. But in Figure 2, which gives theoretical curves as well as experimental points, β shows a dependence on \bar{U}/U_0 and is given as follows:

$$\beta = 1 - \frac{1}{1 + BK} \quad (9)$$

and B , a non-dimensional function, is given by:

$$B = 2 + 0.617 \frac{\bar{U}}{U_0} \quad (10)$$

(b) Sampling from calm air or stationary aerosols has been investigated much less than sampling from flowing aerosols. Figures 3 and 4 demonstrate that the character of the flow fields at the entrance to a tube from a stationary medium and from a stream $0 < U_0/\bar{U} < 1$ is quite different¹⁵.

Levin¹⁶ considered the sampling from stationary aerosols as a flow into a point sink. He developed a relation for A_i , the inertial aspiration coefficient, which is:

$$A_i = 1 - 0.8K + 0.08K^2 + \dots \quad (11)$$

where $K = \tau(4 V_s^3/F)^{1/2}$ is a parameter acting as a Stokes number, F is the flow rate into the sink, and V_s is the sedimentation velocity of the particle.

In his well known theory of sampling, Davies^{12,13,15,23,33} used the stopping distance of a particle to characterize inertial effects and terminal settling velocity to characterize sedimentation of particles. For inertia to be negligible, the stop distance should be small compared to the radius of the tube $D/2$. For sedimentation to be negligible, the flow velocity in the probe should be much larger than the terminal settling velocity. Then the complete condition to obtain a true sample is:

$$\left(\frac{F\tau}{4\pi}\right)^{1/3} \ll \frac{D}{2} \ll \left(\frac{F}{\pi g\tau}\right)^{1/2} \quad (12)$$

where F is the rate of suction of the sample (cm^3/sec), τ is the relaxation time of particles (sec), and g is acceleration due to gravity (cm/sec^2). Using an arbitrary criteria of $1/5$ he arrives at the following condition:

$$5 \left(\frac{F\tau}{4\pi}\right)^{1/3} \leq \frac{D}{2} \leq \frac{\left(\frac{F}{\pi g\tau}\right)^{1/2}}{5} \quad (13)$$

Table 1 shows the permissible tube sizes for sampling aerosols as a function of suction rate and particle size. When the tube radius is greater than the lower figure, sampling errors due to inertia are not significant. When the radius is less than the upper limit, sedimentation is not significant. The two criteria can be satisfied simultaneously for the unbracketed entries in the table but not for bracketed entries. Satisfactory samples can be obtained by using the tube size satisfying the lower limit condition and orienting the sampler vertically to eliminate sedimentation.

Agarwal³⁶ studied the problem of aerosol sampling under calm air conditions by solving the Navier-Stokes equations and equation of variable motion. The study was continued to circular inlets. The sampling efficiency of an inlet was found to depend upon two dimensional parameters, the Stokes Number, K , and the relative velocity, Vs^1 . Using an arbitrary criteria of 90% efficiency, he arrives at the following condition:

$$2.K.Vs^1 \leq 0.1$$

This criterion is less restrictive than the condition given by equation (13) and provides adequate accuracy.

Ter Kuile³⁷ made the distinction between "representative sampling" and "comparable sampling". This results in two criteria.

1. The criterion for representative sampling which combines a modification of DAVIES' theory for representative sampling and LEVIN's sampling theory into one criterion which is limited by three physical effects:

- impaction on the wall of the inlet;
- sedimentation on the wall of the inlet;
- dynamic escape from the sampling region.

2. The criterion for comparable sampling requires that the inlet is to point vertically downwards with a filter near the inlet, resulting in a higher efficiency, sharper cut-off limits, better reproducibility and better comparability.

Both these criteria were given in graphs in which the sampling efficiency is a function of a dimensionless particle size number (k_{dQ}), and a tube size number (m_{DQ}). Theoretical limits of the region where the efficiency is more than 90% for representative sampling and more than 94% for comparable sampling are plotted in these graphs. The tube size number only depends on parameters of the sampling device, so that the design of this device determines the nature of the physical limitation. As a result of this, sampling devices can be divided into three classes for which different physical mechanisms limit the aspiration efficiency of large particles.

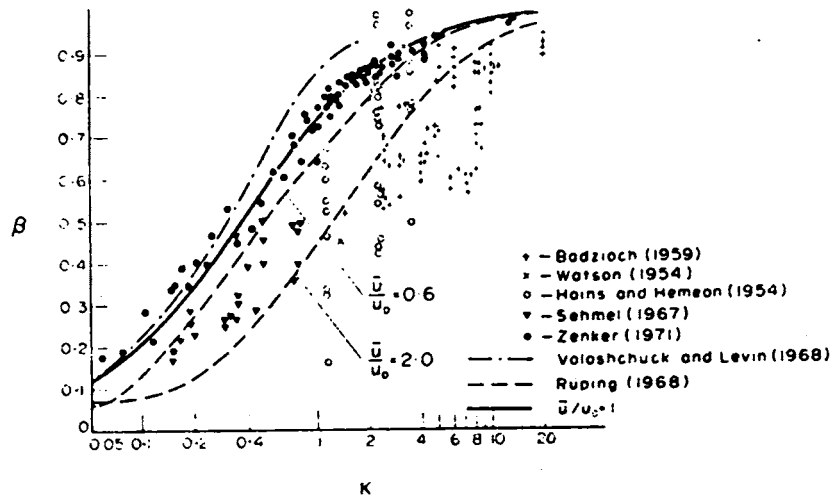


Figure 2. Comparison of experimental and theoretical data taken from papers of various authors (from reference [14]).

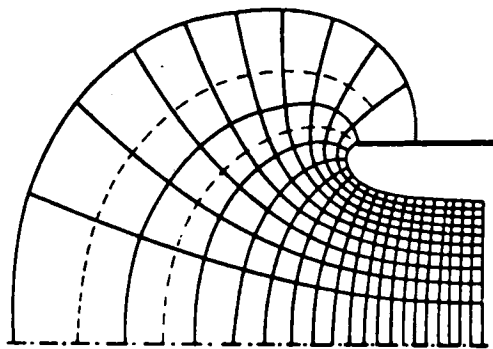


Figure 3. Flow field in the case of sampling a stationary fluid into a tube (from reference [17]).

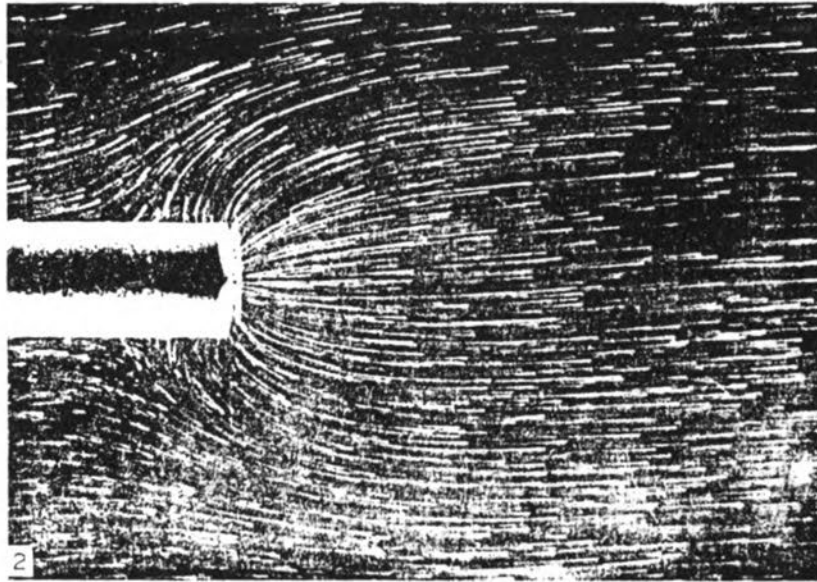


Figure 4. Particle trajectories at $U/U_0 = 25$, $K = 0.3$ (from reference [17]).

Fuchs presented a review of methods of sampling and methods to estimate the bias. During this literature search the author came across a number of experimental studies on the effect of probe shape, orientation and velocity of sampling on entry efficiencies.

Glauber⁹ studied the directional dependence of air samplers using uranium oxide dusts. Two filtration type air samplers were tested. In turbulent air no bias was found due to orientation. In a directional air stream, a sampler head facing into the air stream collected more dust by a factor of two compared to a sampler facing up or down. Schmel¹⁹ investigated particle sampling errors from several sources. The sampling errors were significant for particles as small as 1 micron in some cases. Pickett and Sansone²² studied the effect of varying inlet geometry on collection characteristics of a 10-millimeter Nylon Cyclone. Samples of coal dust aerosol were collected simultaneously with two filter holders: one designed to conform to Davies' criteria, and one with smaller inlet dimensions corresponding to those of the 10 mm Nylon Cyclone. No differences in mass concentration or size distribution were obtained.

Breslin and Stein²⁶ considered sampling inlets in calm air. Their results showed that Davies' criteria for inlet conditions for correct sampling are overly restrictive.

Raynor³⁰ studied the effect on the entrance efficiency of a filter holder caused by variations in the following parameters--air speed, flow rate, angle between the air flow and the filter holder, and particle size. Efficiencies for various particles were determined over a range of angles from 60-120 degrees from horizontal for wind speeds of 100, 200, 400 and 700 cm/sec and filter flow rates of 6.4, 12.7 and 25.4 liters/min. The entrance efficiency varied with all parameters from less than 1% at highest wind speed and lowest flow rate to over 100% at forward angles. Efficiency was lowest with filter holder entrance at right angles to the air stream.

Table 1. Permissible radii of tubes (cm) for sampling aerosols in calm conditions*

Particle diameter, μ	Rate of suction, F (cm ³ /sec)					
	1	10	100	1,000	10,000	100,000
1	0.033 - 1.9	0.071 - 6.0	0.15 - 10	0.33 - 60	0.71 - 190	1.5 - 600
2	0.051 - 1.0	0.11 - 3.2	0.23 - 10	0.51 - 32	1.1 - 100	2.3 - 320
5	0.093 - 0.41	0.20 - 1.3	0.43 - 4.1	0.93 - 13	2.0 - 41	4.3 - 130
10	0.15 - 0.21	0.31 - 0.65	0.68 - 2.1	1.5 - 6.5	3.1 - 21	6.8 - 65
20	(0.23 ~ 0.10)	(0.50 ~ 0.33)	(1.1 ~ 1.0)	2.3 - 3.1	5.0 - 10.3	11.0 - 31
50	(0.42 ~ 0.042)	(0.90 ~ 0.13)	(1.9 ~ 0.42)	(4.2 ~ 1.33)	(9.0 ~ 4.2)	(19 ~ 13.3)
100	(0.63 ~ 0.023)	(1.4 ~ 0.071)	(2.9 ~ 0.23)	(6.3 ~ 0.71)	(14.0 ~ 2.3)	(29 ~ 7.1)
200	(0.89 ~ 0.014)	(1.9 ~ 0.037)	(4.1 ~ 0.14)	(8.9 ~ 0.37)	(19 ~ 1.4)	(41 ~ 3.7)
500	(1.26 ~ 0.008)	(2.7 ~ 0.025)	(5.8 ~ 0.08)	(12.6 ~ 0.25)	(27 ~ 0.80)	(58 ~ 2.5)

* From Reference [12]

THEORETICAL MODEL

An overall theoretical model to simulate a personal sampler requires modeling of the following:

- Model for environmental flow patterns
- Model for flow pattern in and around the sampler
- Model for motion of particles

The strategy used to obtain the overall model for personal sampling is given in the form of a block diagram in Figure 5.

ENVIRONMENTAL FLOW PATTERNS: MODEL FOR INDUSTRIAL ENVIRONMENT

Industrial environmental flow patterns are so complex and individual that any one particular model cannot describe the actual field for all types of working environments. Hence, it is necessary to make some simplifying assumptions so that a model can be developed. Different types of flow patterns exist in a variety of working environments.

- (1) An environment essentially calm except for microscopic fluctuations. This type of pattern can be found in research laboratories, nuclear reactor plants, etc.
- (2) A steady flow exists in a particular direction even though the direction cannot be fixed. The effect of varying directions can be studied by using it as a parameter. This kind of flow pattern will exist in industries which need high ventilation.
- (3) In some working environments, the flow volume is so large that the medium is essentially turbulent in nature. In this type of environment the flow does not realize the existence of an object (sampling head, for instance) and barges into it. This kind of flow would be predominant in environments which need very high ventilation, such as mines.

Hence, the model uses the calm air type of sampling for environments of type 1 and a steady flow type for industrial environments of type 2. Type 3 environments could be realized by increasing the flow velocity of the uniform flow of type 2 environments.

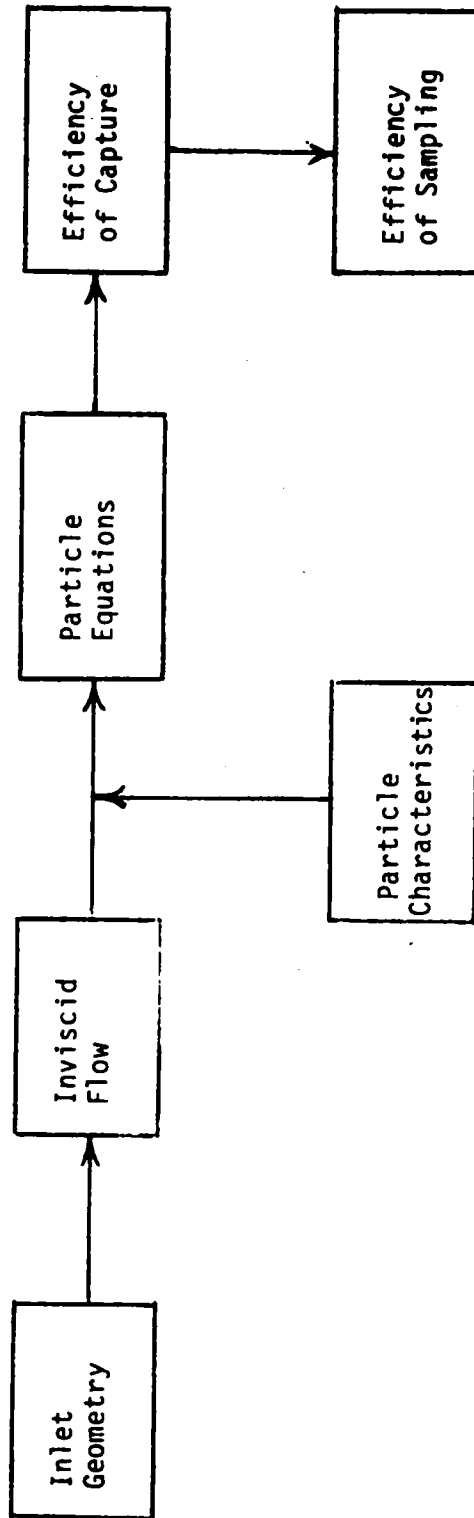


Figure 5. Modeling Strategy

FLOW RATE AND INLET GEOMETRY: MODEL FOR FLOW PATTERN IN AND AROUND THE PROBE

The model for flow pattern in and around the probe is assumed to be given by the inviscid flow pattern. In solving the inviscid problem above, it was assumed the fluid was ideal, without any viscosity as it glides over the walls of the boundary. In reality all fluids have viscosity, hence friction. So the fluid in contact with the wall will be subjected to a no slip condition, that is, the velocity at the wall is zero. This viscous effect extends only to a very small distance from the wall and was not taken into account in this study.

Sampler Facing the Stream

Equations in this section are formulated in the general form so that they can be applied to any given geometry. Ideal fluid flow patterns and velocity distributions can be determined by solving the Laplace equation for the stream function, ψ .¹⁶

$$\nabla^2 \psi = 0 \quad (14)$$

where ∇^2 is the Laplace operator.

$$\nabla^2 = \frac{\partial^2}{\partial x^2} + \frac{\partial^2}{\partial y^2} \text{ for two dimensions}$$

where ∇^2 is the second order central difference operator. The shape of the body determines the boundary conditions on the stream function. General conditions will be:

- (1) $\psi = \text{constant}$ at the body surface
 - (2) $\psi = 0$ at the axis of symmetry
 - (3) $\psi = \psi$ of the environmental flow pattern upstream and downstream from the body
- (15)

The velocity of flow can be calculated from ψ as:

- (i) for Cartesian coordinates (x,y,z) (see Figure 6)

$$U_x = \frac{\partial \psi}{\partial y}$$
$$U_y = \frac{\partial \psi}{\partial x}$$
(16)

- (ii) for cylindrical coordinates (r,z) (see Figure 6)

$$U_r = -\frac{1}{r} \frac{\partial \psi}{\partial y}$$
$$U_z = \frac{1}{r} \frac{\partial \psi}{\partial r}$$
(17)

Hence, once ψ is calculated from equation (14) with the use of conditions (15) then the velocity distribution can be found from either (16) or (17).

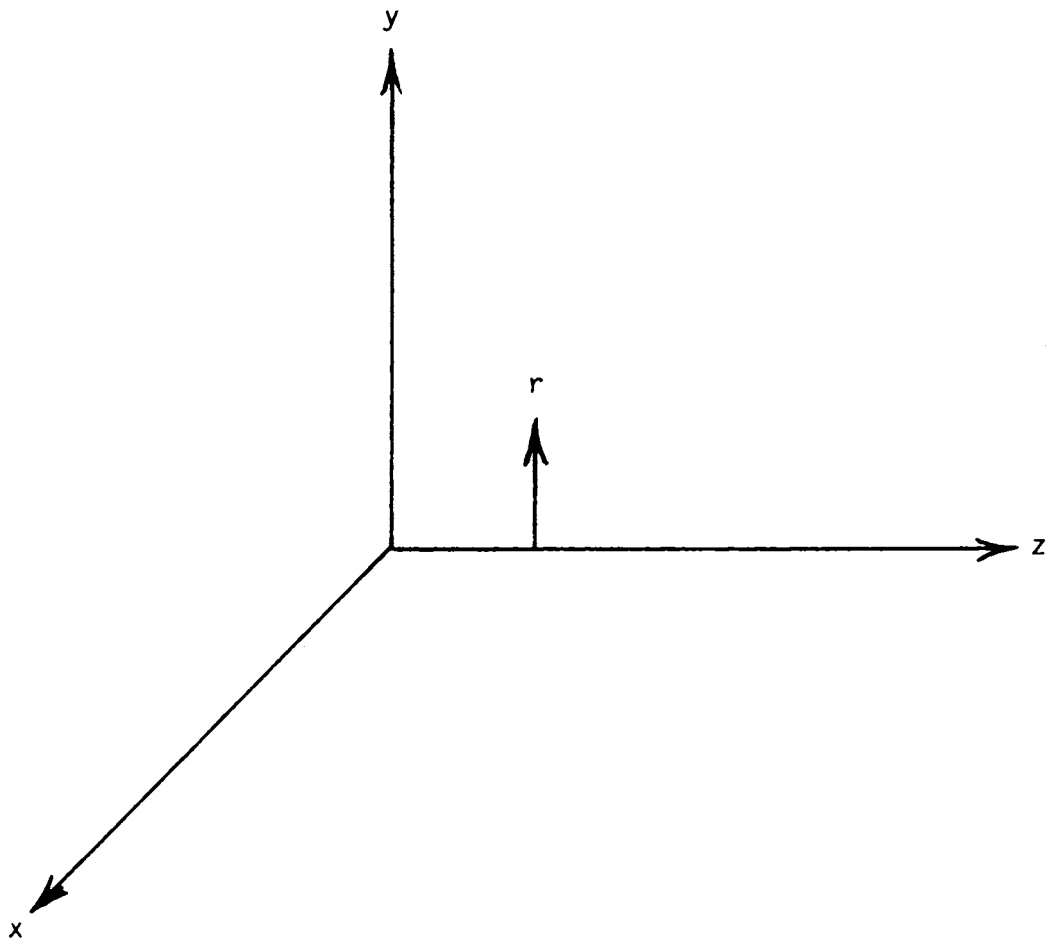


Figure 6. Coordinate system for solving Equation (14).

The stream function ψ does not exist for three dimensional flows. That is, there is no function ψ such that a isoline is a stream line. But for a solenoidal vector field (where \bar{U} satisfies the 3-D continuity equation, $\nabla \cdot \bar{U} = 0$), a so-called vector potential $\bar{\psi} = \psi_x \bar{i} + \psi_y \bar{j} + \psi_z \bar{k}$ does exist, such that the velocity components are given by:

$$\begin{aligned} U_x &= \frac{\partial \psi_z}{\partial y} - \frac{\partial \psi_y}{\partial z} \\ U_y &= \frac{\partial \psi_z}{\partial x} - \frac{\partial \psi_x}{\partial z} \\ U_z &= \frac{\partial \psi_y}{\partial x} - \frac{\partial \psi_x}{\partial y} \end{aligned} \quad (18)$$

and $\bar{\psi}$ satisfies

$$\nabla^2 \bar{\psi} = 0 \quad (19)$$

Equation (18), when written in terms of the vector components, constitutes a set of three equations to be solved for ψ_x , ψ_y , and ψ_z . They are:

$$\begin{aligned} \nabla^2 \psi_x &= 0 \\ \nabla^2 \psi_y &= 0 \\ \nabla^2 \psi_z &= 0 \end{aligned} \quad (20)$$

Equations (20) are similar to equation (14). But the boundary conditions are not as simple as (15) and body shape needs to be specified to formulate them. Due to the complexity involved in the boundary conditions and solution procedures the flow model covers only the two dimensional and axisymmetrical cases.

The two-dimensional equation (14) for ψ is useful where the sampling inlet is either axisymmetrical or when the ratio of height to width of the inlet is large enough to discard one dimension. Even if these conditions are not satisfied for a particular inlet, equation (14) will still approximate the flow in the core region of the sampler inlet.

Formulation of the Problem for Specific Inlet Geometries

Parallel Plate Inlet--

This type of inlet is often encountered in the horizontal elutriator. Figure 7 shows the nomenclature for the fluid flow region. As can be seen from the figure, some transverse distance Y_0 from the centerline of the probe defined where the fluid stream line maintains a flow unperturbed by the sampler. This assumption is necessary because a numerical solution for the problem can be obtained only for a finite number of mesh points.

The required boundary conditions now have to be specified at the centerline, the probe surface, the constant ordinate Y_0 and section I and II as shown in Figure 7.

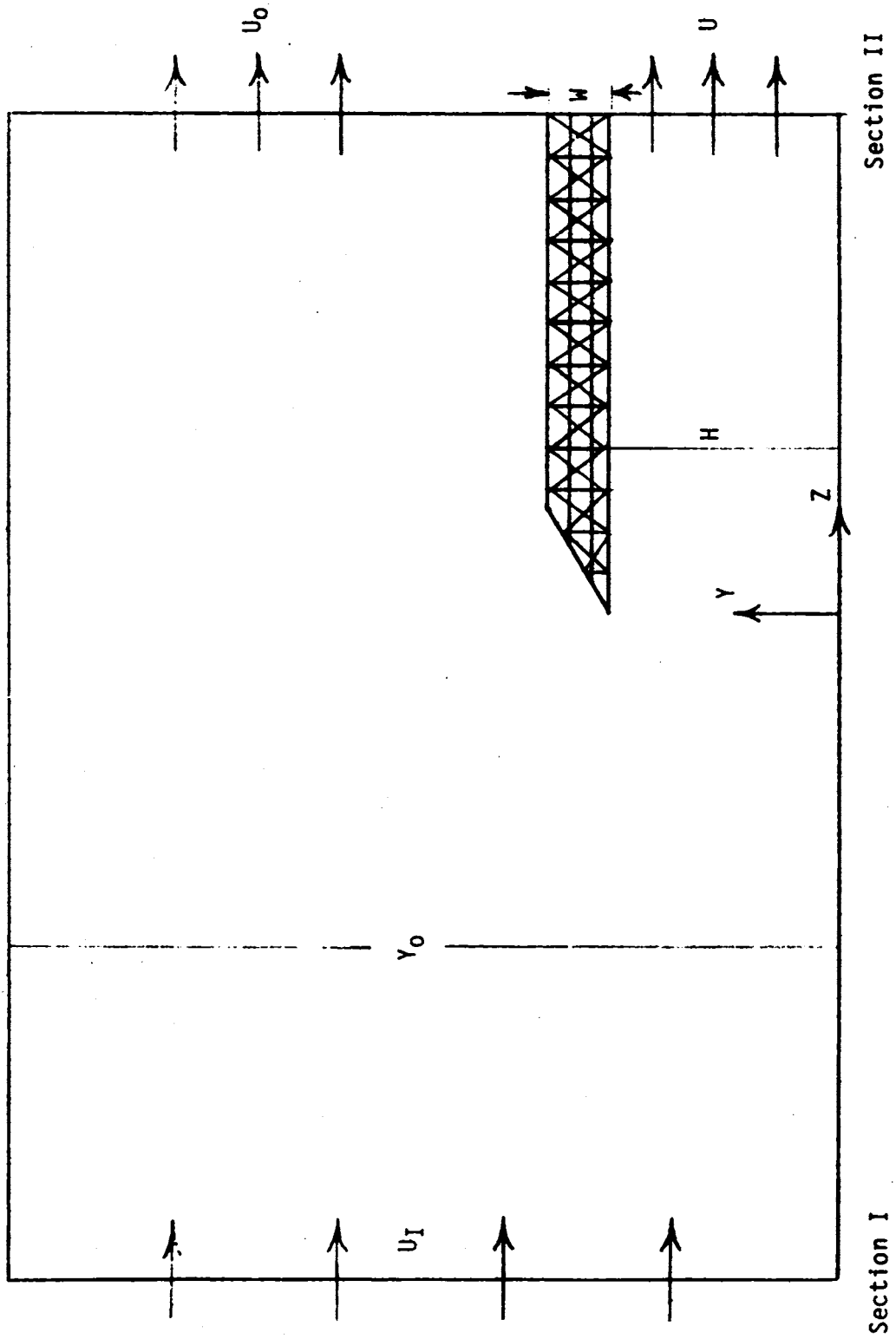


Figure 7. Nomenclature for flow region-- two dimensional case.

When Section I and II are sufficiently far up and downstream from the inlet and the disturbed flow region, the velocities at these stations can be considered uniform and axial only. The axial component of velocity U_z and transverse component U_y are related to the stream as follows:

$$U_z = \frac{\partial \psi}{\partial y} \quad (21)$$

$$U_y = -\frac{\partial \psi}{\partial z} \quad (22)$$

The expression for ψ at sections I and II can be obtained by integrating equation (21):

$$\psi = U_y y + C_1 \quad (23)$$

Where U is the appropriate velocity of the fluid and C_1 is an arbitrary constant of integration for which a value of zero can be assigned.

Then on the centerline of the probe (upstream and inside the probe) the value of the stream function becomes:

$$\psi_{\text{cl}} = \psi \text{ at centerline} = 0 \quad (24)$$

By virtue of equation (23), the values for ψ at other boundaries follow:

$$\psi \text{ at Section I} = \psi_I = U_I y \quad (25)$$

$$\psi \text{ at } y_0 = \psi_{y_0} = U_I y_0$$

y at Section II is given in by three equation valid over various regions.

$$\begin{aligned} \psi_{IP} &= \psi \text{ at Section II inside the probe} \\ &= U_y y \quad 0 \leq y \leq H \end{aligned} \quad (26)$$

$$\begin{aligned} \psi_{OP} &= \psi \text{ at Section II outside the probe} \\ &= U_o y \quad (H+W) \leq y \leq y_0 \end{aligned}$$

By use of mass balance at Sections I and II, expression for ψ_{OP} becomes (Appendix A)

$$\psi_{OP} = \frac{(U_I y_0 - UH)}{(y_0 - (H+W))} * (y - (H+W)) + UH \quad (27)$$

for $(H+W) \leq y \leq y_0$

$$\psi_{PS} = \psi \text{ on the probe surface} = UH \text{ for } H \leq y \leq (H+W) \quad (28)$$

Divide the velocities by U_I and the distances by H to make them nondimensional. Denoting the nondimensional quantities by stars, the boundary conditions become:

$$\begin{aligned}
\psi_I^* &= y^* \\
\psi_{IP}^* &= U^* y^* \\
\psi_{OP}^* &= \frac{(\psi_0^* - U^*)}{(\psi_0^* - (H+W^*))} * (y^* - (1+W^*)) + U^* \\
\psi_{CL}^* &= 0 \\
\psi_{PS}^* &= U^*
\end{aligned} \tag{29}$$

Equation (14) together with the boundary conditions (29) pose a well defined problem.

Circular Tube--

Circular inlets are the most commonly used geometry in aerosol sampling. Although circular tubes are very rarely found in the personal samplers for aerosols, the inlets to the closed face filters can be approximated by the circular tube geometry. Open faced filters can be regarded as a wide and very short circular tubes terminating in a filter.

Figure 8 gives the flow field boundary description and nomenclature. A circular tube of radius R, and wall thickness W, is considered to be located at Z = 0. The axial and radial velocity components, U_z and U_r are given as follows:

$$\begin{aligned}
U_z &= \frac{1}{\gamma} \frac{\partial \psi}{\partial r} \\
U_r &= -\frac{1}{\gamma} \frac{\partial \psi}{\partial z}
\end{aligned} \tag{30}$$

Following similar procedure used for parallel plates,

$$\begin{aligned}
\psi_I &= \frac{1}{2} U_I r^2 \\
\psi_{IP} &= \frac{1}{2} U r^2 \\
\psi_{OP} &= \frac{1}{2} \frac{(U_I R_0^2 - UR^2)}{(R_0^2 - (R+W)^2)} * (r^2 - (R+W)^2) + \frac{1}{2} UR^2 \\
\psi_{CL} &= \psi \text{ at centerline} = 0
\end{aligned} \tag{31}$$

Nondimensionalizing velocities by $\frac{1}{2} U_I$ and distances by R boundary conditions become:

$$\begin{aligned}
\psi_I^* &= r^{*2} & 0 \leq r^* \leq R_0^* \\
\psi_{IP}^* &= U^* r^{*2} & 0 \leq r^* \leq 1 \\
\psi_{OP}^* &= \frac{(R_0^{*2} - U^*)}{(R_0^{*2} - (1+W^*)^2)} (r^{*2} - (1+W^*)^2) + U^* & (1+W^*) \leq r \leq R_0^* \\
\psi_{CL}^* &= 0
\end{aligned} \tag{32}$$

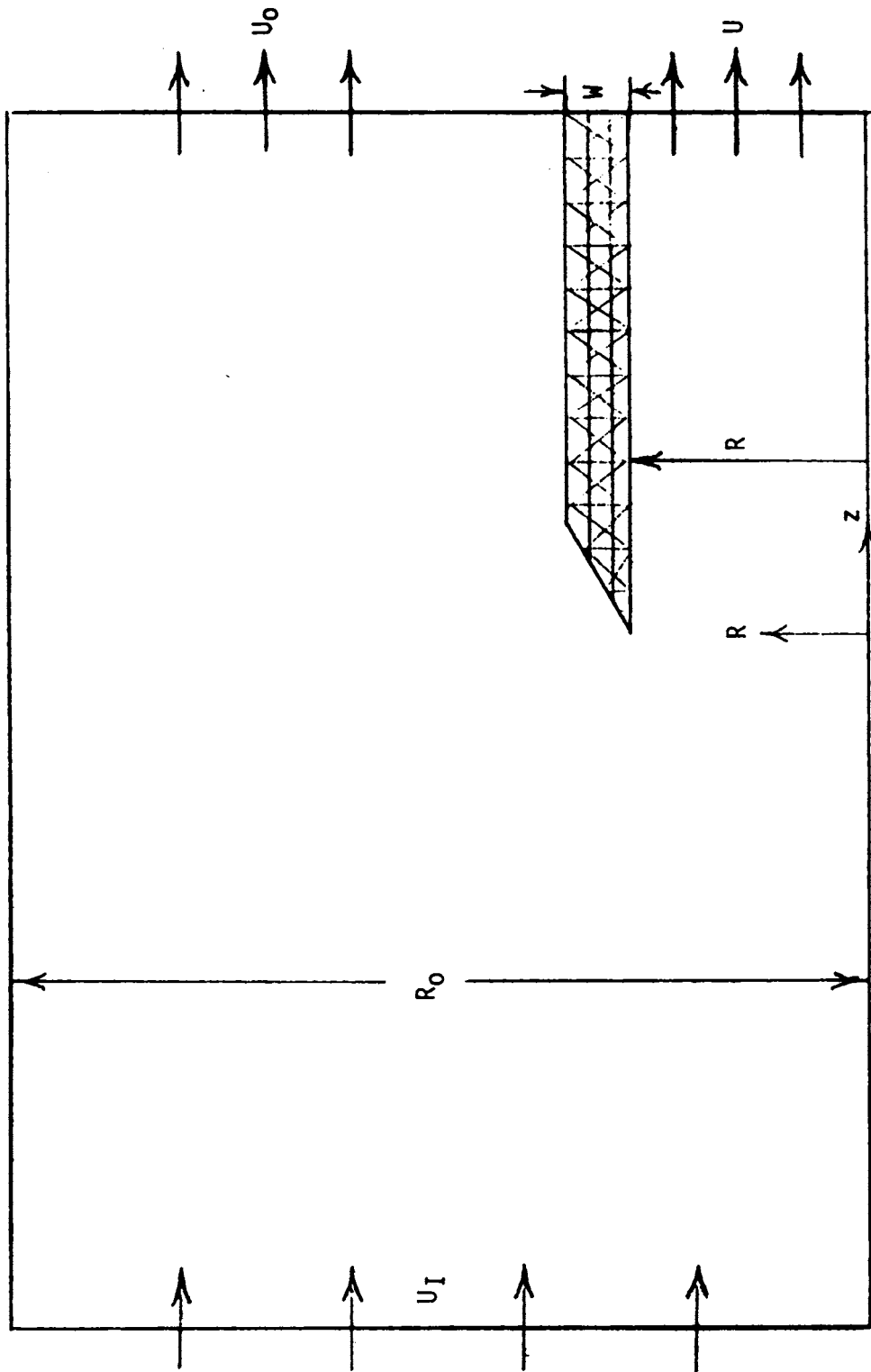


Figure 8. Nomenclature for flow region for circular inlet.

Inviscid flow equations together with Equation (31) pose a well-defined problem.

Sampler with General Orientation to the Stream--

In the two models discussed above, the stream function ψ existed because the problem was reduced to two dimensions. With the parallel plate sampler, the width of the plates along the x-axis is assumed to be so great that the flow field is unchanged. For the circular tube, the angular dimension can also be factored out of the problem when the sampler's axis is parallel to the initial flow. When the circular sampler face is oriented at an angle $\alpha \neq 90^\circ$ towards the oncoming stream, the axial symmetry is not preserved. In the three-dimensional case, the stream function ψ does not exist and Equation (19) is not valid.

Even for the case of parallel plates, solution to Equation (14) for an arbitrary orientation requires a very large flow region to be solved. Hence other approximate methods to simulate the flow are necessary. One such method is to superpose simple potential flows to simulate the flow in question. In this study, superposition of uniform flow over a line sink was used to simulate the flow around a sampling head. In the past a number of investigators^{7,12,13,15,16} have used a point sink and a uniform flow to simulate the flow around the sampling head. But the point sink is isotropic and the sampling head orientation cannot be incorporated. This difficulty is overcome by the use of a line sink.

Uniform Strength Sink Distribution--

Let a line sink of length d be distributed along the face plane OA of the sampler head. Let α be the angular orientation of the sampler head with the oncoming stream, and m the sink strength per unit length. Then the stream function ψ at any point P (Figure 9) can be divided into two parts, ψ_{sink} and $\psi_{\text{uniform stream}}$. The following equation provides ψ_{sink} and ψ_{us} .

$$\psi_{\text{sink}} = -m \left[\tan^{-1} \frac{y}{x} \cdot x - \tan^{-1} \frac{y}{(x-d)} \cdot (x-d) + y \ln \frac{\sqrt{x^2 + y^2}}{\sqrt{(x-d)^2 + y^2}} \right] \quad (33)$$

$$\psi_{\text{u.s.}} = U_I y \cos \alpha + U_I x \sin \alpha \quad (34)$$

U_x = velocity in the x direction

$$= \frac{\partial \psi}{\partial y}$$

$$= U_I \cos \alpha - m \ln \frac{\sqrt{x^2 + y^2}}{\sqrt{(x-d)^2 + y^2}} \quad (35)$$

$$= U_I \cos \alpha - m \ln \frac{OP}{AP}$$

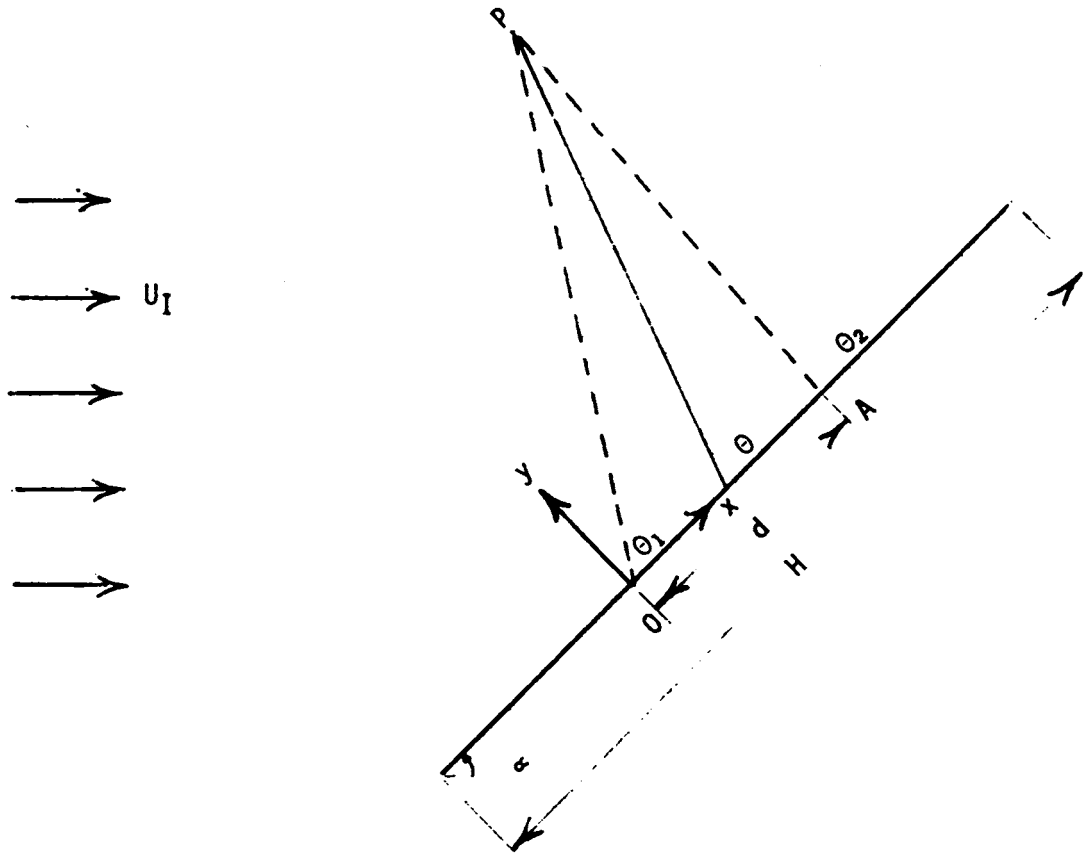


Figure 9. Line sink distribution along face plane of the sampler.

$$\begin{aligned}
U_y &= \text{velocity in } y \text{ direction} \\
&= - \frac{\partial \psi}{\partial x} \\
&= U_I \sin \alpha + m \left[\tan^{-1} \frac{y}{x} - \tan^{-1} \frac{y}{x-d} \right] \\
&= U_I \sin \alpha + m (\theta_1 - \theta_2)
\end{aligned} \tag{36}$$

If U is the anisokinetic velocity ratio and f the ratio of $\frac{d}{2H}$, then through mass balance

$$m = \frac{U - \sin \alpha}{\pi f} \tag{37}$$

If U is greater than $\sin \alpha$ then m is positive and denotes a sink. If U is smaller than $\sin \alpha$ then m is negative and denotes a source. The detailed derivation of Equations (33), (38) and (36) is given in Appendix B.

Triangular Strength Distribution--

A uniform sink/source strength distribution along the face plane of the sampler does not take into account the effect of the sampler wall. The effect of sampler wall propagates towards the center of the sampler inlet and varies with the distance from the centerline. In essence, the flow through the center of the sampler is more than the flow closer to the walls. In order to approximate this effect of retarded flow near the walls, the sink/source strength distribution was made triangular (Figure 10). Using an approach similar to the case of uniform strength, the stream function can be written as the sum of two stream functions, ψ sink/source and ψ uniform stream.

Then from Figure 9

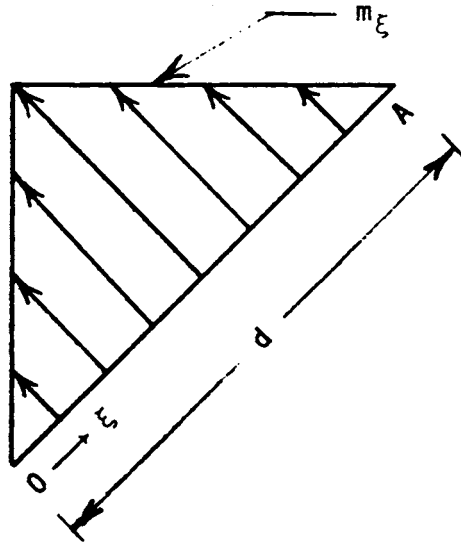
$$S = \int_0^d m_\xi \cdot \theta \cdot d\xi \tag{38}$$

Where

$$\begin{aligned}
m_\xi &= m\xi; & 0 \leq \xi \leq d/2 \\
&= m(d-\xi); & d/2 \leq \xi \leq d
\end{aligned} \tag{39}$$

and

$$\theta = \cot^{-1} \frac{(x-\xi)}{\bar{w}} \tag{40}$$



$$\begin{aligned}
 m_{\xi} &= m \xi & 0 \leq \xi \leq d/2 \\
 &= m (d - \xi) & d/2 \leq \xi \leq d
 \end{aligned}$$

Figure 10. Triangular source/sink strength distribution.

The details of integration of equation (38) with equation (39) and (40) are given in Appendix C. The stream function due to source/sink Ψ is given by

$$\begin{aligned}
 \Psi &= \text{Cot}^{-1} \frac{x}{y} \left[\frac{mx^2}{2} - \frac{my^2}{2} \right] \\
 &+ \frac{\text{Cot}^{-1} \frac{x-d/2}{y} \left[my^2 - m(x-d/2)^2 \right]}{y} \\
 &+ \text{Cot}^{-1} \frac{x-d}{y} \left[\frac{m(d-x)^2}{2} - \frac{my^2}{2} \right] \\
 &+ \frac{mx}{2} \ln \left[\frac{y^2 + x^2}{y^2 + (x-d/2)^2} \right] \\
 &+ \frac{my(d-x)}{2} \ln \left[\frac{y^2 + (x-d/2)^2}{y^2 + (x-d)^2} \right] \quad (41)
 \end{aligned}$$

The velocities U_x and U_y in x and y direction due to the sink are given as follows.

$$\begin{aligned}
 U_x &= \frac{\partial \Psi}{\partial y} \\
 &= \frac{mx}{2} \frac{x^2 - y^2}{x^2 + y^2} - my \cot^{-1} \frac{x}{y} \\
 &+ m(x-d/2) \frac{y^2 - (x-d/2)^2}{y^2 + (x-d/2)^2} + 2my \cot^{-1} \frac{x-d/2}{y} \\
 &+ \frac{m(x-d)}{2} \frac{(d-x)^2 - y^2}{(d-x)^2 + y^2} - my \cot^{-1} \frac{x-d}{y} \\
 &+ \frac{mx}{2} \ln \left[\frac{y^2 + x^2}{y^2 + \left(\frac{x-d}{2}\right)^2} \right] + my \times \left[\frac{1}{x^2 + y^2} - \frac{1}{y^2 + \left(x - \frac{d}{2}\right)^2} \right] \\
 &+ m(d-x) \ln \left[\frac{y^2 + (x-d/2)^2}{y^2 + (x-d)^2} \right] + my^2 (d-x) \left[\frac{1}{y^2 + (x-d/2)^2} - \frac{1}{y^2 + (x-d)^2} \right] \quad (42)
 \end{aligned}$$

$$\text{and } U_y = - \frac{\partial \Psi}{\partial x}$$

$$\begin{aligned}
 &= \frac{my}{2} \frac{x^2 - y^2}{x^2 + y^2} - mx \cot^{-1} \frac{x}{y} \\
 &+ my \frac{y^2 - (x-d/2)^2}{y + (x-d/2)^2} + 2m(x-d/2) \cot^{-1} \frac{x-d/2}{y} \\
 &+ \frac{my}{2} \frac{(d-x)^2 - y^2}{(d-x)^2 + y^2} + m(d-x) \cot^{-1} \frac{x-d}{y}
 \end{aligned}$$

$$\begin{aligned}
& + my/2 \ln \left[\frac{y^2 + x^2}{y^2 + (x-d/2)^2} \right] + my/2 \ln \left[\frac{y^2 + (x-d/2)^2}{y^2 + (x-d)^2} \right] \\
& - myx \left[\frac{x}{y^2 + x^2} - \frac{(x-d/2)}{y^2 + (x-d/2)^2} \right] \\
& - my(d-x) \left[\frac{x-d/2}{y^2 + (x-d/2)^2} - \frac{(x-d)}{y^2 + (x-d)^2} \right] \tag{43}
\end{aligned}$$

The velocities in the flow field with the uniform stream will be

$$\begin{aligned}
U_x &= U_x + U_0 \cos \alpha \\
U_y &= U_y + U_0 \sin \alpha \tag{44}
\end{aligned}$$

The value of m in equations (41), (42) and (43) can be obtained by mass balance as per Appendix C.

$$m = - 2(U \sin \alpha) / \pi f^2 \tag{45}$$

where

- U is the anisokinetic velocity ratio.
- α the angular orientation of the sampler head.
- f the fraction of the diameter over which the sink/source is assumed to be distributed.

The equation (41) - (45) define the flow field completely. This simulation of flow by superposition accounts for the angular orientation and the anisokinetic sampling. The effect of inlet geometry is not taken into account.

PARTICLE MOTION

AEROSOL MECHANICS OF RESPIRABLE PARTICLES

The general theory of the dynamics of spherical bodies suspended in a fluid as a continuum restricts analysis to the condition where the Knudsen number of the body, Kn , approaches zero. In practice, these results can be applied to particle behavior under conditions of $Kn \gg 1$, then the continuum theory cannot be applied and free molecular theory takes over. For intermediate Knudsen number particle dynamics, the continuum theory needs to be supplemented with a slip correction factor. All the above theories have been well documented in the literature.^{13,14}

The various forces acting on a particle are as follows:

- inertial
- gravitational
- diffusional
- electrostatic

Inertial

In the course of movement, particles of aerosol may acquire motion relative to the suspending gas, due to their inability to conform to the fluid flow instantaneously. There is a certain amount of time lag in which the particle is not affected by local velocity changes in the flow. This is characterized by τ , the relaxation time of the particles. τ is defined as the ratio of particle terminal settling velocity to the acceleration due to gravity. In the same manner, if an aerosol at rest is accelerated to a velocity V/e in time τ . Hence, in a velocity gradient field, the particle overshoots the fluid when decelerating or it undershoots it when accelerating.

Stokes number, K (the ratio of the stop distance of the particle to the characteristic length of the system), is used to indicate the importance of inertial effects for a given set of conditions. The smaller the value of K , the more negligible the inertia:

$$K = \frac{U_0 \tau}{L} = \frac{\rho d^2 U_0}{18 \eta L} \quad (46)$$

where U_0 = the free stream velocity
 τ = the relaxation time of particles
 L = characteristic length (cm)
 ρ = the density of the aerosol particle (gm/cc)
 d = diameter of the particle (cm), and
 η = the viscosity of the medium (gm cm/sec).

Gravitational

Gravitational force on particles is given by mg , where m is the mass of the particles and g is the acceleration due to gravity. The terminal settling velocity, V_s , is given by

$$V_s = \tau g \quad (47)$$

where

τ = the relaxation time of particles, and
 g = acceleration due to gravity (cm/sec).

The importance of gravitational effect is indicated by the Froude number (Fr):

$$Fr = \frac{V_s^2}{Lg} = \frac{V_s \tau}{L} \quad (48)$$

Diffusional

Diffusion is the most dominant force on small particles ($d < 2 \mu\text{m}$). Particles not under the influence of external forces diffuse in a random fashion called Brownian motion. Diffusion also occurs because of velocity gradients, concentration gradients, and thermal gradients.

The characteristic numbers are the Schmidt number, Sc , and the Peclet number, Pe .

$$Sc = \frac{\gamma}{\epsilon} \quad (49)$$

where

γ = kinematic viscosity (cm /sec), and
 ϵ = diffusivity of particles (cm /sec).

The Schmidt number indicates the ratio of momentum transfer to mass transfer. Higher Sc values mean Brownian Diffusion is not as important as convective diffusion. The combined effects of diffusion and fluid motion (convection) on particle transport can be expressed as a function of the Peclet number, Pe :

$$Pe = \frac{V_o D}{\epsilon} \quad (50)$$

where

V_o = the initial inviscid velocity (cm/sec), and
 D = the diameter of the sampler inlet (cm).

In this study diffusion was not included.

Electrostatic Force

The electrostatic force considered in the model is only the coulombic force between point charges of magnitude Q_p and Q_c located at the center of the particle and the collector respectively. The coulombic force between a charged particle and sampler head is given by

$$F_c = - \frac{Q_c Q_p}{4\pi\epsilon_0 R^2} \quad (51)$$

where

Q_c = charge on the collector/unit length
 Q_p = charge on the particle
 ϵ_0 = dielectric constant of air, and
 R = distance between the center of particle
to the surface of collector.

If the linear dimension of the collector surface is L , the electrostatic force can be obtained by integrating equation (51) over the length of the collector. Using the coordinate system shown in Figure 11, the total force on the particle can be written as follows

$$F = \int_0^L F_c dx \quad (52)$$

$$\begin{aligned} F_x &= x \text{ component of the force} \\ &= \frac{K}{(y-a)} (\sin \theta_1 - \sin \theta_2) \end{aligned} \quad (53)$$

and

$$\begin{aligned} F_y &= y \text{ component of the force} \\ &= \frac{K}{(y-a)} (\cos \theta_2 - \cos \theta_1) \end{aligned}$$

where

$$K = \frac{Q_c Q_p}{4\pi\epsilon_0}$$

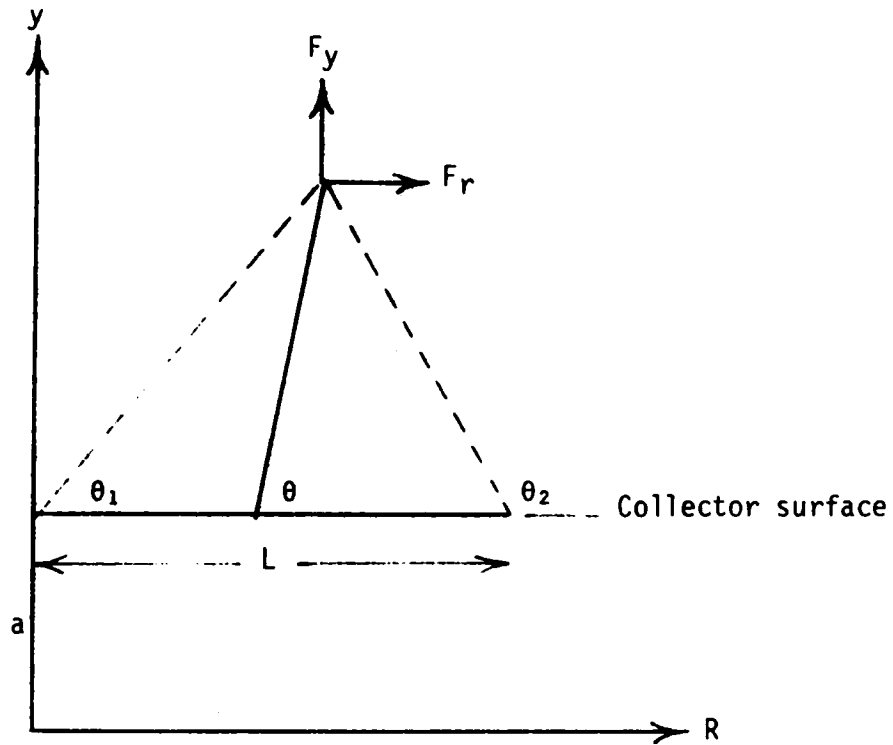


Figure 11. Coordinate system for electrostatic force calculation.

Equation (51) is valid as long as the particle and the collector are not very close. For closer distances, the equations (52) and (53) become infinite and image forces have to be taken into account. This study does not take into account the image forces.

Table 2 provides values of non-dimensional parameters such as Stokes number K , Peclet number Pe , and Froude number Fr for various particles.

Table 2. Typical values of Stokes number K, Peclet number Pe, Froude number Fr for unit density spheres.*

Particle Radius (μ)	Flow Velocity (cm/sec)		10		50		100		Fr**
			K	Pe	K	Pe	K	Pe	
0.25			1.02(-05)	1.6 (07)	5.1 (-05)	8.0 (07)	1.02(-04)	1.6 (08)	1.03(-09)
0.50			3.6 (-05)	3.65(07)	1.8 (-04)	1.83(08)	3.6 (-04)	3.65(08)	1.25(-08)
1.00			1.3 (-04)	7.85(07)	6.5 (-04)	3.93(08)	1.3 (-03)	7.85(08)	1.73(-07)
2.00			5.1 (-04)	1.63(08)	2.55(-03)	8.15(08)	5.1 (-03)	1.63(09)	2.56(-06)
5.00			3.1 (-03)	4.17(08)	1.55(-02)	2.09(09)	3.1 (-02)	4.17(09)	9.55(-05)
10.00			1.24(-02)	8.43(08)	6.2 (-02)	4.22(09)	1.24(-01)	8.43(09)	1.50(-03)

* Characteristic dimension 'L' of the sampler is assumed to be 1 cm.

** Froude number 'Fr' is independent of flow velocities.

EQUATION OF MOTION OF PARTICLES

When an aerosol particle travels in a moving medium the particle generally tends to lag behind the flow of fluid. Assuming that the Stokes relation for the particle drag may be used, then within the continuum approximation of the fluid the equation of motion of the particle may be written as:¹⁴

$$\begin{aligned} \frac{\pi}{6} d^3 \rho \frac{d\bar{v}}{dt} = 3\pi\eta d (\bar{U} - \bar{v}) + \frac{\pi}{6} d^3 \rho_g \frac{d\bar{U}}{dt} + \frac{\pi}{12} d^3 \rho_g \left(\frac{d\bar{U}}{dt} - \frac{d\bar{v}}{dt} \right) \\ + \frac{3}{2} d^2 \sqrt{\pi \rho_g \eta} \int_{t_0}^t \frac{dt^1 \left(\frac{d\bar{U}}{dt^1} - \frac{d\bar{v}}{dt^1} \right)}{(t - t^1)^{3/2}} + F_e \end{aligned} \quad (54)$$

The first term on the left in equation (54) is the resultant force acting on the particle. The first term on the right is the viscous resistance given by the Stokes law. The second term is due to the pressure gradient in the gas surrounding the particle, caused by the acceleration of the particle. The third term denotes the force required to accelerate the apparent mass of the particle relative to the ambient gas. The fourth term, known as the Basset term, accounts for the deviation from the steady state in the gas flow pattern. The last term is the force resulting from external potential. In general, the second, third and fourth terms will be negligible, so equation (54) in simplified form will be

$$\frac{\pi}{6} d^3 \rho \frac{d\bar{v}}{dt} = 3\pi\eta d (\bar{U} - \bar{v}) + \bar{F}_e \quad (55)$$

or

$$\frac{d\bar{v}}{dt} = \frac{\bar{U} - \bar{v}}{\tau} + \bar{F}_{em} \quad (56)$$

where \bar{F}_{em} is the external force per unit mass. Divide velocities by U_I and time by L/U_I to obtain nondimensional form of equation (56). Denoting the nondimensional quantities by stars, the equation of motion becomes:

$$\frac{d\bar{V}^*}{d\bar{t}^*} = \frac{\bar{U}^* - \bar{V}^*}{K} + \bar{F}_{em}^* \quad (57)$$

where

$$\begin{aligned} K = \text{Stokes number of particle} &= \frac{U_I \tau}{L} \\ \bar{F}_{em} &= \frac{\bar{F}_{em} \cdot L}{U_I^2} \end{aligned} \quad (58)$$

METHODS OF SOLUTION

In order to estimate the sampling error, it is necessary to solve the equation of particle motion (equation 48) together with the fluid flow equations. Analytical solutions to partial differential equations such as equations (57) or (14) can be obtained for only very simple boundary configurations. Approximate solutions, however, can be obtained by numerical methods by solving the finite differenced equations of the governing differential equation.

FLUID FLOW

As indicated in the previous section, the model for the fluid flow has two options. The first option is to solve the flow equation (19) with proper boundary conditions to obtain the numerical solution to the exact problem. The second option is to use the superposition of simple flows to approximate the actual flow conditions. The first option requires numerical solution of equation (14) and can be used only when the sampling head is facing the on-coming stream. For general orientation of the sampling head, the second option is used and requires numerical evaluation of the flow velocities given by equations (41)-(45) for use in determining the trajectory of particles.

Sampler Facing the Stream

Thin-walled Plates--

Let the flow field be divided into a grid as shown in Figure 12. Then, Laplace's equation (14) can be written in finite difference form and solved by iteration.

Each iteration of the finite difference equation is analogous to solving the time-dependent version of equation (14):

$$\frac{\partial \psi}{\partial \tau} = \nabla^2 \psi \quad (59)$$

We are not interested in the physical significance of this transient solution, but a step in time Δt in the time-dependent ψ is a convenient representation for an iteration of the time-independent function. As the solution to equation (59) approaches steady state, we have also converged to the desired solution of Laplace's equation (14).

Now, we write equation (59) in discrete form for point I, J using FTCS (Forward Time Centered Space) differencing

$$\frac{\psi_{IJ}^{k+1} - \psi_{IJ}^k}{\Delta t} = \frac{\delta_x^2 \psi}{\Delta x^2} + \frac{\delta_y^2 \psi}{\Delta y^2} \quad (60)$$

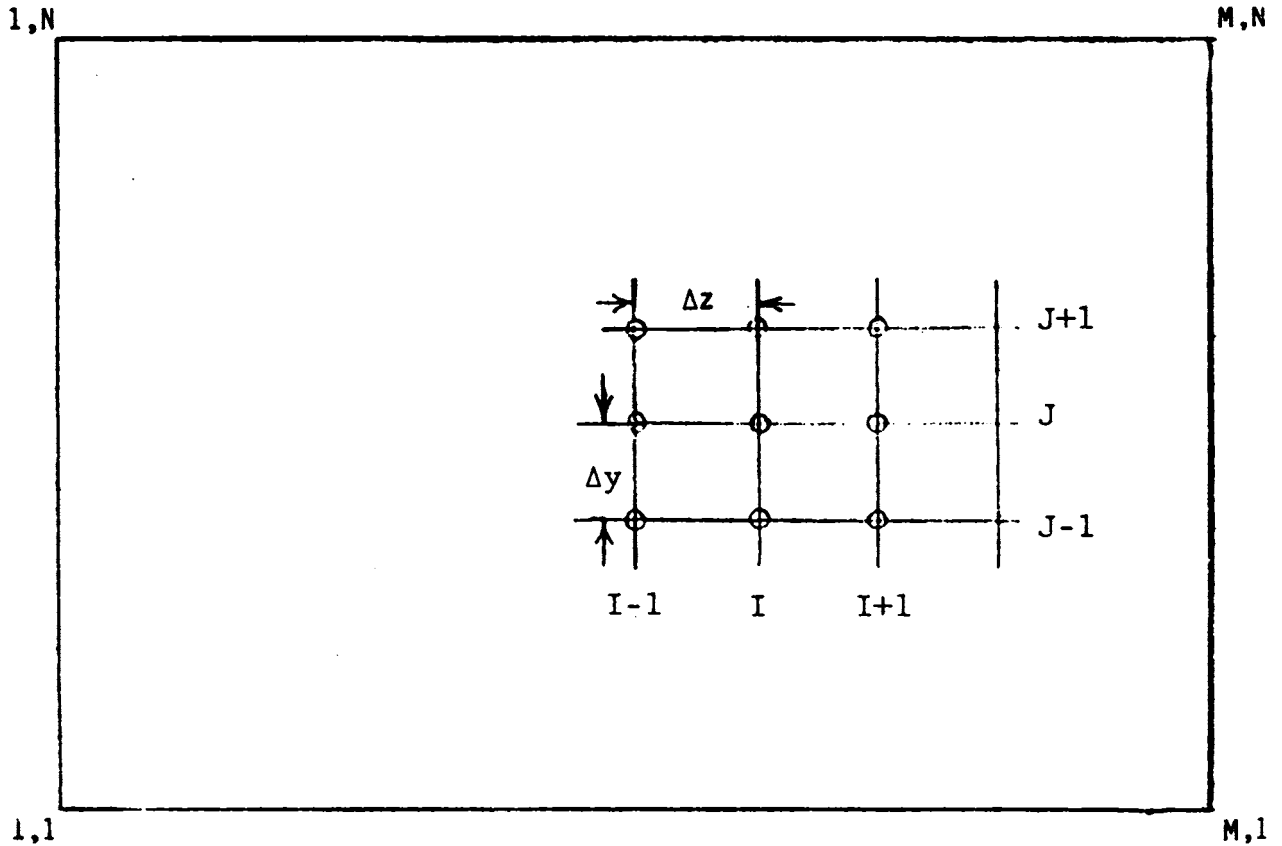


Figure 12. Rectangular mesh geometry.

where

$\psi_{I,J}^k$ = the stream junction ψ at (I,J) at the k^{th} time step.

$$\frac{\delta^2 \psi^k}{\Delta z^2} = \frac{\psi_{I-1,J}^k - 2\psi_{I,J}^k + \psi_{I+1,J}^k}{\Delta z^2} \quad (61)$$

$$\frac{\delta^2 \psi^k}{\Delta y^2} = \frac{\psi_{I,J-1}^k - 2\psi_{I,J}^k + \psi_{I,J+1}^k}{\Delta y^2}$$

For the difference equation (60) to be stable the condition is:

$$\frac{\Delta t}{\Delta z^2} + \frac{\Delta t}{\Delta y^2} \leq 1/2 \quad (62)$$

Since we wish to approach the solution as rapidly as possible, we take the largest possible Δt from equation (62).

Defining the mesh aspect $\beta = \Delta z/\Delta y$, then:

$$\psi_{I,J}^{k+1} = \psi_{I,J}^k + \frac{1}{2(1+\beta^2)} \left[\psi_{I+1,J}^k + \psi_{I-1,J}^{k+1} + \beta^2 \psi_{I,J+1}^k + \beta^2 \psi_{I,J-1}^{k+1} - 2(1+\beta^2) \psi_{I,J}^k \right] \quad (63)$$

The convergence of equation (63) can be made faster by multiplying the bracketed terms by a factor ω such that $1 < \omega < 2$ [28,29]. Then

$$\psi_{I,J}^{k+1} = \psi_{I,J}^k + \frac{\omega}{2(1+\beta^2)} \left[\text{Bracketed terms as above} \right] \quad (64)$$

A solution for $\psi_{I,J}^{k+1}$ would be computed from the lower order solution $\psi_{I,J}^k$. An initial lower order solution has to be provided either by a previous problem or by arbitrary assumptions for ψ . When $\psi_{I,J}^{k+1} \rightarrow \psi_{I,J}^k$, then the solution is reached. This can be programmed in a digital computer and the iteration will be stopped when

$$\frac{|\psi_{I,J}^{k+1} - \psi_{I,J}^k|}{\psi_{I,J}^k} \leq \xi \quad (\text{error limit}) \quad (65)$$

The velocities are calculated as follows.

$$\begin{aligned} U_z(I,J) &= (\psi(I,J+1) - \psi(I,J-1))/2 \cdot \Delta y \\ U_y(I,J) &= -[\psi(J+1,J) - \psi(J-1,J)]/2 \cdot \Delta z \end{aligned} \quad (66)$$

Thin-walled Tube--

The time dependent problem for circular tube is given by

$$\frac{\partial \psi}{\partial t} = \frac{\partial^2 \psi}{\partial z^2} - \frac{1}{r} \frac{\partial \psi}{\partial r} + \frac{\partial^2 \psi}{\partial r^2} \quad (67)$$

Writing equation (67) in discretized form for point I,J using FTCS differencing

$$\frac{\psi_{IJ}^{k+1} - \psi_{IJ}^k}{\Delta t} = \frac{\delta^2 \psi^k}{\Delta z^2} + \frac{\delta^2 \psi^k}{\Delta r^2} - \frac{1}{R} \frac{\delta \psi^k}{\Delta r} \quad (68)$$

where

$$\psi_{IJ}^k = \text{stream function at (I,J) at } k^{\text{th}} \text{ time step}$$

R = Radial Coordinate at (I,J)

$$\frac{\delta^2 \psi^k}{\Delta z^2} = \frac{\psi_{I-1,J} - 2\psi_{I,J}^k + \psi_{I+1,J}^k}{\Delta z^2}$$

$$\frac{\delta^2 \psi^k}{\Delta r^2} = \frac{\psi_{I,J-1}^k - 2\psi_{I,J}^k + \psi_{I,J+1}^k}{\Delta r^2}$$

$$\frac{\delta \psi^k}{\Delta r} = \frac{\psi_{I,J+1}^k - \psi_{I,J-1}^k}{2 \cdot \Delta r}$$

The convergence of equation (68) is made faster by multiplying the right hand side of the equation by a factor w such that $1 < w < 2$. The flow velocities are calculated as follows

$$U_z(I,J) = \frac{1}{R} \frac{\psi_{I,J+1} - \psi_{I,J-1}}{2 \cdot \Delta r}$$

$$U_r(I,J) = -\frac{1}{R} \frac{\psi_{I+1,J} - \psi_{I-1,J}}{2 \cdot \Delta z}$$
(69)

Thick-Walled Tube/Plate

Depending on the shape and thickness of the sampler wall the grid size in any one direction may not be equal throughout the flow region (Figure 13).

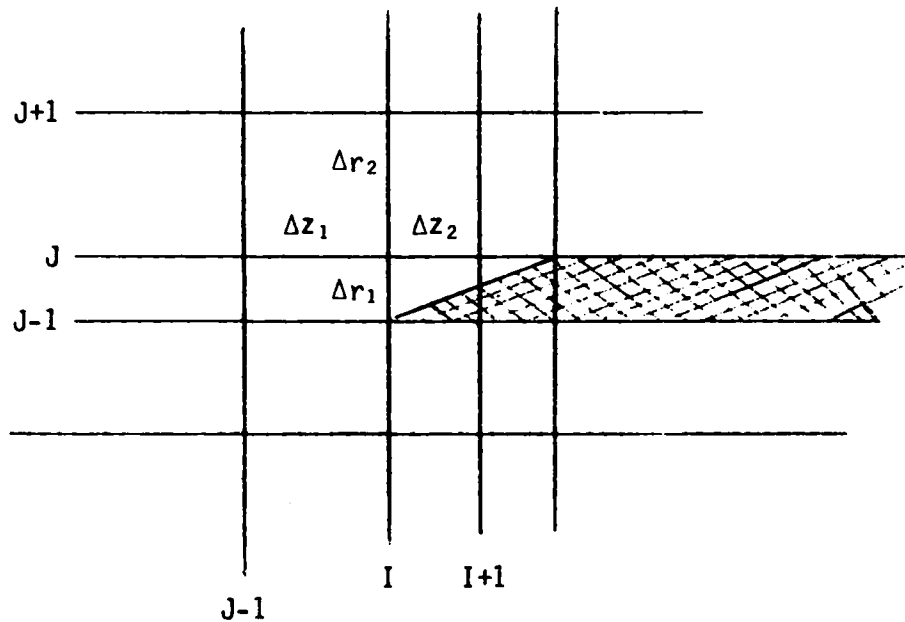


Figure 13. Unequal grid size.

Writing the governing equation (67) in discretized form for unequal grid size and grouping the terms gives:

$$\begin{aligned}
 & \psi_{I,J} \left\{ \frac{2}{(\Delta z_1 \cdot \Delta z_2)} - \frac{1}{R} \left(\frac{\Delta r_1 - \Delta r_2}{\Delta r_1 \cdot \Delta r_2} \right) + \frac{2}{\Delta r_1 \cdot \Delta r_2} \right\} \\
 &= \psi_{I-1,J} \left\{ \frac{2}{(\Delta z_1 + \Delta z_2) \cdot \Delta z} \right\} + \psi_{I+1,J} \left\{ \frac{2}{(\Delta z_1 + \Delta z_2) \cdot \Delta z_2} \right\} \\
 &+ \psi_{I,J-1} \left\{ \frac{1}{R} \cdot \frac{\Delta r_2}{(\Delta r_1 + \Delta r_2) \cdot \Delta r_1} + \frac{2}{(\Delta r_1 + \Delta r_2) \cdot \Delta r_1} \right\} \\
 &+ \psi_{I,J+1} \left\{ -\frac{1}{R} \cdot \frac{\Delta r_1}{(\Delta r_1 + \Delta r_2) \cdot \Delta r_2} + \frac{2}{(\Delta r_1 + \Delta r_2) \cdot \Delta r_2} \right\} \tag{70}
 \end{aligned}$$

for circular tube,

$$\begin{aligned}
 \psi_{I,J} \left\{ \frac{2}{\Delta z_1 \cdot \Delta z_2} + \frac{2}{\Delta r_1 \cdot \Delta r_2} \right\} &= \psi_{I-1,J} \left\{ \frac{2}{(\Delta z_1 + \Delta z_2) \cdot \Delta z_1} \right\} \\
 &+ \psi_{I+1,J} \left\{ \frac{2}{(\Delta z_1 + \Delta z_2) \cdot \Delta z_2} \right\} \\
 &+ \psi_{I,J-1} \left\{ \frac{2}{(\Delta r_1 + \Delta r_2) \cdot \Delta r_1} \right\} \\
 &+ \psi_{I,J+1} \left\{ \frac{2}{(\Delta r_1 + \Delta r_2) \cdot \Delta r_2} \right\} \tag{71}
 \end{aligned}$$

for plates

The stream function at the boundary points are given by either equation (29) or by equation (32).

The various wall shapes that can be realized by use of wall thickness 'w' and chamfer angle 'α' are shown in Figure 14. These shapes can be obtained for both two-dimensional and axisymmetrical cases.

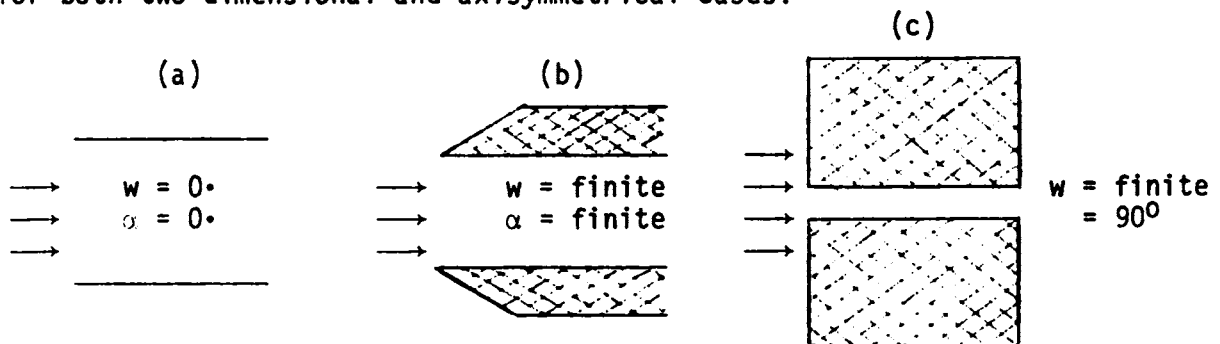


Figure 14. Various inlet geometries.

Sampler with General Orientation

When the sampler is oriented at an angle ' α ' to the on-coming stream, the approximate solution developed earlier is used. Equations (41)-(45) will be evaluated for use in particle trajectory calculation.

PARTICLE MOTION

The equation of motion of particles as given by equation (48) is solved by calculating the trajectories of particles. The method that is used to do this is the predictor-corrector method together with an iterative convergence. Even though the predictor-corrector method is a standard one and can be found in any numerical methods book, we will give a short description of the method here.

Prediction

If the particle is at position $\vec{x}=\vec{x}_0$ at time $t=0$, then at $t=t+\Delta t$, the particle is predicted to be at

$$\vec{x}_p = \vec{x}_0 + \Delta t \cdot \vec{v} \quad \left| \quad \vec{x} = \vec{x}_0 \quad (72)$$

Correction

The above equation assumes that the velocity, v , of the particle remains constant within the step. But actually it is a changing function:

$$\vec{x}_c = \vec{x}_0 + \Delta t \cdot v \quad \left| \quad \vec{x} = \frac{\vec{x}_0 + \vec{x}_p}{2} \quad (73)$$

Equation (73) is iterated until the corrected value \vec{x}_c converges.

The above procedure is continued until the particle either touches the wall of the sampling probe, in which case it is captured and lost from the sample, or enters the probe inlet, in which case it could either be transported to the sensing instrument or be lost by deposition to the walls. A limiting trajectory which will just graze the inside of the probe wall can then be calculated.

In order to calculate the velocity v for equation (73), the simplified equation for particle motion (48) is used. Equation (48) is the result of the various forces influencing the particle. In this study, the particle motion is determined by inertial and gravitational forces. Electrostatic and diffusion forces are neglected.

Assumptions

The following assumptions are used in obtaining a solution to the particle motion equation.

- The particles are uniformly distributed and, at a large distance upstream from the probe inlet, move with the same velocity as the free stream fluid.
- The particles are spherical and do not change in size due to agglomeration, evaporation or condensation.
- The particles are considered to be sufficiently small in comparison with probe size and they move as individual particles with no hydro-dynamic interactions among themselves or between themselves and the probe walls.

Solution Procedure

At a large distance upstream (5 radii) from the probe inlet the fluid flow is uniform and the particles move with the stream. As the flow approaches the sampling probe the disturbance due to the presence of the probe is felt and the particles due to their inertia are not able to follow the fluid flow.

The equation (48) can be written in terms of the velocity components as

$$\begin{aligned}\frac{dV_x}{dt} &= \frac{U_x - V_x + V_{ext-x}}{K} \\ \frac{dV_y}{dt} &= \frac{U_y - V_y + V_{ext-y}}{K}\end{aligned}\tag{74}$$

Now let the particle be at position (x_0, y_0) at time $t=t_0$. Then at time $t=t_0+\Delta t$, $V_x=V_{xP}$, $V_y=V_{yP}$ are the predicted values of velocities.

$$\begin{aligned}V_{xP} &= V_x + \left. \frac{dV_x}{dt} \right|_{\substack{x=x_0 \\ y=y_0}} \cdot \Delta t \\ V_{yP} &= V_y + \left. \frac{dV_y}{dt} \right|_{\substack{x=x_0 \\ y=y_0}} \cdot \Delta t\end{aligned}\tag{75}$$
$$\begin{aligned}x_P &= x_0 + V_{xP} \cdot \Delta t \\ y_P &= y_0 + V_{yP} \cdot \Delta t\end{aligned}$$

The corrected values are

$$\begin{aligned}
 V_{xC} &= V_x + \frac{dV_x}{dt} \Bigg|_{\substack{x = \frac{x_0+x_p}{2} \\ y = \frac{y_0+y_p}{2}}} \cdot \Delta t \\
 V_{yC} &= V_y + \frac{dV_y}{dt} \Bigg|_{\substack{x = \frac{x_0+x_p}{2} \\ y = \frac{y_0+y_p}{2}}} \cdot \Delta t
 \end{aligned}
 \tag{76}$$

$$x_c = x_0 + V_{xC} \cdot \Delta t$$

$$y_c = y_0 + V_{yC} \cdot \Delta t$$

The equations (76) are iterated, replacing the x_p , and y_p values by the corrected values x_c and y_c until the successive values are within a preselected tolerance.

For the cases of very small Stokes number, it becomes necessary to adopt very small time steps to compute the trajectory accurately in any flow region with steep velocity changes (near the sampler head, for example). To overcome this difficulty, the velocities of particle V_x and V_y can be approximated and the following procedure is used.

$$V_x = U_x - K \frac{\partial U_x}{\partial x} \cdot U_x + VG_x \tag{77}$$

$$V_y = U_y - K \frac{\partial U_y}{\partial y} \cdot U_x + VG_y$$

where

V_x = particle velocity in x direction

V_y = particle velocity in y direction

U_x = fluid velocity in x direction

U_y = fluid velocity in y direction

K = Stokes number of the particle

VG_x = sedimentation velocity in the x direction

VG_y = sedimentation velocity in the y direction

$$\frac{dx_p}{dt} = V_x$$

$$\frac{dy_p}{dt} = V_y$$
(78)

where

x_p, y_p = coordinates of particles
 t = time coordinate

From (78) we get

$$\frac{dy_p}{dx_p} = \frac{V_y}{V_x}$$
(79)

Equations (77) and (78) are used to compute the trajectory of the particles.

Particle velocities V_x, V_y are computed from the equation (77). By using (79), the new position of the particle is predicted as:

$$Y_{PN} = Y_{PO} + \left. \frac{V_y}{V_x} \right|_{XPO} \cdot \Delta x$$
(80)

where

Y_{PN} = new position of particle in Y
 Y_{PO} = old position of particle in Y
 Δx = a preselected step size in x
 XPO = old position of particle in x

If the ratio of Y_{PN}/Y_{PO} is greater than 1.05, then the step size x is reduced until this criteria is met. Then a corrected new position of the particle is computed by calculating the velocities at the new position by equation (77) and using an average value of the velocity ratios in equation (80). That is

$$Y_{PN}(\text{corrected}) = Y_{PO} + \frac{1}{2} \left(\left. \frac{V_y}{V_x} \right|_{\text{old}} + \left. \frac{V_y}{V_x} \right|_{\text{new}} \right) \cdot \Delta x$$
(81)

If we denote the corrected value of Y_{PN} as Y_0 then Equation (81) is iterated until Y_0 converges. That is

$$Y_0^n = Y_0^{n-1} + \frac{\left(\left. \frac{V_y}{V_x} \right|_{\text{old}} + \left. \frac{V_y}{V_x} \right|_{\text{new}}^{n-1} \right)}{2} \cdot \Delta x$$

where superscript n represents iteration number. The procedure is stopped when the successive values of Y_0 are within a chosen error limit.

The above procedure is repeated until the particle passes the probe inlet, at which point it either gets captured by the probe or escapes it.

Calculation of the Efficiency of the Sampling

Let C_0 denote the number of particles/unit volume in the free stream and let C be the actual number of particles sensed by the instrument, then

$$\eta = \frac{C}{C_0} = \frac{C_I}{C_0} \cdot \frac{C}{C_I}$$

where

η = the efficiency of the sampling, and

C_I = the concentration at the inlet to the probe

$$\frac{C_I}{C_0} = E \cdot \frac{U_0}{U}$$

where

E = the efficiency of capture of inlet

$$\frac{C}{C_I} = \frac{C_I - \Delta C}{C_I}$$

where

ΔC = the loss of particles in the probe.

In the case of a polydispersed system, the distribution can be divided into n number of small groups. Each one can be treated in the same way as described above. The effective η will be given as

$$\eta_{\text{eff}} = \sum_{i=1}^n \eta_i f_i$$

where

η_i = the efficiency of the i^{th} group

f_i = the fraction of i^{th} group, and

n = the number of groups.

In most of the cases, the measured size distribution under non-ideal conditions

are available and one likes to find the actual distribution. Denoting the fraction of i^{th} group by ' $f_i \text{ act}$ ', then:

$$f_{i \text{ act}} = \frac{f_i/n_i}{\sum_{i=1}^n \frac{f_i}{n_i}} \quad (82)$$

COMPUTER PROGRAM SYSTEM

The computer program system consists of two separate programs. Program 'FLOWFI' solves for the flow field and program 'TRAJEC' computes the particle trajectories in the specified flow region. Since the model uses the stream function equation (14) only when the sampling head faces the stream, program 'FLOWFI' has to be run only with this option. For angular orientations the flow field is approximated by a line sink/source in a uniform stream and the flow field is incorporated in the 'TRAJEC' program. A description of both programs follows.

Program 'FLOWFI'

This program to solve for the values of Stokes/Lagrange stream function ψ and to calculate the fluid velocity components U_r , U_z has been written in Fortran V for Univac 1108 digital computer. The program solves the flow fluid in and around the sampling head with circular/parallel plate geometry. The thickness of the sampling head W , chamfer angle α , and the velocity of suction ratio U are treated as parameters. An explanation of various program subroutines follows.

The calling sequence of the subroutines according to the user option of the flow field is accomplished in the Main Program.

Subroutine FLBOUN, meaning FLOW BOUNDary, specifies the boundary of the flow field in the upstream (ZM), downstream (ZMA), and the radial (RO) direction. It also specifies the sampling velocity ratio (U), chamfer angle (ANG) and the sampler wall thickness (W). The values of the upstream boundary ZM, downstream boundary ZMA, and the radial boundary RO have to be chosen arbitrarily. Typical nondimensional distances are ZM=5, ZMA=5 and RO=5 for sampling heads with 'W' \leq 0.2. For very thick-walled tubes, these boundary values have to be increased so as to realize the uniform undisturbed flow condition.

The above values are input to the program and have to be supplied by the user. The subroutine calculates a value (ZOW) which is the axial coordinate of the outer edge of the sampler for use in further calculations.

Subroutine GRID places a grid of specified grid spacing in axial (Z) and radial (R) direction and calculates the coordinates of a given point. It also calculates the maximum number of points in axial direction (IM) and maximum number of points in radial direction (JM). The total number of grid points in the flow field would be IM x JM. The coordinates of any given point (I,J) would be given by (Z(I),R(J)). ITW is an indicator for the sampler wall

thickness. ITW:0 for $W=0$, ITW:1, for finite W and ANG=0 and ITW:-1 for finite W and finite ANG. Calculation regions for various options are shown in Figure 15. IGR, and JGR are number of grid points per unit distance in the axial direction and radial direction.

Subroutine BCOND formulates the boundary conditions of the problem. The boundary conditions are to be formulated at Section I, II, and III. The sampler wall conditions are also stipulated. Figure 16 gives the values of PSI at the boundary for circular tube.

Subroutine LAPLA solves the Stokes' stream function equation formulated for the problem earlier by using the boundary conditions provided by BCOND. The solution for the flow field is provided at the grid points specified by GRID. Successive over relaxation procedure is used to approach the solution. The iteration procedure is stopped either when the successive values of PSI are within the specified error tolerance (EPPS) or when the number of iterations has exceeded the maximum number of iterations (ITERMA) specified by the user. The relaxation factor (RELAX) has to be supplied by the user and the value varies from 1.0 to 2.0 depending upon the conditions of the problem. Optimum value has to be found by trial and error. The finite difference equation formulated in the previous sections is used. This equation is solved at each grid point of the flow field except the boundary points specified by BCOND. The maximum error occurring at each iteration is printed out under convergence rate.

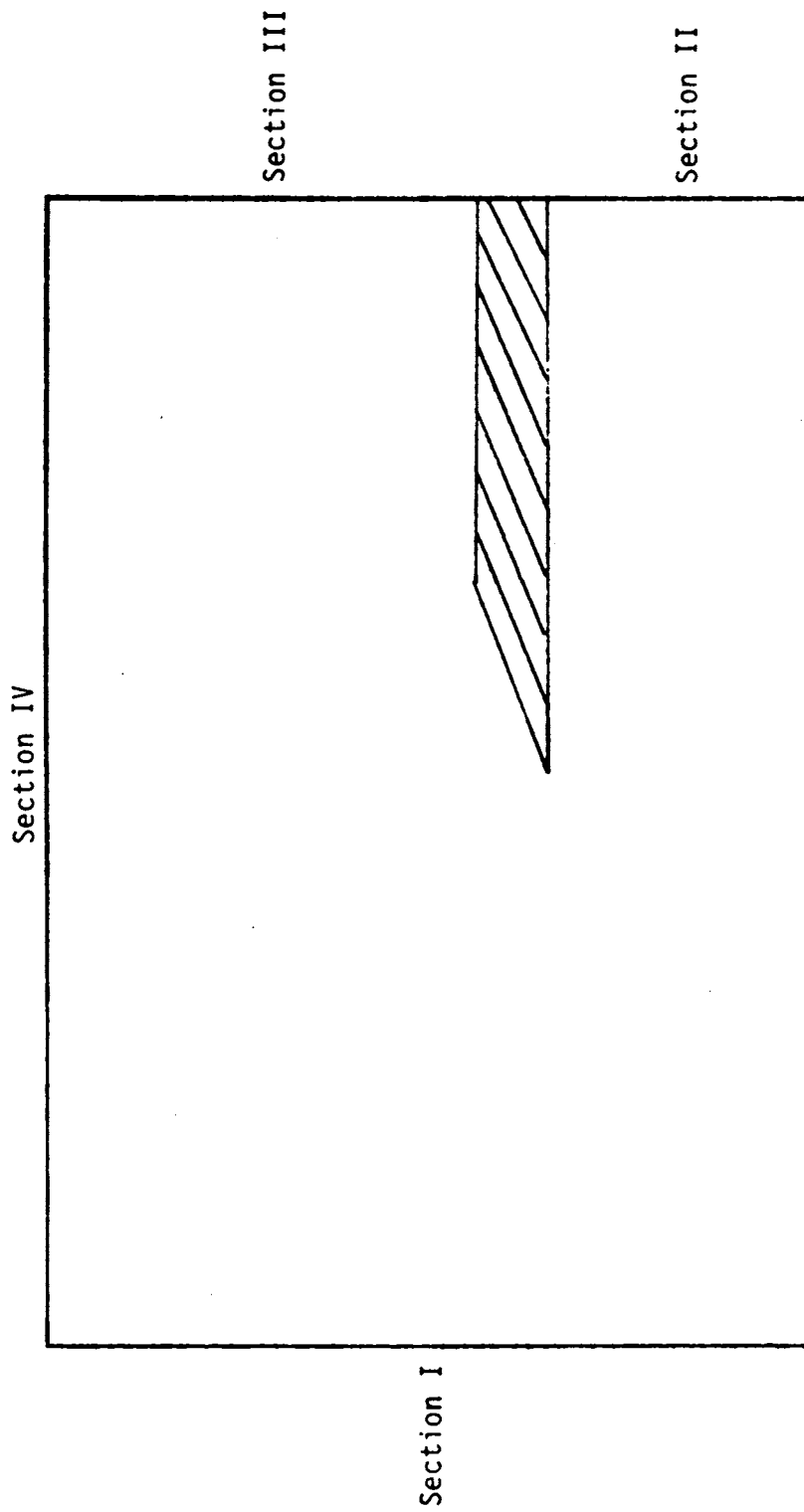
Subroutine VELO calculates the axial and radial velocity components U_z , U_r , respectively, from the stream function solution provided by the subroutine LAPLA. Velocities are calculated by determining by second order accurate finite difference expressions. Depending upon the position of the grid point, either one of the following finite difference forms is chosen:

- 1) ESC (Equal Spaced, Centered)
- 2) ESB (Equal Spaced, Backward)
- 3) ESF (Equal Spaced, Forward)
- 4) UESB (Unequal Spaced, Backward)
- 5) UESF (Unequal Spaced, Forward)
- 6) UESC (Unequal Spaced, Centered)

Subroutine RESULT prints out the results obtained from various subroutines. User can manipulate the output statements to suit his needs.

Subroutine STREAM calculates the locus of any specified stream line for use in the plotting of stream lines. A lagrange interpolation is used to calculate the locus. Function statement SAG is the lagrange interpolation formula for three points with unequal intervals.

The program listing is provided in Appendix D.



Section	PSI
I	$R(J)^{**2}$
II	$U * R(J)^{**2}$
III	$A * (R(J)^{**2} - (1+W)^{**2}) + U$ where $A = \frac{(R0^{**2} - U)}{(R0^{**2} - (1+W)^{**2})}$
IV	$R0^{**2}$

Figure 16. Boundary conditions for circular tube.

Program 'TRAJEC'

This program to solve for the limiting particle trajectory and to calculate the true particle distribution from the measured distribution has been written in Fortran V for Univac 1108 digital computer. For certain flow field options, the flow has to be predetermined and is input to 'TRAJEC'. The particle trajectories are determined by solving the equation of motion of particle with Stokes' drag. The program uses a predictor-corrector method with iterative convergence. A description of various program subroutines follows.

Program 'INER' is the Main Program and computes the particle trajectories. The user has three options in choosing the flow field. These are controlled by an integer 'NDIM'.

- NDIM = 0 The flow field used is that of two parallel plate inlets facing the stream.
- NDIM = 1 The flow field used is that of a circular tube inlet facing the stream.
- NDIM = 2 The flow field used is obtained by superposition of line sink/source with uniform stream.

Choosing the option 0 or 1 requires the output from 'FLOWFI'. However, for option 2 the flow field is incorporated in the program 'TRAJEC'. Various inlet geometries and physical conditions can be obtained by the parameters U, W, ANG, NDIM, IDIM, ALPHA. Table 3 shows the physical conditions that can be obtained by various combinations.

Table 3. Parameter description and physical significance.

NDIM	W	ANG	ALPHA	ZLIP	Physical Meaning
0	0	0	90°	0	Two D thin-walled plates facing the stream.
	Wo	90°	90°	0	Two D thick-walled plates facing the stream.
	Wo	α	90°	0	Two D thick-walled plates with sharp edge facing the stream.
1	0	0	90°	0	Thin-walled circular tube facing the stream.
	Wo	90°	90°	0	Thick-walled circular tube facing the stream.
	Wo	α	90°	0	Thick-walled circular tube with sharp edge facing the stream.
2	-	-	90°	-	Approximate solution to sampler facing the stream.
					IDIM = 0 - Two · D
					IDIM = 1 - circular tube
	-	-	α	0	Sampler with an orientation angle α .
		α	ZL	Sampler with an orientation angle α with a lip depth 'ZL'.	

Program TRAJEC starts the trajectory calculation at position ZI, RI input by the user. ZI is the upstream distance at which the particle is moving with the stream and is usually at least 5 radii from the sampling head. RI is the radial position to start the process to find RC, the radial position of limiting trajectory at ZI. If the trajectory of the particle starting at position RI enters the probe then the next trajectory is started from a position $RI = RI + DR$, where DR is a preselected radial increment. If the trajectory from RI escapes the sampler then the new RI is given by $RI - DR$. This process continues until the trajectories from successive radial positions alternate (i.e., one gets captured and another escapes). This process is repeated with successive halving of DR until the radial positions RES (at which the particle escapes) and RCA (at which the particle gets captured) are within a preselected tolerance EPP.

To calculate the trajectory accurately it is necessary that the time or space step is not very large. This is accomplished by taking the ratio RAT of predicted radial position RP to initial radial position R0. If the ratio RAT is greater than a prespecified value CAT then the time/space step is halved and recalculation starts. The value of CAT used in the program is 1.05. Even with a step size that satisfies the ratio test if the iterative convergence fails within LIMIT iteration then the step size is halved and the calculation procedure is restarted. The origin of the coordinate system lies at the center of the sampling head. The Z axis is along the centerline and R axis along the face plane. The efficiency calculation is performed for IST number of particles.

Subroutine FCT calculates the derivatives of the velocities at a given position R, Z. When NDIM option of 2 is used, the fluid velocity can be calculated at any given point but for option 0 and 1 the velocities are available only at the grid points and interpolation is needed. Subroutine INTERP performs the interpolation and computes the fluid velocity at a given particle location. A two-dimensional linear interpolation is used.

Subroutine OUTP prints the particle position at various time intervals. The printing interval INT is chosen by the user. For example, when $INT = 50$, the result is printed once in every 50 steps. Subroutine OUTP also tests for the deposition, capture or escape, of particle from the sampler and is indicated by KODE. When $KODE = 0$, particle is escaped and when 1 particle is captured, $KODE = 2$ indicates that particle has deposited on the sampler wall.

Subroutine BIAS calculates the actual size distribution from the measured size distribution. It uses the efficiency calculated by the program INER. The Stokes number of a given particle K is also calculated by BIAS. The measured fraction PF, particle size P, relaxation time TAU are input to the subroutine BIAS. The maximum number of particle intervals that can be used is 10.

A computer listing of the program is provided in Appendix D. The users manual and an example problem is provided in Appendix E.

LIMITATIONS OF THE MODEL

- (1) The model uses inviscid flow pattern around the sampler to compute particle trajectories. Close to the sampler wall the effect of boundary layer dominates the flow pattern and modifies the particle trajectories.
- (2) The error in collection efficiency for particles with much smaller Stokes number K (<0.001) is high when using the flow field option NDIM=2. The main cause of the error is the deviation of the model flow lines to the actual flow lines.
- (3) The effect of the physical presence of sampler and inlet geometry are not incorporated in the model for angular orientations of the sampler (option NDIM=2).

RESULTS AND DISCUSSION

Even though there are a number of theoretical and empirical models available to estimate the sampling errors due to anisokinetic sampling they fail to account for the effect of sampler orientation. The major difficulty in incorporating the effect of orientation is solving the flow field. This is circumvented by approximating the flow field around the sampling head with a two-dimensional line sink superposed on uniform flow. Such an assumption will render the exact flow field when the sampler inlet is a slit but for other inlet geometries the assumption is valid in the core region of the inlets. Even with such a simple model, one can gain a physical insight to the effect of sample orientation.

The computer program system was used to obtain the sampling bias for various particles when sampled by a thin-walled circular tube. Sampler inlet geometry of thin-walled circular tube approximates the flow around the vicinity of the closed face filter used in personal sampling. The velocity ratios used are: 1.2; 2.0; 0.75; 0.375; 0.1875; and 0.0938.

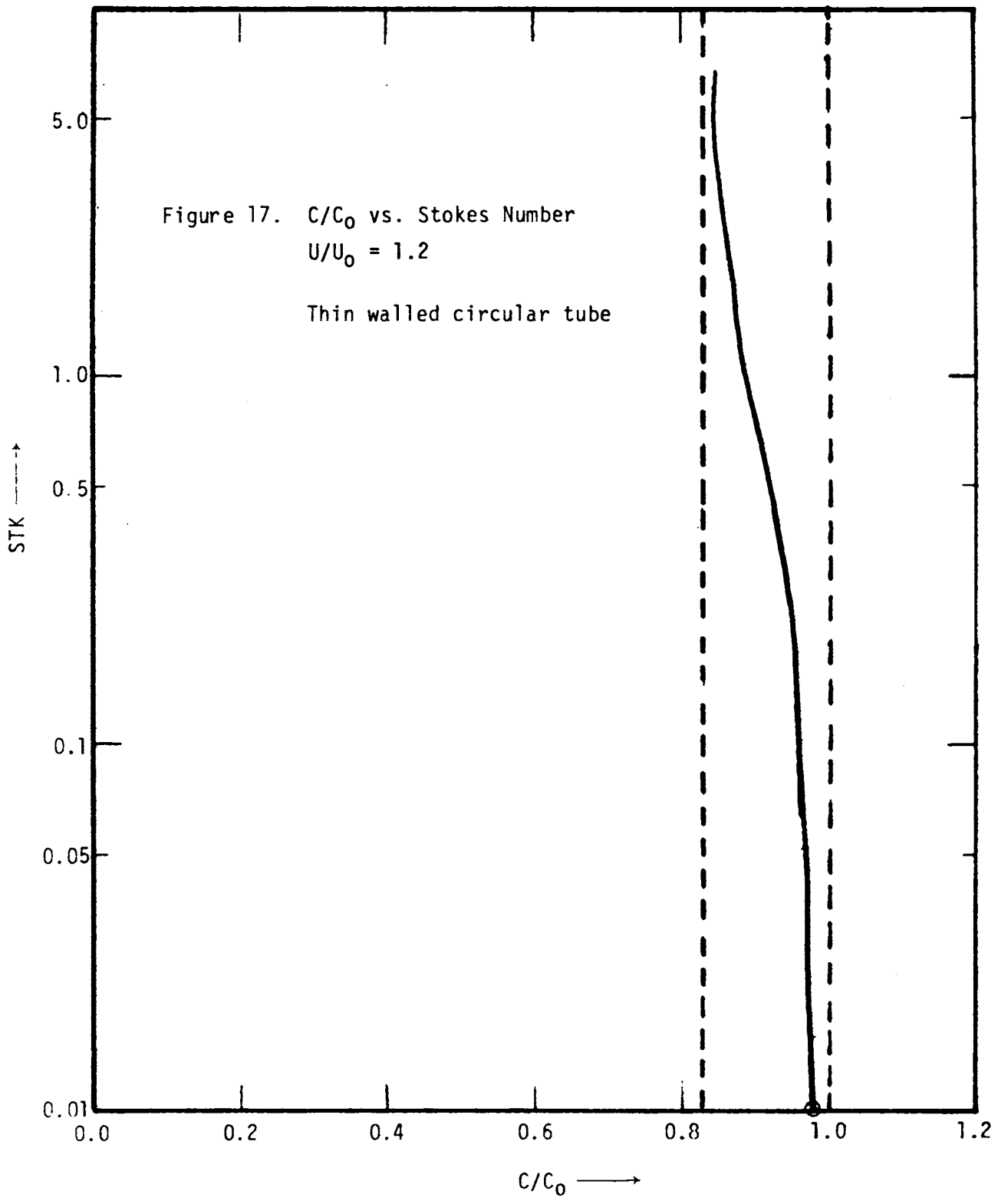
The concentration ratios were calculated at least at 8 Stokes numbers K . The results are given in Figures 17-22. The X axis represents the ratio of measured concentration C /actual concentration C_0 . The Y axis represents particle Stokes number K . For all the cases sedimentation and electrostatic effect has been neglected.

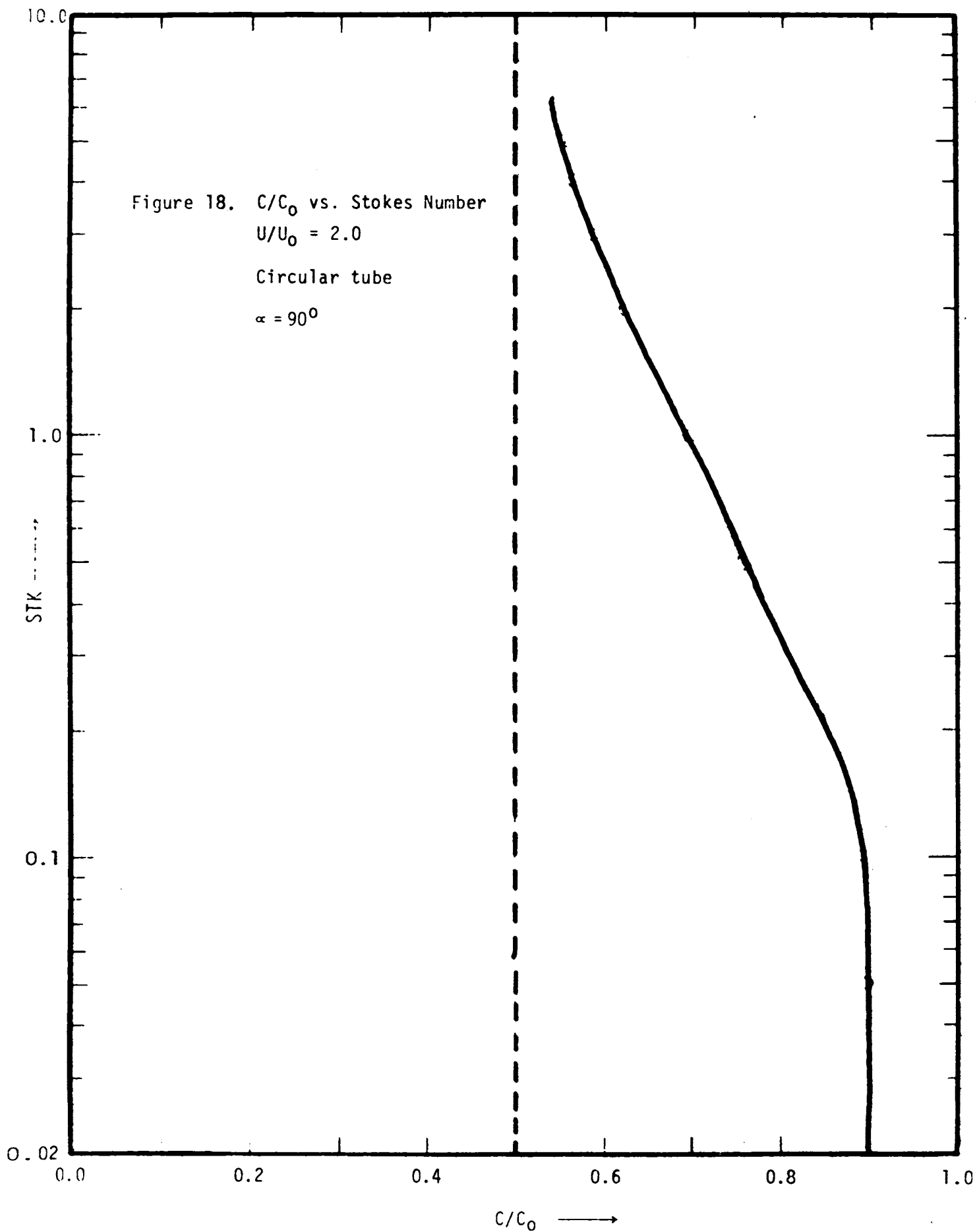
Particles with negligible inertia ($K \rightarrow 0$) move with the fluid stream, thus the concentration ratio C/C_0 approaches unity. But particles with infinite inertia ($K \rightarrow \infty$) continue in their original direction of motion and the concentration ratio C/C_0 approaches the velocity ratio U_0/U .

At velocity ratios close to one such as 1.2 or 0.75, the maximum error in concentration measurement is approximately 30%. But at extreme velocity ratios the error becomes as high as 100% for super isokinetic velocity ratios (>1) and infinite at subisokinetic velocity ratios (<1). Hence, sampling error for subisokinetic velocity ratios are more important and significant than the error for superisokinetic velocity ratios.

For the case of open-faced filter sampling, flow field option of NDIM=2 was used. In calculating the limiting trajectory of particles, the filter cassette was considered to have a lip depth of $0.2 \times$ radius. The sampling bias for various particles when sampled at an angle α to the oncoming stream was calculated for a velocity ratio of 0.375.

Figures 23 through 27 show the trajectory of particles when sampled at a velocity ratio of 0.375. Effect of Stokes number of the particle trajectory is shown in Figures 23 through 25 at the orientation angle of 90° . Flat trajectories are characteristic of large Stokes number K . Figures 26 and 27





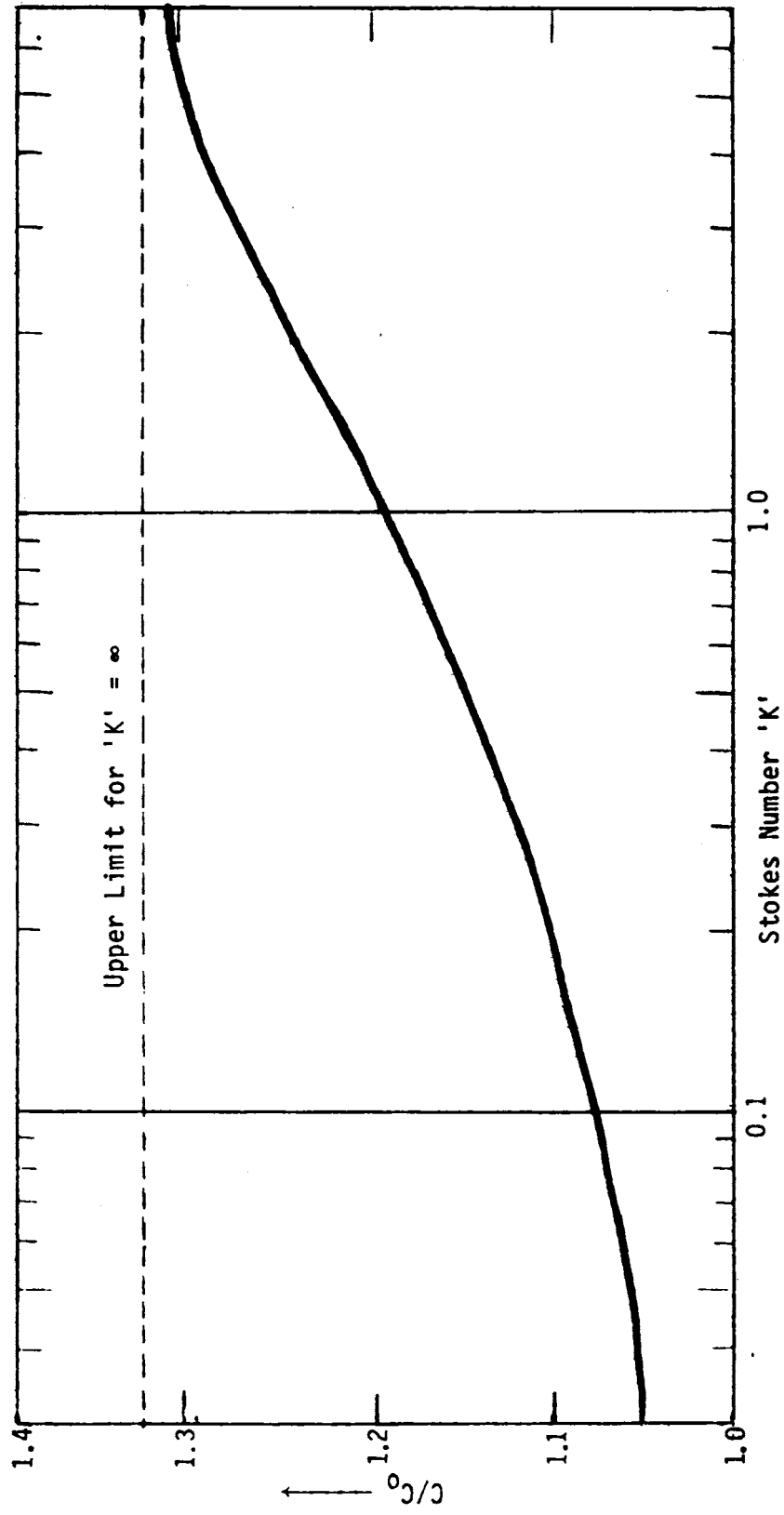


Figure 19. Sampling bias for a thin-walled circular tube facing the stream velocity ratio = 0.75.

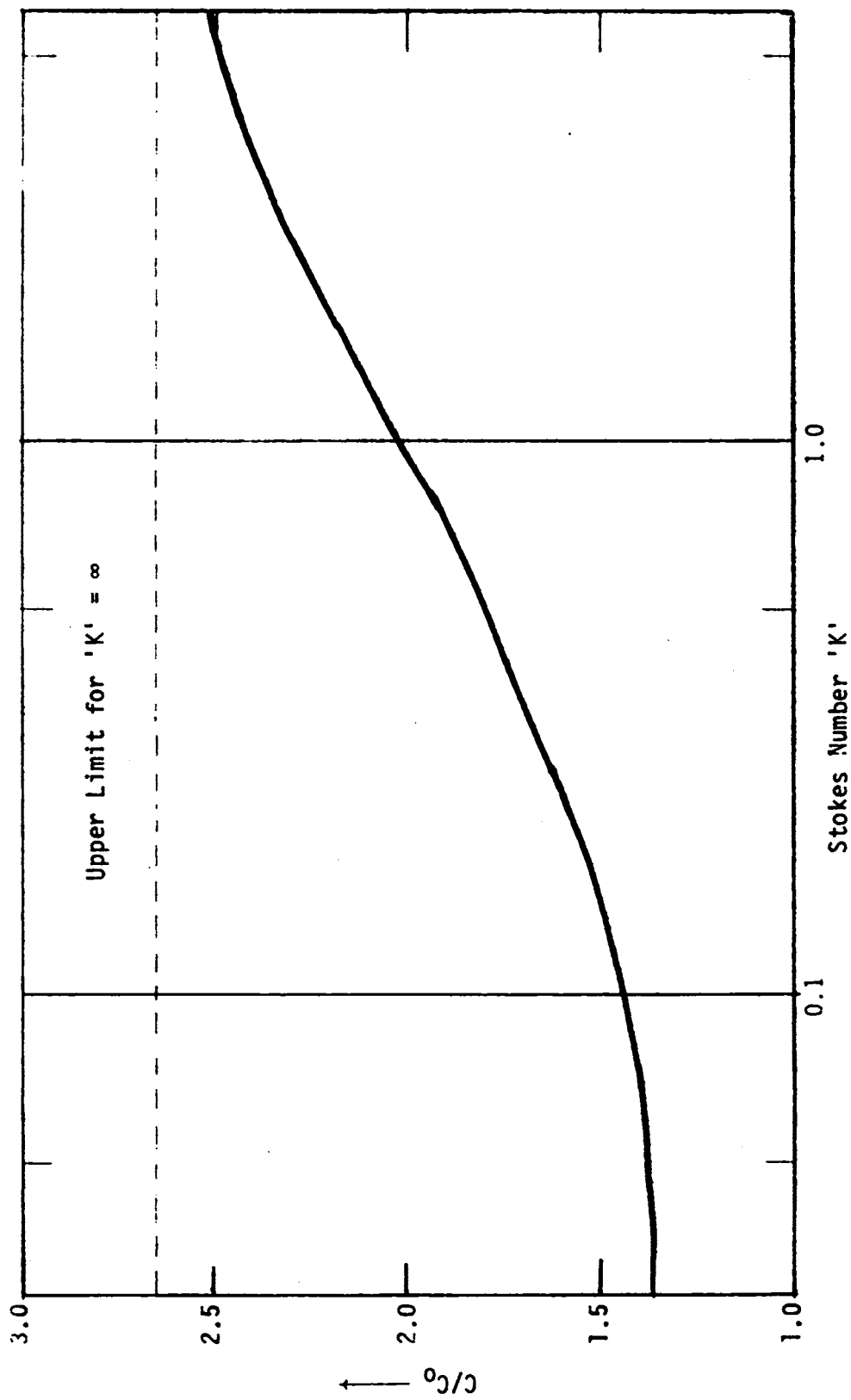


Figure 20. Sampling bias for a thin-walled circular tube facing the stream velocity ratio = 0.375.

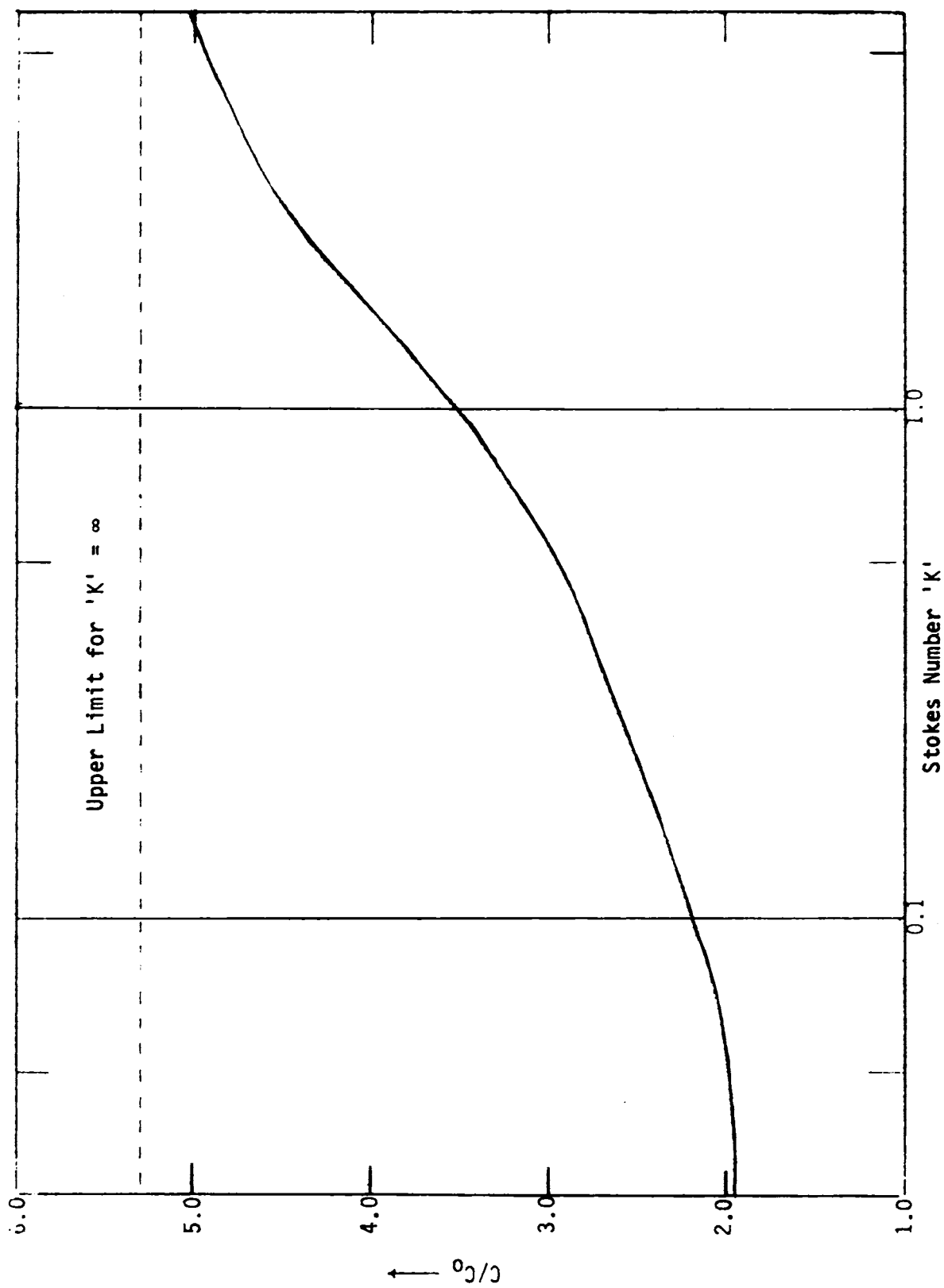


Figure 21. Sampling bias for a thin-walled circular tube facing the stream velocity ratio = 0.1875.

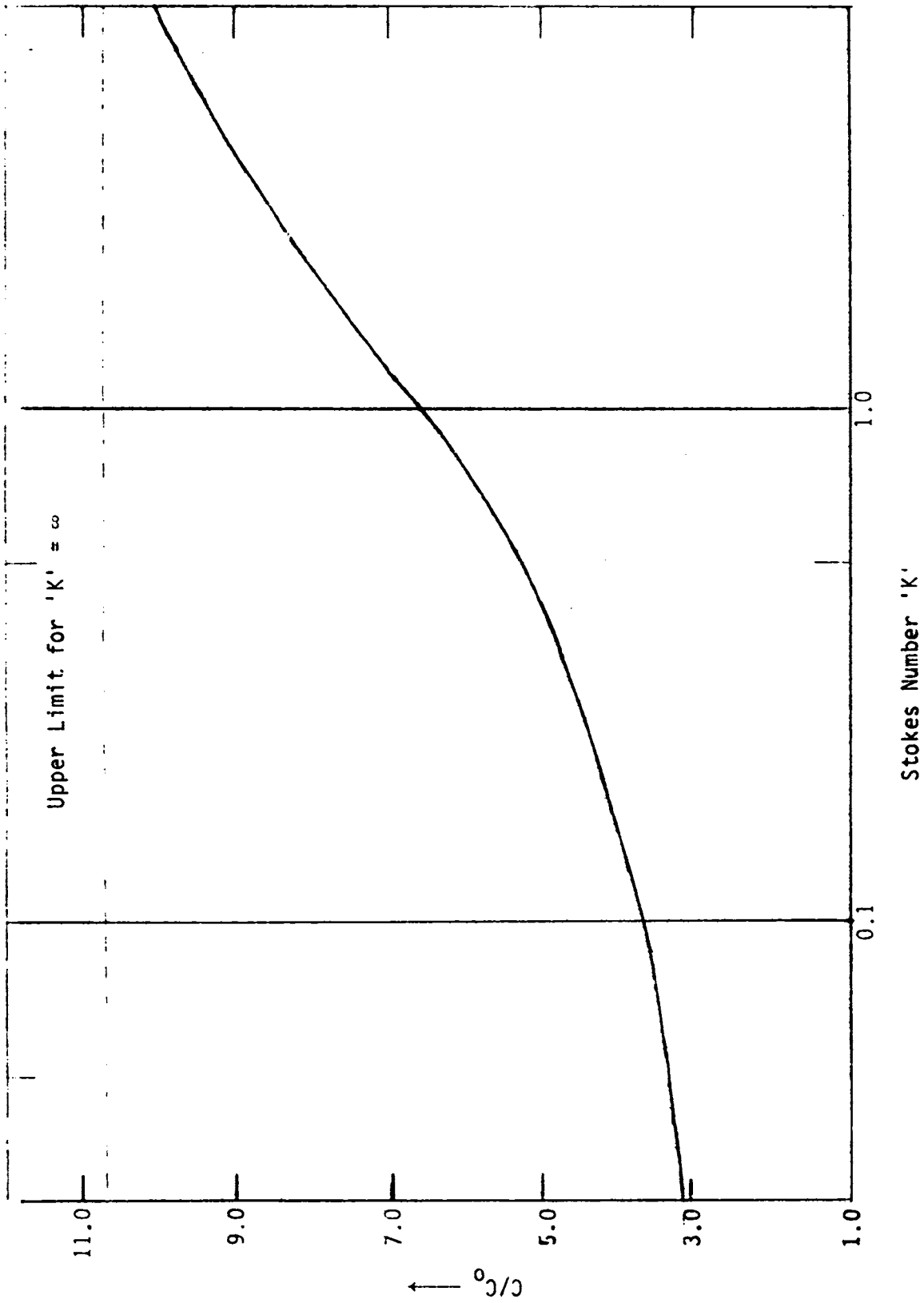


Figure 22. Sampling bias for thin-walled circular tube facing the stream velocity ratio = 0.0938.

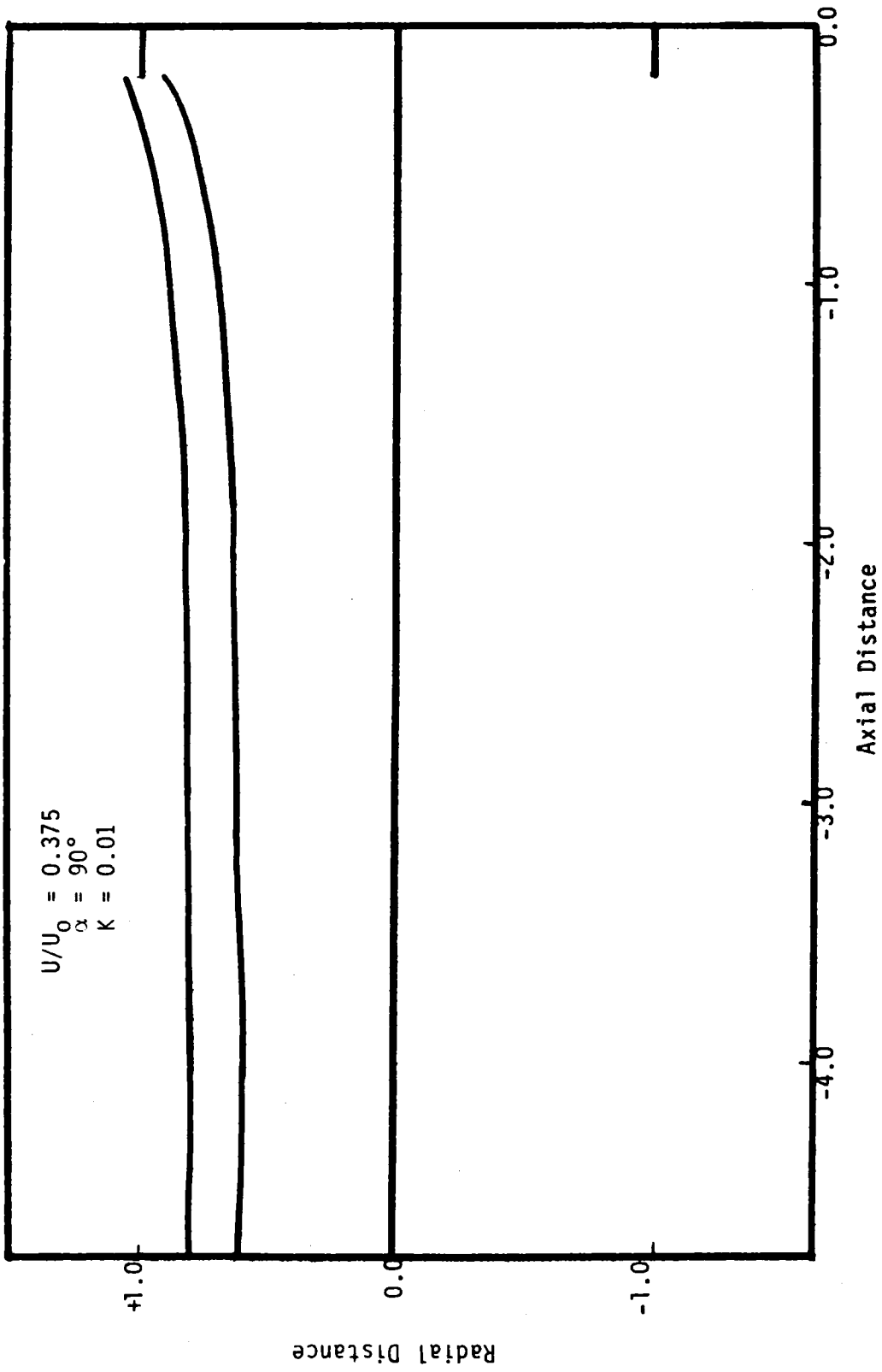


Figure 23. Trajectory of particles.

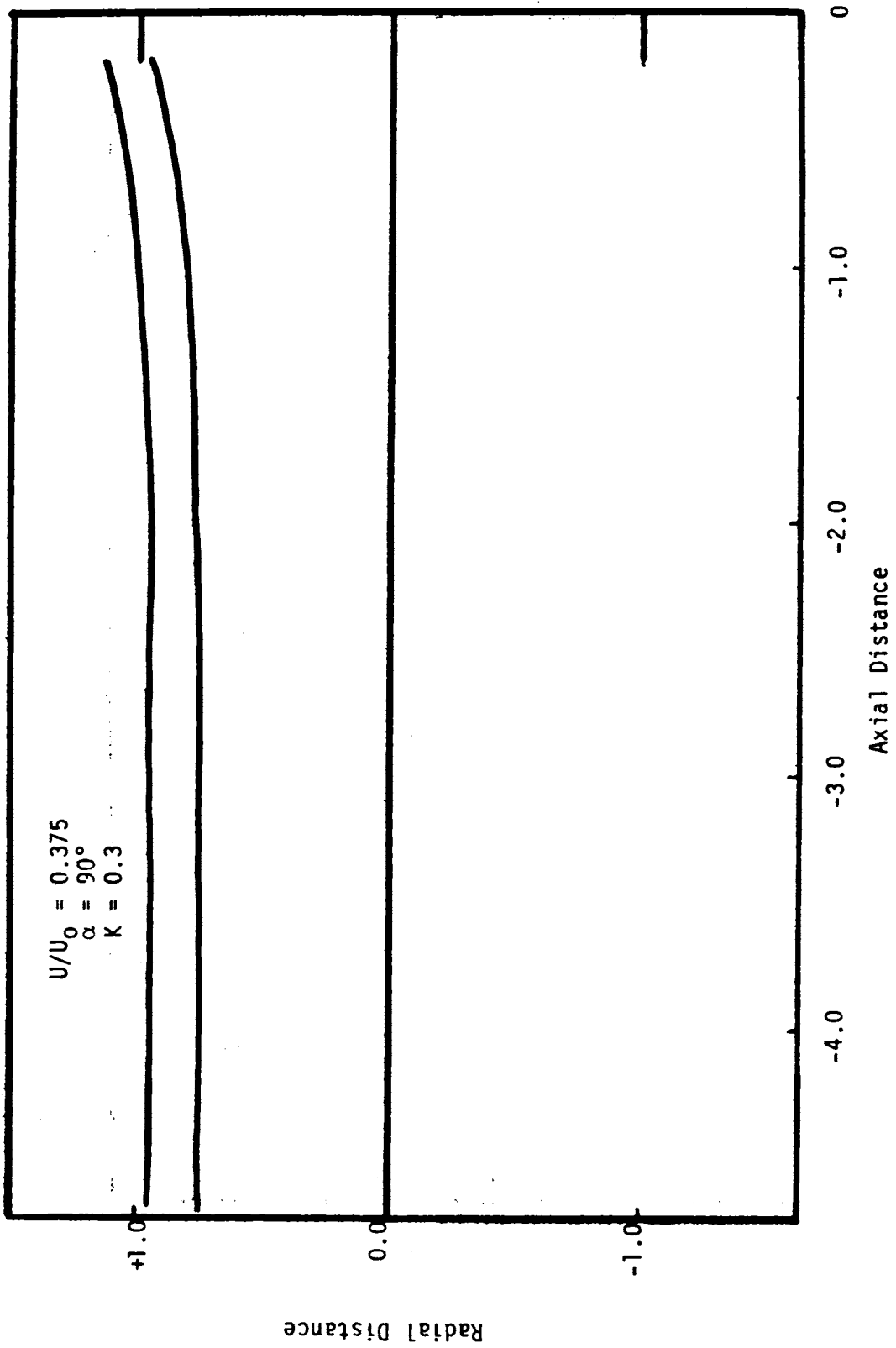


Figure 24. Trajectory of particles.

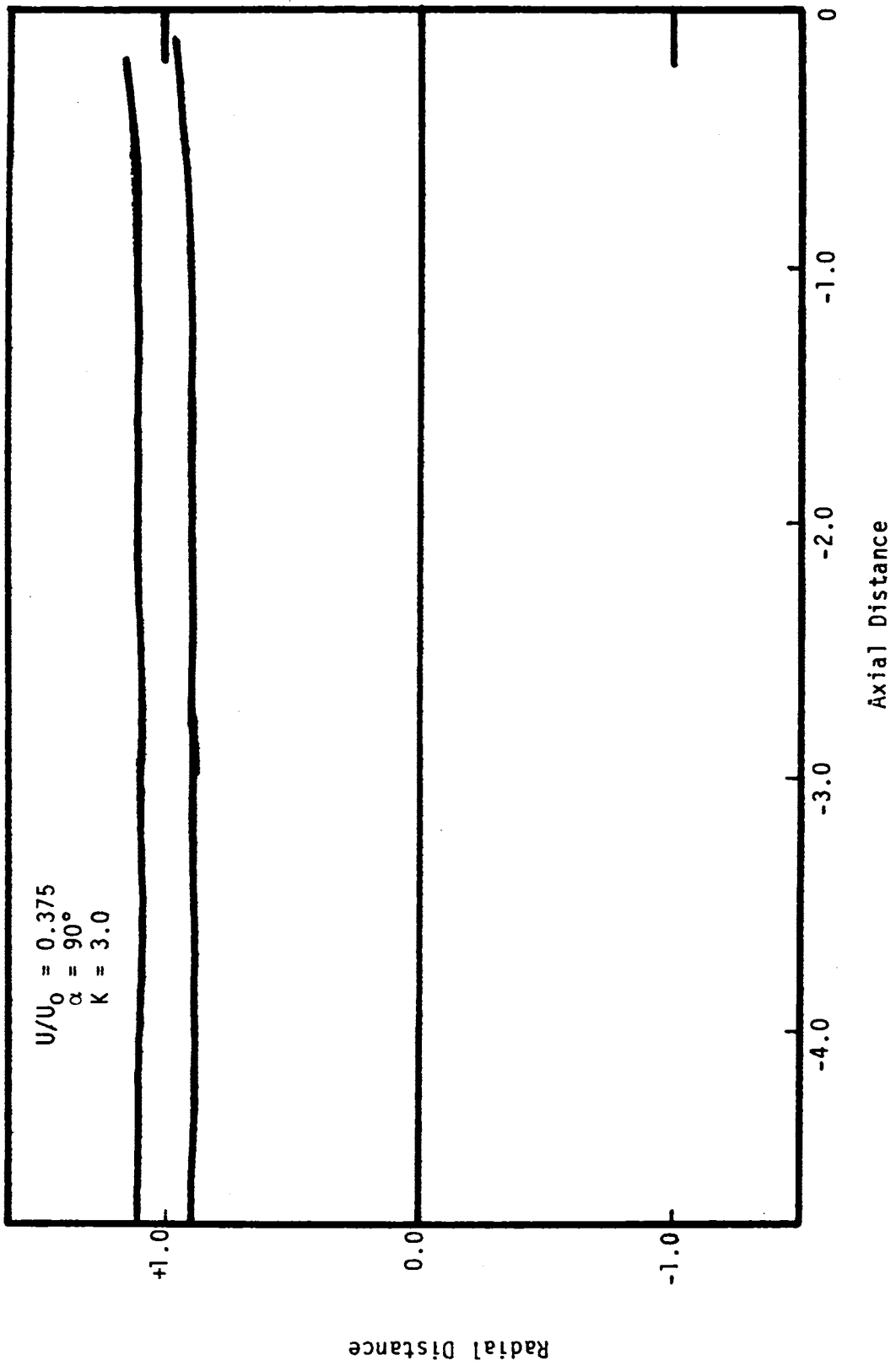


Figure 25. Trajectory of particles.

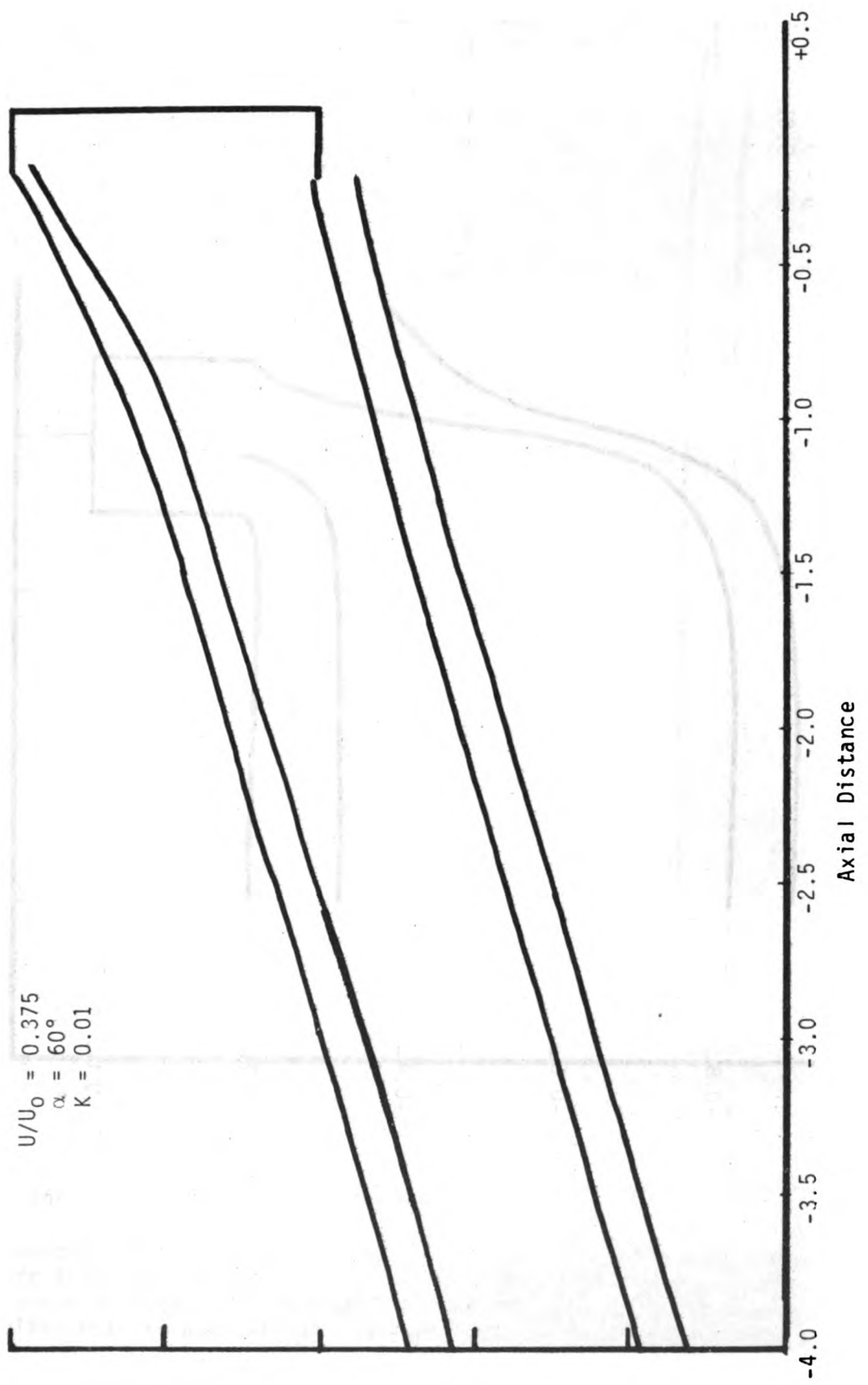


Figure 26. Trajectory of particles.

$U/U_0 = 0.375$
 $\alpha = 0^\circ$
 $K = 0.01$

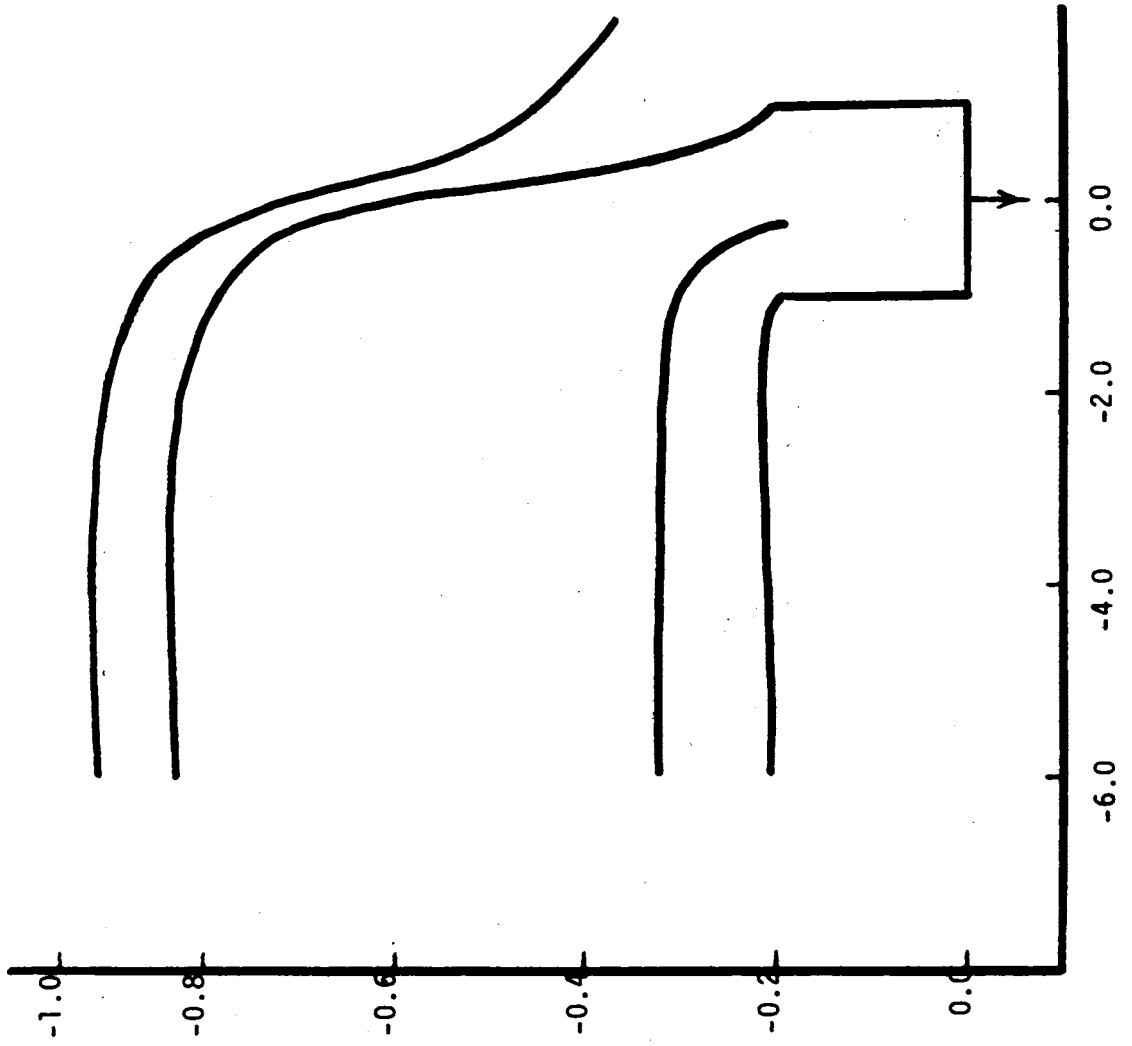


Figure 27. Trajectory of particles

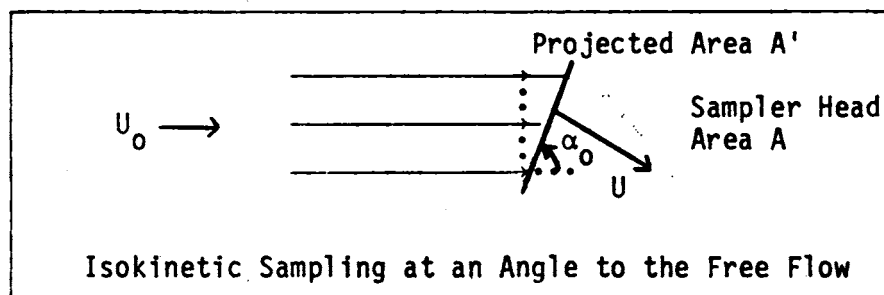
show the trajectory of a particle of Stokes number 0.01 at the orientation angles of 60° and 0° , respectively.

Figure 28 shows the efficiency of sampling of various particles at different orientation angles. The velocity ratio is 0.375. The theoretical limits of efficiency for Stokes numbers of ∞ and 0 are shown in solid lines. The experimental values of efficiency for a particle of Stokes number 0.553, as obtained by G.S. Raynor³⁰ is also shown. The values predicted by the current model are higher than the experimental values. The reason for over estimation is probably due to effects such as particle bounce-off, flow turbulence, etc.

Figure 28 predicts that there is an angular orientation α_0 at which all the particles are sampled isokinetically.

$$\sin \alpha_0 = U/U_0 \quad (83)$$

This holds only when the sampler wall is very thin and the sampler body doesn't affect the flow.



The physical meaning of equation (83) is that the correct tilt of the sampler α_0 can reduce the volume of air sampled to compensate for sampling velocities $U < U_0$. Isokinetic sampling happens in general when the volume of fluid incident on the sampler cross-section equals the volume of fluid sampled:

$$V_i = V_s$$

where $V_i = U_0 A'$ (a)

$$V_s = UA$$

A' is the projection of A on the plane perpendicular to the free flow, as shown in the figure. Therefore,

$$A' = A \sin \alpha_0. \quad (b)$$

Equation (83) is derived by substituting (a) into (b).

The sampling bias for various particles, when sampled anisokinetically by a square inlet was obtained by use of the computer program system. The results are shown in Figures 29 through 33. The flow field in the vicinity of the sampling head is approximated by superimposing a two-dimensional uniform flow

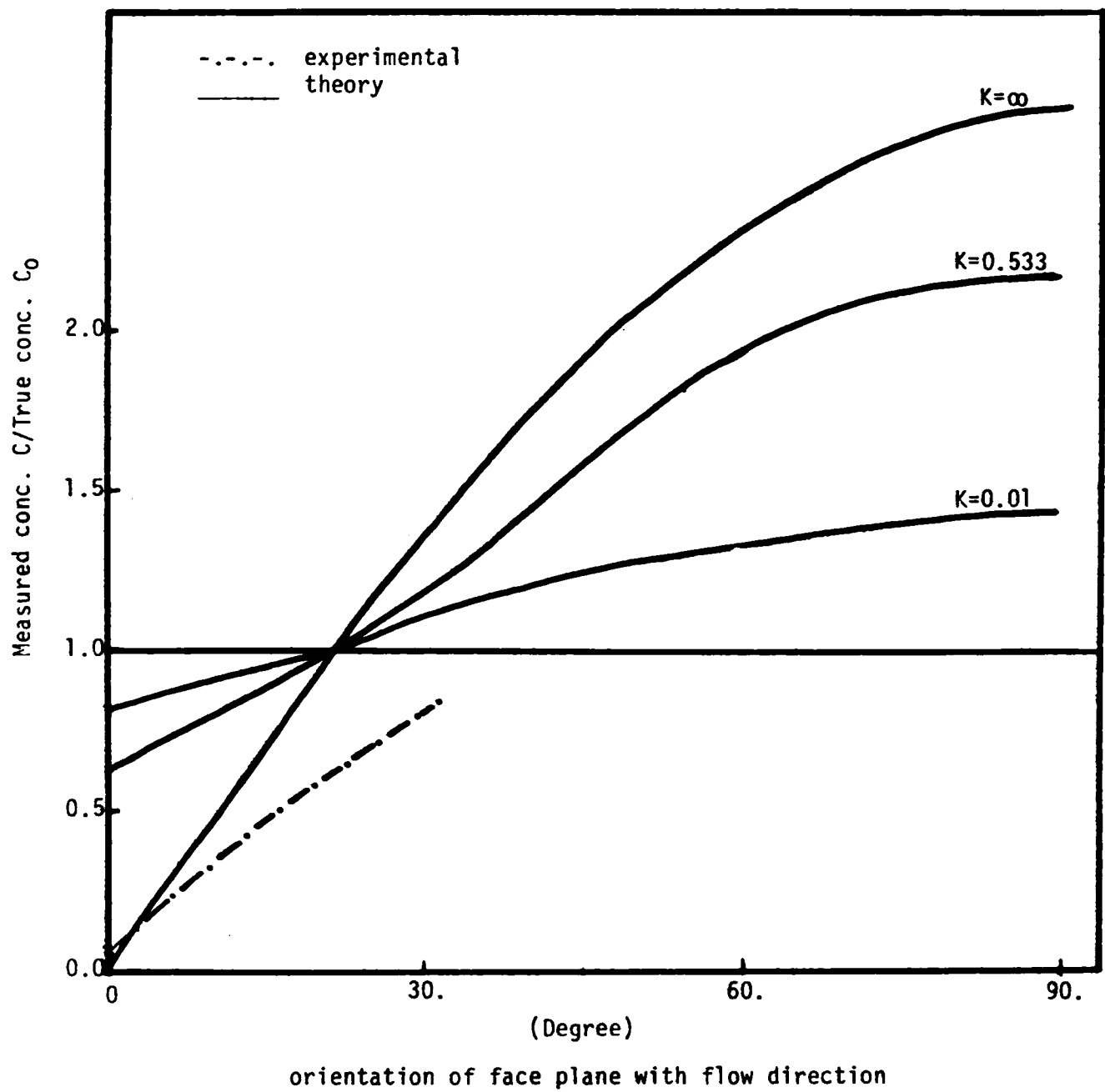


Figure 28. C/C_0 vs. orientation angle for $U/U_0 = 0.375$ and lip depth is 0.2.

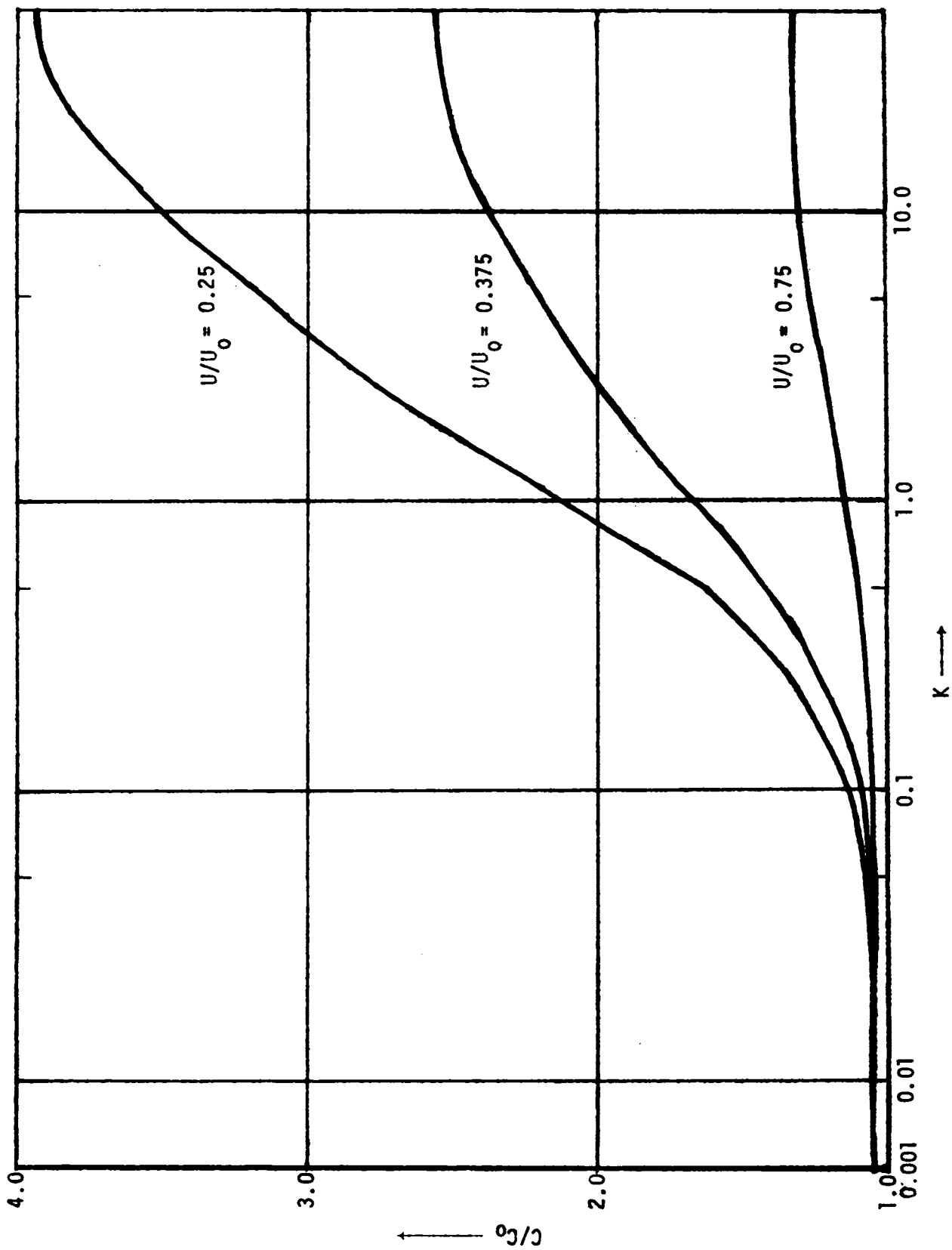


Figure 29. C/C_0 vs. K for $\alpha = 90^\circ$ square inlet, ZLIP = 0.

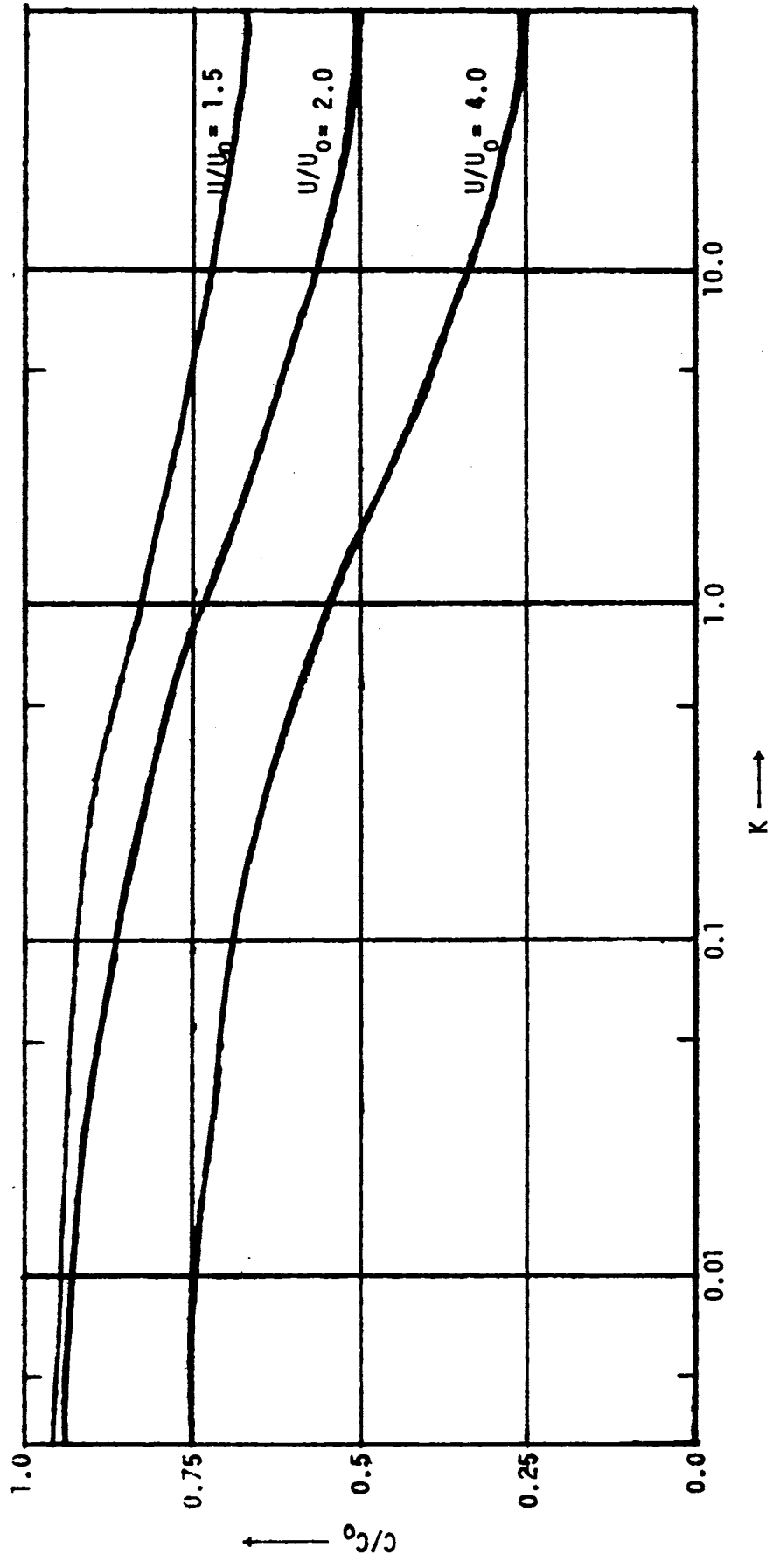


Figure 30. C/C_0 vs. K for $\alpha = 90^\circ$ square inlet, $ZLIP = 0$.

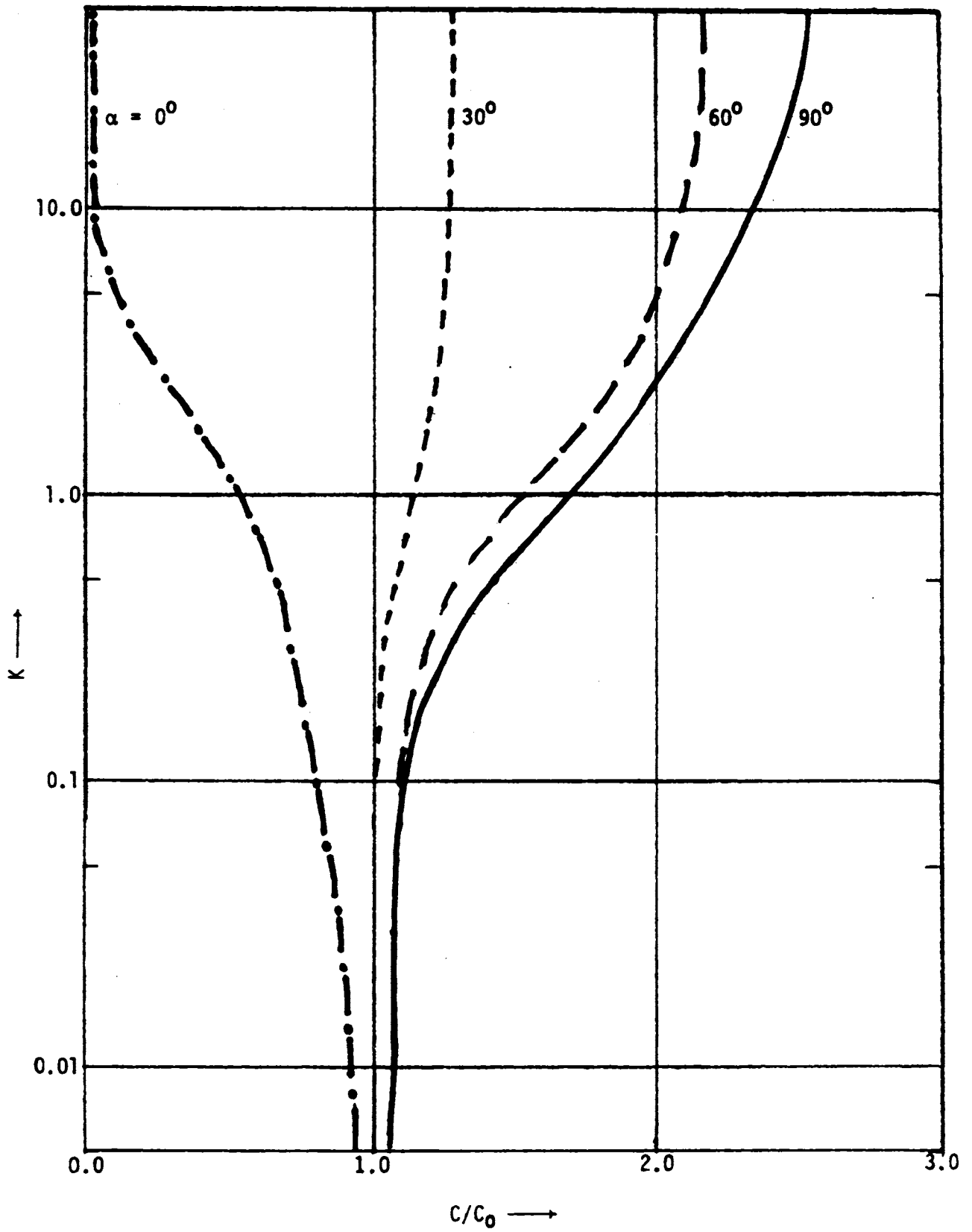


Figure 31. K vs. C/C_0 for $U/U_0 = 0.375$ square inlet, $ZLIP = 0$.

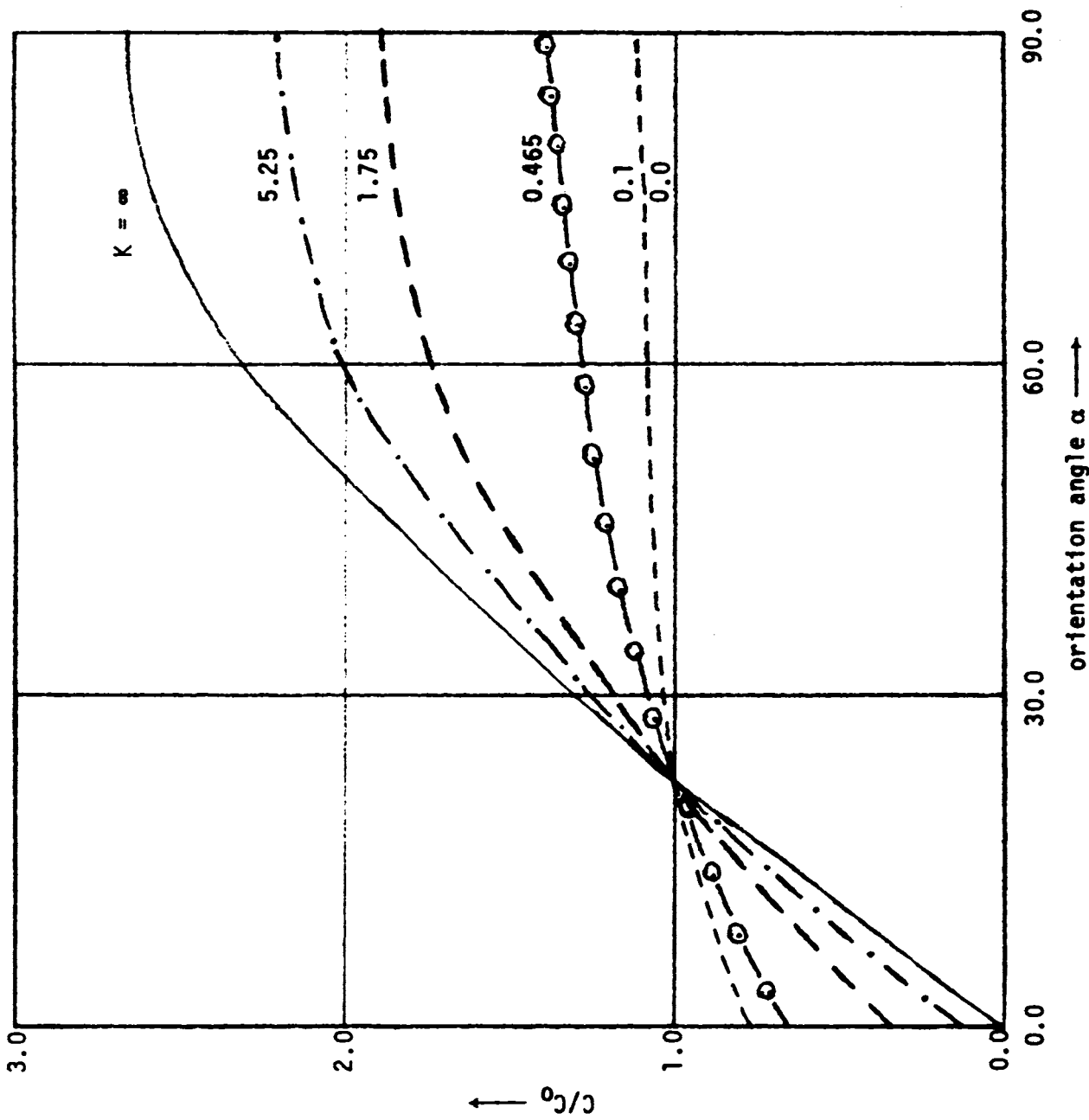


Figure 32. C/C_0 vs. α for $U/U_0 = 0.375$ square inlet, $ZLIP = 0$.

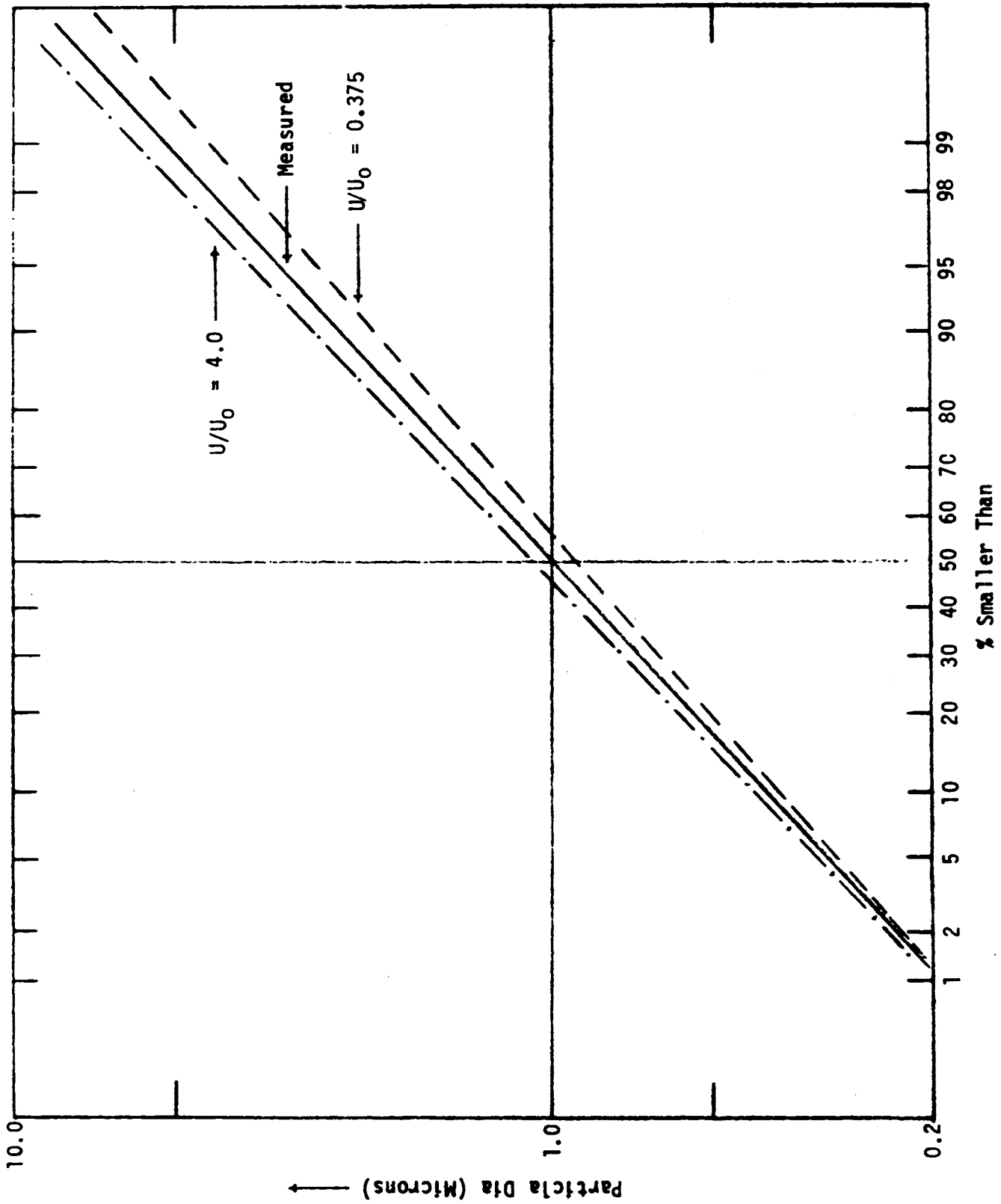


Figure 33. Effect of Bias on the Distribution $\alpha = 90^\circ$, square inlet, ZLIP = 0.

with a line sink located at the face of the inlet (NDIM=2). The lip length ZLIP is assumed to be 0 and α the orientation angle is 90° .

Figures 29 and 30 show the plot of the ratio C/C_0 vs. K for various values of the velocity ratio U . At lower Stokes numbers the value of C/C_0 approaches 1 indicating that the measured concentration C is the same as the true concentration C_0 . This is true even in the case of extreme velocity ratios of $U=0.25$ and 4.0 . At higher Stokes number values, the concentration ratio reaches the asymptotic limit of $1/U$.

Figure 31 shows the plot of C/C_0 vs. K for various orientation angles α . When α equals 90° the sampler faces the oncoming stream and when α equals 0° the face plane of the sampling head is tangential to the oncoming stream. For low Stokes number values, the angular orientation seems to be immaterial. The asymptotic value for the larger Stokes number is $\sin \alpha/U$. Figure 32 presents the plot of C/C_0 vs. α for various values of K . The curves for K equal to zero and K equal to ∞ are also known.

Figure 33 shows the effect of sampling bias on the cumulative size distribution for two velocity ratios. The measured distribution with the anisokinetic velocity ratio is assumed to be a lognormal distribution with a σ of 2.0. The corrected "True" distribution for various values of U is shown.

Figure 34 shows the effect of sampling bias as a function of velocity ratio for various Stokes numbers K . For smaller Stokes numbers such as 0.1, the ratio C/C_0 remains close to 1 even at extreme velocity ratios. For large Stokes numbers, $K = 10$ the curve approaches the asymptotic limit for $K = \infty$, i.e., $C/C_0 = U_0/U$.

The effect of wall thickness of the sampler on the sampling bias was determined for a circular tube. The flow field was obtained with option NDIM=1. The sampler was assumed to be facing the stream. A velocity ratio of 0.375 was used. The maximum value of W the wall thickness used was $0.2 \times$ radius. Figure 35 presents the results. As W increases, the sampling bias decreases. The reason for this is that the velocity ratio of 0.375 makes the stream lines move away from the center of the sampler, whereas the effect of wall thickness is to move the stream lines toward the center thereby nullifying the effect of an anisokinetic velocity ratio to a certain extent.

The present model was used to compare with the experimental results of Badzioch³¹ for a circular tube inlet. The comparison is shown in Figure 36. Theory agrees very well with the experimental data. Here the Stokes number of the particle used is 10.5 which is very much larger than usual values encountered in personal sampling conditions. Experimental data for lower Stokes numbers are not available at present.

For the physical conditions encountered in personal sampling the Stokes number of particles in the respirable range is much smaller than unity. Typically, for a $10\mu\text{m}$, particle sampled with a tube of 1cm radius at a velocity of 100 cm/sec the Stokes number K is on the order of 3.1×10^{-2} . Particles with

such a small Stokes number will follow the fluid stream lines even if the curvature of the stream line is quite high. So the anisokinetic velocity ratio or the inlet geometry is not expected to play a major role in influencing the collection efficiency.

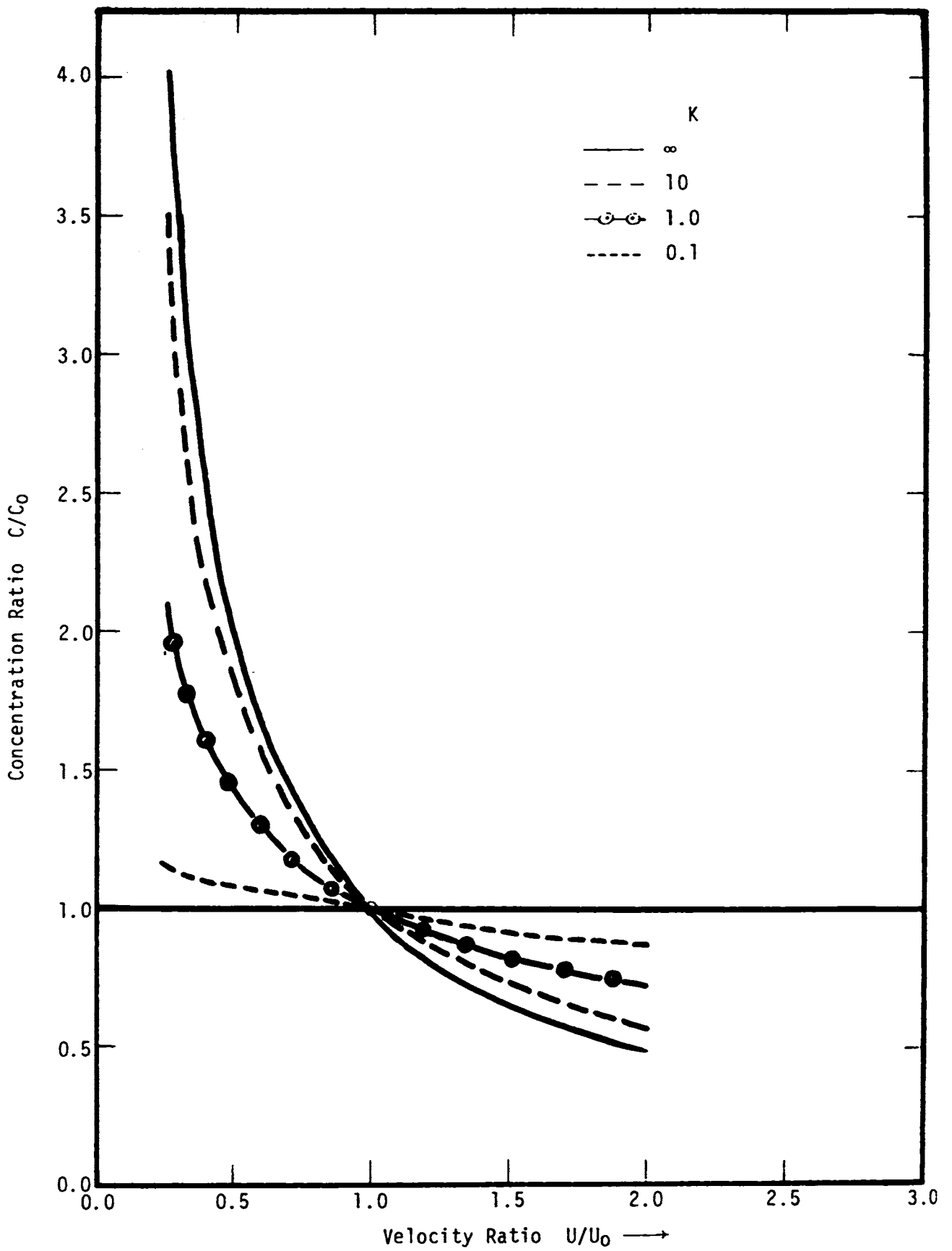


Figure 34. C/C_0 vs. U/U_0 for Square Inlet Facing the Stream.

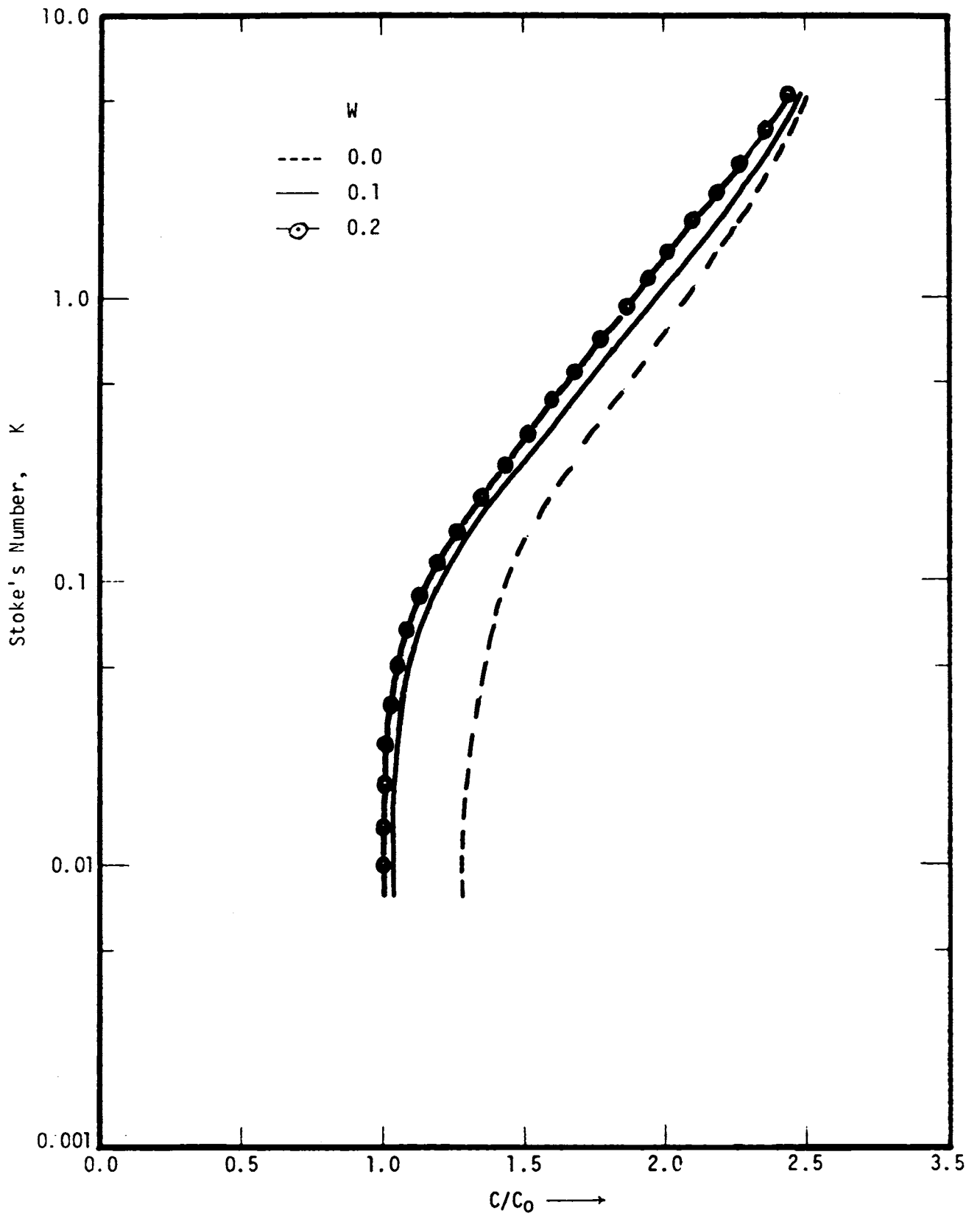


Figure 35. C/C_0 vs. K for Various Thickness of Wall with Circular Inlet Facing the Stream $U/U_0 = 0.375$

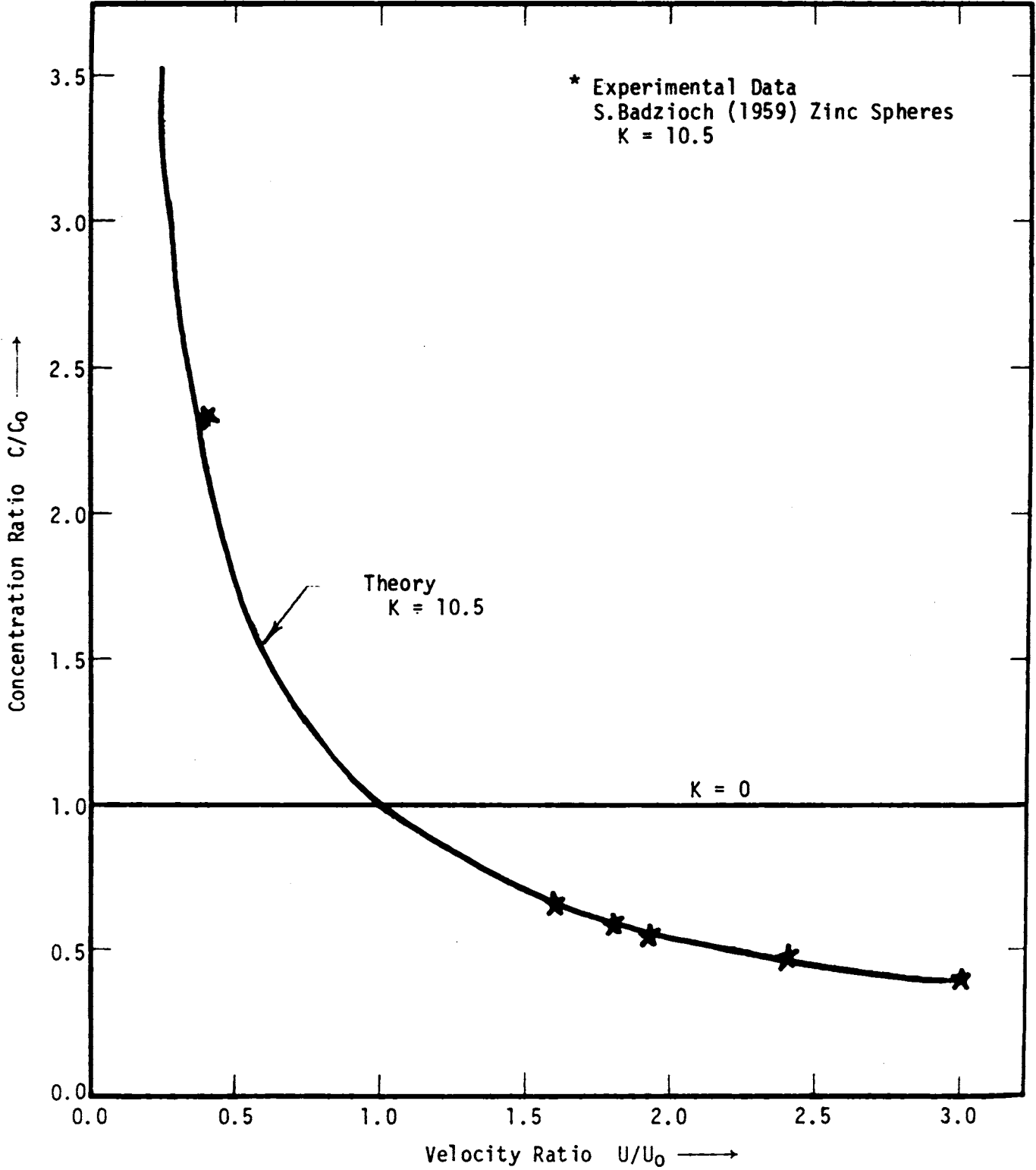


Figure 36. Comparison of Theoretical Results with Experimental Data of S. Badzioch (1959). Circular Tube Facing the Stream.

CONCLUSIONS

There exists a complete lack of purely theoretical investigations on the effects of sampler orientation and the effects of sampler head. The present research demonstrates the feasibility of such a study. The conclusions from the results of this study are summarized below.

- (1) The actual fluid flow patterns encountered around two-dimensional or axisymmetrical inlet geometries can be obtained. The flow around a square inlet presents a formidable problem and approximations are necessary to obtain flow patterns.
- (2) Anisokinetic sampling errors are more important and significant for subsokinetic velocity ratios ($U/U_0 < 1$) than for supersokinetic velocity ratios ($U/U_0 > 1$).
- (3) Theoretical error estimates may be regarded as upper limits. The actual error is lower due to turbulence, particle bounce-off, and variability of drag on the particles.
- (4) For subsokinetic sampling ($U/U_0 < 1$) the sampler wall thickness has a counter effect on the sampling bias.
- (5) Sampling bias for polydispersed aerosols can be obtained by use of number of monodisperse aerosols.
- (6) The experimental data available for circular inlets compare very well with the theoretical collection efficiencies.
- (7) For cases when the sampler is oriented at an angle to the stream, the exact solution to the flow field is very difficult to obtain and approximations are necessary. A line sink was used in the present model.
- (8) Sampling efficiencies obtained for angular orientations compare well with the presently available experimental data. But expanded experimental data are needed to ascertain the reliability of the model.
- (9) It is very difficult to arrive at a single or a multiple optimum inlet geometries because of the variety of factors that influence the particle collection. For the physical conditions encountered in personal sampling, the inlet geometry is not expected to play a major role in influencing the collection efficiency.

- (10) The major difficulty in evaluating various inlet geometries is obtaining the flow field around the sampler. Experimentally determined flow field can be used with the particle motion part of the program to accurately evaluate various inlets.

REFERENCES

1. Brady, W. and L. A. Touzalin, J. Ind. Eng. Chem., 3 :662 (1911).
2. Lappel, C. E. and C. B. Shepherd, J. Ind. Eng. Chem., 32:605 (1940).
3. Dalla Valle, J. M., Micrometrics, 2nd edition, Pitmann Publ. Corp. New York. (1948).
4. Watson, H. H., Amer. Ind. Hyg. Assoc. Quart., 15 :21 (1954).
5. Badzioch, S., British J. Of. App. Physics, 10, 10:26 (1959).
6. Badzioch, S., J. Inst. Fuel, 33, :106 (1960).
7. Levin, L. M., Izv. Adad. Nauk. Ser. Geoph, 7, :914 (1957).
8. Whiteley, A. B., and L. E. Reed., J. Inst. Fuel; 32:316
9. Glauberman, H., Amer. Ind. Hyg. Assoc. Quart, 23.235 (1962)
10. Vitols, V., Determination of Theoretical Collection Efficiency of Aspirated Particulate Matter Sampling Probes Under Anisokinetic Flow, Ph.D. Thesis, University of Michigan (1964).
11. Vitols, V., J. Air. Poll. Con. Assoc., 16:2, :79-84 (1966).
12. Davies, C. N., Staub Reinhalt, Luft (English), 28:6, :1-9, (1968).
13. Davies, C. N., Dust is Dangerous, Faber London, P. 21, (1954).
14. Belyave, S.P., and L. M. Levin, J. Aero. Sci., 5, :325, (1974).
15. Belyave, S.P., and L. M. Levin, J. Aero. Sci., 3, :127, (1972).
16. Levin, L. M., "Studies on coarsely dispersed aerosols", P. 3, Acad. Sci., U.S.S.R. (1961).
17. Fuchs, N. A., Atmos. Envir., 9, :697, (1975).
18. Gooddale, T. C., B. M. Carder, E. C. Evans, Ind. Hyg. Quart, 13.4, :226 (1952).

REFERENCES (continued)

19. Schmel, G. A., Amer. Ind. Hyg. Assoc. J. 31:758 (1970).
20. Carson, G. A., Ashrae Journal, :45-49, May (1974).
21. Bien, C. T., and Morton Corn, Amer. Ind. Hyg. Assoc. J., 32:7, :453, (1971).
22. Pickett, W. E., and E. B. Sansone, Amer. Ind. Hyg. Assoc. J., 34, :421, (1973).
23. Davies, C. N., Amer. Ind. Hyg. Assoc. J., 36:9, :714, (1975).
24. Strom, L., Atmos. Envir. 6 :133 (1972)
25. Myres, G. E., Amer. Ind. Hyg. Assoc. J., 35:307 (1974).
26. Breslin, J. A., and R. L. Stein, Amer. Ind. Hyg. Assoc. J. 36 :576, (1975)
27. Lundgren, D., and S. Calvert, Amer. Ind. Hyg. Assoc. J. 28: 208 (1967).
28. Roache, P. J., Computational Fluid Dynamics, Hamosa Publication, N.M., (1971).
29. Southwell, R.V., and G. Vaisey, Phil. Trans. Roy. Soc., A 240, :177, (1946).
30. Raynor, G.S., Amer. Ind. Hyg. Assoc. J. 31:294 (1970).
31. Fuchs, N. A., Mechanics of Aerosols, Macmillan Company, N.Y., (1964).
32. Hidy, G.M. and J.R. Brock, Dynamics of Aerocolloidal Systems, Pergamon Press (1970).
33. Davies, C. N., Aerosol Science, Academic Press, N.Y., (1966).
34. Milne-Thomson, L. M., Theoretical Hydrodynamics, 5th ed., Macmillan Company, N.Y., (1968).
35. Schlichting, H., Boundary Layer Theory, 4th edition, McGraw Hill, N.Y., (1960).

REFERENCES (continued)

36. Agarwal, J. K. Aerosol Sampling and Transport. Ph.D. Thesis, University of Minnesota (1975).
37. Ter Kuile, W. M., "Comparable Dust Sampling at the Work Place," Report F 1699, Instituut Vook Milieuhygiene en Gezondheidstechniek, Postbus 214

Appendix A. Derivation of Boundary Condition at Section II

Circular Tube

Using continuity of flow at Sections I and II

$$\frac{1}{2} U_I R_0^2 - \frac{1}{2} UR^2 = \frac{1}{2} U_0 R_0^2 - \frac{1}{2} U_0 (R + W)^2$$

so

$$U_0 = \frac{U_I R_0^2 - UR^2}{R_0^2 - (R + W)^2}$$

denoting the stream function outside the probe at Section II ψ_{op} then

$$\psi_{op} = \frac{1}{2} U_0 r^2 + C$$

on the probe wall ψ is unique and ψ_{op} must be equal to ψ_{Ip} , the stream function inside the probe. So

$$\frac{1}{2} \frac{U_I R_0^2 - UR^2}{R_0^2 - (R + W)^2} (R + W)^2 + C = \frac{1}{2} UR^2$$

and C is given by

$$C = -\frac{1}{2} U_0 (R + W)^2 + \frac{1}{2} UR^2$$

∴

$$\psi_{op} = \frac{1}{2} \frac{U_I R_0^2 - UR^2}{[R_0^2 - (R + W)^2]} \cdot [r^2 - (R + W)^2] + \frac{1}{2} UR^2$$

$$(R + W) \leq r \leq R_0$$

in non-dimensional form

$$\psi_{op} = \frac{R_0^2 - U}{[R_0^2 - (1 + W)^2]} \cdot [r^2 - (1 + W)^2] + U$$

$$(1 + W) \leq r \leq R_0$$

Two Parallel Plates

Following similar procedure as before

$$U_0 = \frac{U_I Y_0 - UH}{Y_0 - (H + W)}$$

$$\psi_{op} = \frac{U_I Y_0 - UH}{[Y_0 - (H + W)]} \cdot [y - (H + W)] + UH$$

$$(H + W) \leq y \leq Y_0$$

In non-dimensional form

$$\psi_{op} = \frac{Y_0 - U}{[Y_0 - (1 + W)]} \cdot [y - (1 + W)] + U$$

$$(1 + W) \leq y \leq Y_0$$

Appendix B. Uniform Sink Strength Distribution

$$\psi_{\text{sink}} = -\int_0^d m \cdot dx_1 \cdot \theta$$

$$x_1 = x - y \cot \theta$$

$$dx_1 = y \operatorname{cosec}^2 \theta \cdot d\theta$$

$$\psi_{\text{sink}} = -\int_{\theta_1}^{\theta_2} m \cdot \theta \cdot \operatorname{cosec}^2 \theta \cdot d\theta \cdot y$$

$$= -my \left[\theta_1 \cdot \cot \theta_1 - \theta_2 \cdot \cot \theta_2 + \ln \frac{\sin \theta_2}{\sin \theta_1} \right]$$

$$\psi_{\text{sink}} = -m \left[\tan^{-1} \frac{y}{x} \cdot x - \tan^{-1} \frac{y}{x-d} \cdot (x-d) + y \cdot \ln \frac{\sqrt{x^2+y^2}}{\sqrt{(x-d)^2+y^2}} \right] \quad (\text{B1})$$

$\psi_{\text{U.F}}$ = ψ due to uniform stream

$$= U_I y \cos \alpha + U_I x \sin \alpha$$

$$\psi = \psi_{\text{sink}} + \psi_{\text{U.F}}$$

$$U_x = \frac{\partial \psi}{\partial y}$$

$$U_x = U_I \cos \alpha - m \ln \frac{\sqrt{x^2+y^2}}{\sqrt{(x-d)^2+y^2}} \quad (\text{B2})$$

$$U_y = -\frac{\partial \psi}{\partial x}$$

$$= -U_I \sin \alpha + m \left[-\frac{xy}{x^2+y^2} + \tan^{-1} \frac{y}{x} + \frac{(x-d)y}{(x-d)^2+y^2} - \tan^{-1} \frac{y}{(x-d)} \right. \\ \left. + \frac{xy}{x+y} - \frac{(x-d)y}{(x-d)^2+y^2} \right]$$

$$= -U_I \sin \alpha + m \left[\tan^{-1} \frac{y}{x} - \tan^{-1} \frac{y}{x-d} \right] \quad (\text{B3})$$

$$= U_I \sin \alpha + m(\theta_1 - \theta_2)$$

The sink strength m is given as follows

$$H \sin\alpha \cdot U_I + \pi dm = H \cdot U$$

$$\therefore m = \frac{U - \sin\alpha}{2\pi \cdot f} \quad (B4)$$

$$\text{where } f = \frac{d}{2H}$$

Appendix C. Triangular Sink Strength Distribution

$$\begin{aligned}
 m_{\xi} &= m \cdot \xi & 0 \leq \xi \leq \frac{d}{2} \\
 &= m (d-\xi) & \frac{d}{2} \leq \xi \leq d
 \end{aligned} \tag{C1}$$

$$\therefore \psi_{\text{sink}} = \int_0^d m_{\xi} \cdot \theta \cdot d\xi$$

$$\theta = \tan^{-1} \frac{y}{(x-\xi)} \quad \text{or} \quad \theta = \cot^{-1} \frac{(x-\xi)}{y}$$

$$\psi_{\text{source}} = \int_0^{d/2} m_{\xi} \cot^{-1} \frac{(x-\xi)}{y} \cdot d\xi + \int_{d/2}^d m(d-\xi) \cdot \cot^{-1} \frac{(x-\xi)}{y} \cdot d\xi$$

put

$$x = \frac{(x-\xi)}{y}$$

then

$$d\xi = -y \cdot dx$$

then

$$\begin{aligned}
 \psi_{\text{source}} &= myx \int_{\frac{x}{y}}^{\frac{x-d}{y}} \cot^{-1} x \cdot dx + my^2 \int_{\frac{x-d}{y}}^{\frac{x}{y}} x \cdot \cot^{-1} x \cdot dx
 \end{aligned}$$

$$\begin{aligned}
 &+ my(d-x) \int_{\frac{x-d}{y}}^{\frac{x-d}{y}} \cot^{-1} x \cdot dx - my^2 \int_{\frac{x-d}{y}}^{\frac{x-d}{y}} x \cdot \cot^{-1} x \cdot dx
 \end{aligned}$$

Integrating and grouping the terms

$$\begin{aligned}
 \psi_{\text{source}} &= \cot^{-1} \frac{x}{y} \left[\frac{mx^2}{2} - \frac{my^2}{2} \right] \\
 &+ \cot^{-1} \frac{x-\frac{d}{2}}{y} \left[my^2 - m \left(x - \frac{d}{2} \right)^2 \right] \\
 &+ \cot^{-1} \frac{x-d}{y} \left[\frac{m \cdot (d-x)^2}{2} - \frac{my^2}{2} \right] \\
 &+ \frac{mxy}{2} \ln \frac{y^2 + x^2}{y^2 + \left(\frac{x-d}{2} \right)^2} \\
 &+ \frac{my(d-x)}{2} \ln \left[\frac{y^2 + \left(x - \frac{d}{2} \right)^2}{y^2 + (x-d)^2} \right]
 \end{aligned} \tag{C2}$$

$$\begin{aligned}
 \text{The total sink strength} &= \int_0^{\frac{d}{2}} m \cdot \xi \cdot d\xi + \int_{\frac{d}{2}}^d m(d-\xi) \cdot d\xi \\
 &= \frac{md^2}{8} + \frac{md^2}{8} \\
 &= \frac{md^2}{4}
 \end{aligned}$$

The value of m is found by flow balance to the sampler. Let Q be the rate of sampling for a square inlet ($H \times H$). Then flow per unit width is $\frac{Q}{H}$ and

$$\frac{Q}{H} = U_I \sin \alpha \cdot H - \pi \cdot \frac{md^2}{4}$$

$$\text{non-dimensional } m = \frac{mH}{U_I} = - \frac{2(U - \sin \alpha)}{\pi f^2} \tag{C3}$$

where f is given by $\frac{d}{2H}$

$$\text{velocity } U_x = \frac{\partial \psi}{\partial y} = \frac{\partial \psi_{\text{source}}}{\partial y} + \frac{\partial \psi_{U \cdot F}}{\partial y}$$

$$U_y = - \frac{\partial \psi}{\partial x} = \frac{\partial \psi_{\text{source}}}{\partial x} - \frac{\partial \psi_{U \cdot F}}{\partial x}$$

Appendix D. Computer Program Listing

(See following pages.)

```

C *****
C
C           'FLOWFI' DESCRIPTION
C *****
C *****
C THIS PROGRAM SOLVES FOR THE FLOW FIELD IN AND AROUND THE SAMPLING
C HEAD.
C THE PHYSICAL DIMENSIONS ARE NORMALIZED WITH RESPECT TO THE
C PROBE RADIUS
C ALL THE VELOCITIES ARE NORMALIZED WITH RESPECT TO THE FREE
C STREAM VELOCITY
C
C METHOD OF SOLUTION
C
C SECOND ORDER FINITE DIFFERENCE APPROXIMATION
C SUCCESSIVE OVER RELAXATION(SOR) TECHNIQUE IS USED
C
C THE FLUID IS ASSUMED TO BE FRICTIONLESS AND THE FLOW FIELD IS GOVERNED
C BY POTENTIAL FLOW EQUATIONS. THE FLUID FLOW MODEL COVERS THREE DIFFERENT
C SITUATIONS. 1) TWO DIMENSIONAL FLOW BETWEEN PARALLEL PLATES
C 2) AXISYMMETRIC FLOW IN A CIRCULAR TUBE
C 3) LINE SINK WITH ARBITRARY ORIENTATION TO THE ONCOMING FLOW.
C THE USER CAN CHOOSE ANY OF THE ABOVE OPTION WITH PROPER VALUE OF AN
C INTEGER PARAMETER 'NDIM'
C   NDIM = 0 TWO DIMENSIONAL CASE
C   NDIM = 1 AXISYMMETRIC CASE
C   NDIM = 2 LINE SINK
C
C *****
C           'FLOWFI' VARIABLES DESCRIPTION
C *****
C RELAX*****RELAXATION PARAMETER(USER INPUT), VALUES BETWEEN 1.0 AND 2.0
C
C ALPHA*****ANGLE OF ORIENTATION OF SAMPLER HEAD(INPUT), USED ONLY WITH
C NDIM VALUE 2.
C IGR*****GRID POINTS PER UNIT LENGTH IN AXIAL DIRECTION (INPUT)
C
C JGR*****GRID POINTS PER UNIT LENGTH IN TRANSVERSE DIRECTION(INPUT)
C
C ZM *****FLOW FIELD BOUNDARY UPSTREAM(INPUT) <=5.
C
C ZMA*****FLOW FIELD BOUNDARY DOWNSTREAM(INPUT)
C
C RU *****FLOW FIELD BOUNDARY RADIAL DIRECTION(INPUT)
C
C ITERMA*****MAXIMUM ALLOWABLE ITERATIONS FOR FLOW FIELD TO CONVERGE(INPUT)
C
C IM *****MAXIMUM NUMBER OF GRID POINTS IN AXIAL DIRECTION <101
C
C JM *****MAXIMUM NUMBER OF GRID POINTS IN RADIAL DIRECTION <61
C
C ANG *****TAPERING ANGLE OF SAMPLER WALL(INPUT)
C
C ERR *****MAXIMUM ERROR ALLOWABLE IN STREAM FUNCTION SOLUTION(INPUT)
C
C ITER*****NUMBER OF ITERATIONS TO OBTAIN THE SOLUTION
C
C PSI*****IMXJM ARRAY OF STREAM FUNCTION

```

```

C
C IPUNCH****CONTROL PARAMETER FOR GETTING PUNCHED OUTPUT OF
C           PSI,UZ,UR,Z,R,ETC(INPUT)
C           =0 NO PUNCHED OUTPUT DESIRED
C           =1 PUNCHED OUTPUT RESULTS
C
C NCON*****INTEGER PARAMETER INDICATING WHETHER SOLUTION CONVERGED
C           OR NOT WITHIN ITERPA INTERATIONS
C           =0 CONVERGENCE OBTAINED
C           =1 NO CONVERGENCE
C
C U *****SAMPLING VELOCITY RATIO (INPUT)
C
C UR*****VELOCITY OF FLUID IN TRANSVERSE DIRECTION(ARRAY OF [MXJM])
C
C UZ*****VELOCITY OF FLUID IN AXIAL DIRECTION(ARRAY OF [MXJM])
C
C W*****THE SAMPLER WALL THICKNESS(INPUT),USED ONLY WITH
C           NDIM OPTION OF 0 OR 1
C
C ESC*****FUNCTION FOR EQUALLY SPACED CENTRAL DIFFERENCE
C
C ESF*****FUNCTION FOR EQUALLY SPACED FORWARD DIFFERENCE
C
C ESH*****FUNCTION FOR EQUALLY SPACED BACKWARD DIFFERENCE
C
C UESC*****FUNCTION FOR UNEQUALLY SPACED CENTRAL DIFFERENCE
C
C UESF*****FUNCTION FOR UNEQUALLY SPACED FORWARD DIFFERENCE
C
C UESR*****FUNCTION FOR UNEQUALLY SPACED BACKWARD DIFFERENCE
C
C H*****FICTICIOUS SOURCE/SINK STRENGTH(FOR NDIM 2)
C
C *****
C           SUBROUTINE DESCRIPTION
C *****
C
C MAIN*****CALLS VARIOUS SUBROUTINES
C
C FLBOUN****FIXES THE FLOW BOUNDARY
C
C GRID*****LAYS A PRESPECIFIED GRID ON THE FLOW FIELD AND
C           CALCULATES THE COORDINATES OF THE GRID POINTS.
C
C BCOND*****CALCULATES HOUNDARY CONDITIONS FOR THE PROBLEM
C
C LAPLA*****SOLVES THE FINITE DIFFERENCE EQUATION BY SOR METHOD
C
C VELO*****CALCULATES THE VELOCITIES FROM STREAM FUNCTION
C
C STREM*****CALCULATES THE CONTOUR OF A STREAM LINE
C
C RESULT****PRINTS THE RESULTS
C
C SINVEL****CALCULATES THE FLOW FIELD WITH LINE SINK(NDIM=2)
C
C *****
C *****

```

'FLOWFI' DATA INPUT

CARD 1: NDIM,IPUNCH FORMAT()

NDIM.....FLOW FIELD OPTION PARAMETER
=0 TWO DIMENSIONAL CASE
=1 AXISYMMETRIC CASE
=2 LINE SINK

IPUNCH.....CONTROL PARAMETER FOR GETTING PUNCHED OUTPUT OF
PSI,UZ,UR,Z,R,EPC
=0 NO PUNCHED OUTPUT DESIRED.
=1 PUNCHED OUTPUT DESIRED.

CARD 2: ISINK,ALPHA,F FORMAT(15,2F10.4) OMIT IF NDIM,NE.2

ISINK.....SINK DISTRIBUTION PARAMETER
=0 LINE SINK OF UNIFORM STRENGTH.
=1 LINE SINK OF TRIANGULAR STRENGTH DISTRIBUTION.

ALPHA.....ANGULAR ORIENTATION OF THE FACE PLANE OF SAMPLER HEAD.
=90 DEGREES WHEN SAMPLER FACES THE STREAM
=0 DEGREES WHEN STREAM IS TANGENTIAL TO THE HEAD.

F.....FRACTION OF THE PROBE DIAMETER OVER WHICH
THE SINK IS ASSUMED TO BE DISTRIBUTED.
RECOMMENDED VALUE IS 0.01.

CARD 3: ITERMA,RELAX FORMAT(15,F10.4)

ITERMA.....MAXIMUM ALLOWABLE ITERATIONS FOR FLOW FIELD
TO CONVERGE

RELAX.....RELAXATION PARAMETER USED IN THE PROCEDURE OF
SUCCESSIVE OVER RELAXATION(SOR)
VALUES BETWEEN 1.0 AND 2.0.

CARD 4: ZM,ZMA,RO,U,W,ANG FORMAT(6F10.4)

ZM.....UPSTREAM FLOW FIELD BOUNDARY,LE.=5.

ZMA.....DOWNSTREAM FLOW FIELD BOUNDARY

RO.....FLOW FIELD BOUNDARY IN THE RADIAL OR TRANSVERSE
DIRECTION. RO.GE.5.

U.....ANISOKINETIC VELOCITY RATIO.

W.....SAMPLER WALL THICKNESS
WHEN NDIM,EQ.2 W=0.

ANG.....TAPERING ANGLE OF SAMPLER WALL
=0 IF W=0. OR NDIM,EQ.2

CARD 5: IGZ,JGR FORMAT(215)

IGZ.....GRID POINTS PER UNIT LENGTH IN AXIAL DIRECTION
= 1./GRID SIZE +1

JGR.....GRID POINTS PER UNIT LENGTH IN RADIAL DIRECTION
=1./RADIAL GRID SIZE +1


```

1 TWO DIMENSIONAL CASE'//)
9 FORMAT(1H,10X,'FLOW FIELD FOR CIRCULAR TUBE',//,10X,
1 AXIALLY SYMMETRIC CASE'//)
10 FORMAT(1H,9X,'FLOW FIELD WITH A LINE SINK',//,10X,
1 ORIENTATION ANGLE ALPHA=',F10.6,'DEGREES TO THE FLOW')
WRITE(6,6) ZM,ZMA,RO
6 FORMAT(1H,'DISTANCE OF UPSTREAM BOUNDARY=',F10.5//,
1 1H,'DISTANCE OF DOWN STREAM BOUNDARY=',F10.5//,
2 1H,'DISTANCE OF RADIAL BOUNDARY=',F10.5//)
IF(IPUNCH.EQ.1) WRITE(1,1)U,W,ANG
WRITE(6,7) U,W,ANG
7 FORMAT(1H,'SAMPLING CONDITIONS'///,
1 1H,'SAMPLING VELOCITY/FREE STREAM VELOCITY=',F10.5//,
2 1H,'SAMPLER WALL THICKNESS=',F10.5//,
3 1H,'TAPERING ANGLE OF SAMPLER WALL=',F10.5,'DEGREES'//)
RETURN
END
*FOR I GRID
SUBROUTINE GRID(IM,JM,Z,R,ZM,ZMA,RO,W,ZOW,ITW)
COMMON/ABC/JGR,IGR,IBW,ITER
COMMON/ACC/IBW0,JGR0
DIMENSION Z(101),R(61)
READ(5,18) IGZ,JGR
18 FORMAT(2I5)
IGP=IGZ
WRITE(6,1) IGR,JGR
1 FORMAT(1H,'NUMBER OF GRID POINTS FOR UNIT DISTANCE Z=',I5//,
1 1H,'NUMBER OF GRID POINTS FOR UNIT DISTANCE R=',I5//)
FGZ=IGZ-1
FGM=JGR-1
DZ=1./FGZ
DR=1./FGM
C CALCULATE MAXIMUM VALUE OF I
I=1
Z(I)=ZM
2 Z(I+1)=Z(I)+DZ
I=I+1
IF(AHS(Z(I)).LE.(DZ+.0005))GO TO 3
GO TO 2
3 I=I+1
Z(I)=0.
IBW=I
IF(ITW)5,15,15
5 FN=ZOW/DZ
N=1
NN=FN+.99
IF(NN.EQ.N) GO TO 13
FN=NN
N=NN
13 DO 14 J=1,N
FJ=J
I=I+1
Z(I)=FJ*ZOW/FN
14 CONTINUE
Z(I)=ZOW
15 IBW0=I
4 Z(I+1)=Z(I)+DZ
I=I+1
IF(Z(I).GE.(ZMA-.0005))GO TO 6
GO TO 4

```

```

6 IM=1
C CALCULATE MAXIMUM VALUE OF J
  J=1
  R(J)=0.
7 R(J+1)=R(J)+DK
  J=J+1
  IF(J.EQ.JGR)GO TO 8
  GO TO 7
8 R(JGR)=1.
  IF(ITW)9,10,17
17 FN=W/DK
  N=FN
  NN=FN+.99
  IF(NN.EQ.N) GO TO 9
  FN=NN
  N=NN
9 DO 16 JJ=1,N
  FJ=JJ
  J=J+1
  R(J)=1.+FJ*W/FN
16 CONTINUE
  R(J)=1.+W
  JGR=J
10 J=J+1
  R(J)=R(J-1)+DK
  IF((R(J)+.005).GE.R0)GO TO 11
  GO TO 10
11 JM=J
  IF(ITW.EQ.0) JGR=JGR
  WRITE(6,12) IM,JM
12 FORMAT(1H,'MAXIMUM NUMBER OF POINTS IN Z DIRECTION=',I5//,
1      1H,'MAXIMUM NUMBER OF POINTS IN R DIRECTION=',I5//)
  RETURN
  END
*FOR,I BCOND
SUBROUTINE BCOND(PSI,IM,JM,U,ITW,W,R)
COMMON/ABC/JGR,IGR,IBW,ITER
COMMON/ACC/IBWU,JGR0
COMMON/ARD/NDIM,IPUNCH
DIMENSION PSI(IM,JM),R(JM)
C INITIALIZE ALL PSI VALUES.
  N=NDIM+1
  DO 1 1 J=1,JM
  A=R(J)**N
  DO 1 I=1,IM
  PSI(I,J)=A
1 CONTINUE
11 CONTINUE
C AT THE OUTER BOUNDARY
  DO 2 I=1,IM
  PSI(I,JM)=R(JM)**N
2 CONTINUE
C AT THE INLET
  JM1=JM-1
  DO 3 J=2,JM1
  PSI(1,J)=R(J)**N
3 CONTINUE
C AT THE OUTLET
  DO 4 J=2,JGR
  PSI(IM,J)=R(J)**N*U

```

```

4 CONTINUE
  DO 5 I=IBW,IM
    PSI(I,JGR)=U
5 CONTINUE
  JG=JGR+ABS(ITW)
  IF(ITW)6+H,6
6 IH=IHW
  IF(ITW.LE.0)IH=IBW+1
  DO 7 I=IB,IBWU
    JGG=JGR-IHW+I
    IF(ITW.EQ.1)JGG=JGRD
    DO 13 J=JG,JGG
      PSI(I,J)=PSI(I,JGP)
13 CONTINUE
7 CONTINUE
  DO 14 I=IHWU,IM
    DO 15 J=JG,JGG
      PSI(I,J)=PSI(I,JGR)
15 CONTINUE
14 CONTINUE
8 A=R(JM)**N-U
  C=(1.+W)**N
  B=R(JM)**N-C
  IF(ITW.EQ.0)JGG=JG
  DO 9 J=JGG,JM1
    IF(J.FG,JGR)GO TO 9
    PSI(IM,J)=A/B*(R(J)**N-C)+L
9 CONTINUE
  WRITE(6,12)
12 FORMAT(1H,'INITIAL VALUES OF STREAM FUNCTION'//)
  WRITE(6,10)((PSI(I,J),I=1,IM,5),J=1,JM,5)
10 FORMAT(11F10,4)
  RETURN
  END
*FOR,I LAPLA
SUBROUTINE LAPLA(PSI,IM,JM,ITW,RELAX,Z,R,ITERMA,NCON)
COMMON/ABC/JGR,IGR,IHW,ITER
COMMON/AAA/ERR
COMMON/ACC/IBWU,JGRD
COMMON/ARD/NDIM,JPUNCH
DIMENSION PSI(IM,JM),Z(IM),R(JM)
ENDIMENDIM
WRITE(6,11) RELAX
11 FORMAT(1H,'RELAXATION FACTOR='F15,6,/,/,'1H,
1'CONVERGENCE RATE'//)
  IG=0
  NCON=0
  ITER=1
  IM1=IM-1
  JM1=JM-1
  EPPS=1E-3
  IF(ITW.NE.0)IG=1
3 ERR=0.
  DO 1 I=2,IM1
    DZ=Z(I)-Z(I-1)
    IF(IG.EQ.0)GO TO 4
    DZZ=Z(I+1)-Z(I)
    A=2./(DZ+DZZ)
    B=A/DZ
    C=A/DZZ

```

```

D=2./DZ/DZZ
4 DO 2 J=2,JM1
  DR=R(J)-R(J-1)
  IF(J.EQ.JGM.AND.I.GE.IBW) GO TO 2
  IF(IG.EQ.0)GO TO 5
  IF(J.LT.JGM.OR .J.GT.JGRO) GO TO 10
  IF(I.LT.IBW) GO TO 10
  IF(ITW)9+5+2
9 IF(I.GE.IHW0) GO TO 2
  JMAG=I-IBW+JGM+1
  IF(J.GE.JMAG) GO TO 10
  GO TO 2
10 DRK=R(J+1)-R(J)
  A=2./((DR+DRR)
  E=A/DR
  F=A/DRK
  G=E/2.*DR/R(J)*FNDIM
  H=F/2.*DR/R(J)
  H=H*FNDIM
  P=(DK-DRR)/DK/DRR/R(J)
  P=P*FNDIM
  U=2./DR/DRK
  S=U-P+Q
  PS=PSI(I,J)+RELAX/S*(B*PSI(I-1,J)+C*PSI(I+1,J)+(G+E)*PSI(I,J-1)+(F
1-H)*PSI(I,J+1))
  PS=PS-RELAX*PSI(I,J)
  GO TO 6
5 PS=PSI(I,J)+RELAX/4.*(PSI(I-1,J)+PSI(I+1,J)+PSI(I,J-1)*(1.+DR/2.*
2FNDIM/R(J))+PSI(I,J+1)*(1.-DR/2./R(J)*FNDIM))
  PS=PS-RELAX*PSI(I,J)
6 ER=ABS(PSI(I,J)-PS)
  FR=ER/PSI(I,J)
  IF(ER.GE.ERN)ERR=ER
  PSI(I,J)=PS
2 CONTINUE
1 CONTINUE
  WRITE(6,H) ITER,ERR
8 FORMAT(15,F10.7)
  IF(ERR.LE.EPPS)GO TO 7
  ITER=ITER+1
  IF(ITER.GE.ITERMA)NCON=1
  IF(ITER.GE.ITERMA)GO TO 7
  GO TO 3
7 RETURN
  END
#FOR,I RESULT
SUBROUTINE RESULT(PSI,IM,JM,Z,R,RELAX,NCON,UZ,UR)
DIMENSION PSI(IM,JM),Z(IM),R(JM)
DIMENSION UZ(IM,JM),UR(IM,JM)
COMMON/ABC/JGM,IGR,IHW,ITER
COMMON/AAA/ERR
COMMON/AND/NDIM,IPUNCH
COMMON/ACC/IBW0,JGRO
COMMON/HAT/ALPHA,F,ISINK
IF(NDIM.EQ.2) GO TO 12
IF(NCON)1,1,2
2 WRITE(6,3)
3 FORMAT(1H,'NO CONVERGENCE')
1 WRITE(6,5)ITER
5 FORMAT(1H,'NUMBER OF ITERATIONS',2X,I4)

```

```

WRITE(6,4) ERR
4 FORMAT(1H,1MAXIMUM ERROR=1.2X,F10.7)
WRITE(6,7)
7 FORMAT(//,1H,1 FINAL STREAM FUNCTION SOLUTION 1//)
WRITE(6,6)((PSI(I,J),I=1,1M,5),J=1,JM)
12 WRITE(6,8)
WRITE(6,6)((UZ(I,J),I=1,1M,5),J=1,JM)
WRITE(6,9)
WRITE(6,6)((UR(I,J),I=1,1M,5),J=1,JM)
6 FORMAT(11F10.4)
8 FORMAT(//,1H,5X,'UZ')
9 FORMAT(//,1H,5X,'UR')
10 FORMAT(8F10.4)
11 FORMAT(2I4)
IF(IPUNCH)13,13,14
14 CONTINUE
WRITE(1,11) NDIM
WRITE(1,11) JGR,JGR0
WRITE(1,11) IHW,IHW0
WRITE(1,11) IM,JM
IF(NDIM,EQ,2) WRITE(1,11) ISINK
IF(NDIM,EQ,2) WRITE(1,10) F,ALPHA
WRITE(1,10)(Z(I),I=1,IM)
WRITE(1,10)(R(I),I=1,JM)
IF(NDIM,EQ,2) GO TO 13
WRITE(1,10)((UZ(I,J),I=1,1M),J=1,JM)
WRITE(1,10)((UR(I,J),I=1,1M),J=1,JM)
13 RETURN
END
*FOR,I VELO
SUBROUTINE VELO(PSI,IM,JM,UZ,UR,HU,w,ITw,U,Z,R)
DIMENSION Z(IM),R(JM)
DIMENSION PSI(IM,JM),UZ(IM,JM),UR(IM,JM)
COMMON/ACC/IHW0,JGR0
COMMON/ABC/JGR,IGR,IHW,ITEH
COMMON/ARD/NDIM,IPUNCH
ESC(A,B,C)=(A-B)/2./C
ESB(A,B,C,D)=(3.*A+C-4.*B)/2./D
ESF(A,B,C,D)=(4.*B-A-3.*C)/2./D
UESC(A,H,C,E,D)=(D**2*A-(C**2-F**2)*H-E**2*C)/(D+E)/D/E
UESF(A,H,C,D,E)=(R*(D+E)**2-A*D**2-C*(2.*D+E)*E)/D/E/(D+E)
UFSB(A,H,C,D,E)=(A*(2.*D+E)*E-H*(D+E)**2+C*D**2)/D/E/(D+E)
C INITIALIZE ALL VALUES OF VELOCITIES
N=NDIM+1
DO 1 I=1,IM
DO 2 J=1,JM
UZ(I,J)=1.0
UR(I,J)=0.0
2 CONTINUE
1 CONTINUE
DO 3 J=1,JGR
UZ(IM,J)=U
3 CONTINUE
DO 4 J=JGR0,JM
UZ(IM,J)=(RU**N-U)/(RU**N-(1.+w)**N)
4 CONTINUE
DO 28 J=JGR,JGR0
UZ(IM,J)=0.
28 CONTINUE
DO 29 I=1,IM

```

```

      UZ(I,1)=PSI(I,2)/R(2)**N
      IF(NDIM.EQ.0) RR=1.
29  CONTINUE
C  CALCULATE THE VELOCITIES
      IM1=IM-1
      JM1=JM-1
      DO 5 I=2,IM1
      DO 7 J=2,JM1
      DZ=Z(I+1)-Z(I)
      RR=2.*R(J)
      IF(NDIM.EQ.0) RR=1.
      DR=R(J+1)-R(J)
      IF(ITW)8,9,10
 9  UZ(I,J)=ESC(PSI(I,J+1),PSI(I,J-1),DR)/RR
      UR(I,J)=ESC(PSI(I+1,J),PSI(I-1,J),DZ)/(-RR)
      GO TO 7
10 IF(J.LT.JGR.OR.J.GT.JGRO)GO TO 9
      IF(I=IBW)11,12,13
11 IF(J.GT.JGR.AND.J.LT.JGRO )GO TO 9
17 DRR=R(J)-R(J-1)
      UR(I,J)=-ESC(PSI(I+1,J),PSI(I-1,J),DZ)/RR
      UZ(I,J)=UESC(PSI(I,J+1),PSI(I,J),PSI(I,J-1),DR,DRR)/RR
      GO TO 7
12 UR(I,J)=-ESH(PSI(I,J),PSI(I-1,J),PSI(I-2,J),DZ)/RR
      UZ(I,J)=0.0
14 IF(J.EQ.JGR)UZ(I,J)=FSB(PSI(I,J),PSI(I,J-1),PSI(I,J-2),(R(J)-R(J-1)))
      IF(J.EQ.JGRO)UZ(I,J)=ESF(PSI(I,J+2),PSI(I,J+1),PSI(I,J),DR)/RR
      GO TO 7
13 UR(I,J)=0.0
      UZ(I,J)=0.0
      GO TO 14
 8  IF(I.GE.IBW.AND.I.LE.IHWO)GO TO 15
      IF(J.EQ.JGR.OR .J.EQ.JGRO)GO TO 16
      IF(I.LT.IBW)GO TO 9
      IF(J.LT.JGR.OR.J.GT.JGRO)GO TO 9
      UZ(I,J)=0.0
      UR(I,J)=0.0
      GO TO 7
16 IF(I.LT.IBW) GO TO 17
      UR(I,J)=0.0
      GO TO 14
15 IF(I.EQ.IBW.OR.I.EQ.IHWO) GO TO 1A
      IF(J.LT.JGR.OR.J.GT.JGRO) GO TO 9
      IF(J.EQ.JGRO) GO TO 12
      IF(J.EQ.JGR) UR(I,J)=0.0
      IF(J.EQ.JGR) GO TO 14
      IF(I.GT.(IBW+J-JGR)) GO TO 27
      IF(J.GT.(JGR+1-IBW))GO TO 9
      IF(J.EQ.(JGR+1).OR.J.EQ.(JGRO-1))GO TO 19
      IF(J.LT.(JGR+1-IBW)) GO TO 27
      DZ=Z(I)-Z(I-1)
      UR(I,J)=-ESH(PSI(I,J),PSI(I-1,J),PSI(I-2,J),DZ)/RR
21 UZ(I,J)=ESF(PSI(I,J+2),PSI(I,J+1),PSI(I,J),DR)/RR
      GO TO 7
27 UZ(I,J)=0.0
      UR(I,J)=0.0
      GO TO 7
19 IF(J.NE.(JGR+1))GO TO 20
      DZ=Z(I)-Z(I-1)

```

```

D7Z=Z(I-1)-Z(I-2)
UR(I,J)=UESH(PSI(I,J),PSI(I-1,J),PSI(I-2,J),DZ,DZZ)/(-RR)
IF(J.EQ.(JGR-1))GO TO 20
GO TO 21
20 DPR=R(J+2)-R(J+1)
U7(I,J)=UESF(PSI(I+2,J),PSI(I+1,J),PSI(I,J),DP,DRR)/RR
IF(J.EQ.(JGR+1))GO TO 7
D7=Z(I)-Z(I-1)
UR(I,J)=-ESH(PSI(I,J),PSI(I-1,J),PSI(I-2,J),D7)/RR
GO TO 7
18 IF(I.EQ.IHWD)GO TO 22
26 DRH=R(J)-R(J-1)
D7Z=Z(I)-Z(I-1)
UR(I,J)=-UESC(PSI(I+1,J),PSI(I,J),PSI(I-1,J),DZ,DZZ)/RR
U7(I,J)=UESC(PSI(I,J+1),PSI(I,J),PSI(I,J-1),DR,DRR)/RR
GO TO 7
22 IF(J.GT.JGR.AND.J.LT.JGR) GO TO 23
IF(J.EQ.JGR) GO TO 24
IF(J.EQ.JGR) GO TO 25
UR=R(J+1)-R(J)
GO TO 26
24 UR(I,J)=0.0
D7=Z(I)-Z(I-1)
UR(I,J)=-ESH(PSI(I,J),PSI(I-1,J),PSI(I-2,J),DZ)/RR
DR=R(J)-R(J-1)
U7(I,J)=ESH(PSI(I,J),PSI(I,J-1),PSI(I,J-2),DR)/RR
GO TO 7
25 UR(I,J)=0.0
D7=Z(I)-Z(I-1)
UR(I,J)=-ESH(PSI(I,J),PSI(I-1,J),PSI(I-2,J),DZ)/RR
U7(I,J)=ESH(PSI(I,J+2),PSI(I,J+1),PSI(I,J),DR)/RR
GO TO 7
23 UR(I,J)=0.0
U7(I,J)=0.0
7 CONTINUE
5 CONTINUE
RETURN
END
#FOR,I STREAM
SUBROUTINE STREAM(Z,PSI,R,IM,JM,STR,II)
DIMENSION PSI(IM,JM),Z(IM),R(JM),STR(II)
DIMENSION RS(10,101)
SAG(X,Y,V,A,B,C,D)=(A-C)*(A-D)*X/(H-C)/(B-D)+(A-B)*(A-D)*Y/(C-B)
1/(C-D)+(A-B)*(A-C)*V/(D-R)/(D-C)
JM2=JM-2
DO 1 IK=1,II
ST=STR(IK)
DO 2 I=1,IM
DO 3 J=1,JM2
IF(ST.GT.PSI(I,J).AND.ST.LE.PSI(I,J+1)) GO TO 4
3 CONTINUE
4 RS(IK,I)=SAG(R(J),R(J+1),R(J+2),ST,PSI(I,J),PSI(I,J+1),PSI(I,J+2))
2 CONTINUE
1 CONTINUE
WRITE(6,5)((Z(I),(RS(IK,I),IK=1,II)),I=1,IM)
5 FORMAT(11F10.6)
RETURN
END
#FOR,I SINVEL
SUBROUTINE SINVEL(U,Z,R,IM,JM,UZ,UR)

```

```

DIMENSION Z(IM),H(JM),UZ(IP,JM),UR(IM,JM)
COMMON/BAT/ALPHA,F,ISINK
FUN(X,Y)=SQRT(X**2+Y**2)
REAL M
ALPHA=ALPHA*3.141596/180.
C=COS(ALPHA)
S=SIN(ALPHA)
M=(U-S)/4./F
IF(ISINK.EQ.1) M=(S-U)/2./F**2
WRITE(6,4) M,F,ISINK
3 FORMAT(4F10.6)
4 FORMAT(2F10.6,I4)
DO 1 I=1,IM
  Y=Z(I)
  DO 2 J=1,JM
    X=H(J)+F
    XF=X-F
    XFF=XF-F
    IF(ISINK.EQ.0) GO TO 13
    IF(ABS(Y).LE..01) GO TO 10
    A=FUN(X,Y)
    B=FUN(XF,Y)
    D=FUN(XFF,Y)
    F=B+XF
    E=XFF+D
    G=X+A
    UUZ=-X/2./A+XF/H-XFF/2./D+ALOG(H/G)+ALOG(H/E)+
1Y**2/2.*(2./H/B-1./G/A-1./E/D)
    UUR=X**2/2./Y/A-XF**2/Y/B+XFF**2/2./Y/D-Y/2.*(2./B-1./A-1./D)
    UUR=UUR+A/2./Y-B/Y+D/2./Y
    UUZ=UUZ*M
    UUR=UUR*M
    GO TO 11
10 IF(X.GE.U..AND.X.LE.(2.*F)) GO TO 12
    UUR=0.
    UUR=M*ALOG(XF**2/X/XFF)
    GO TO 11
12 UUZ=0.
    UUR=0.
    GO TO 11
13 A=FUN(X,Y)
    B=FUN(XFF,Y)
    IF(A.LE..01) A=.01
    IF(B.LE..01) B=.01
    UUR=M*(1./A-1./B)
    UUR=M*(X/A/Y-(XFF)/B/Y)
11 CONTINUE
  UZ(I+J)=UUR+S
  UR(I+J)=UUZ+C
2 CONTINUE
1 CONTINUE
RETURN
END

```

```

*FIN
**

```


C INT*****INTERVAL FOR TRAJECTORY COORDINATES TO BE PRINTED OUT INPUT
 C
 C IS*****SEDIMENTATION PARAMETER
 C =0 SETTLING IS NOT TAKEN INTO ACCOUNT
 C =1 " " " TAKEN INTO ACCOUNT
 C
 C ISINK*****SINK STRENGTH DISTRIBUTION PARAMETER.
 C =0 UNIFORM STRENGTH
 C =1 TRIANGULAR STRENGTH DISTRIBUTION
 C
 C IST*****NUMBER OF SIZE INTERVALS IN PARTICLES DISTRIBUTION INPUT
 C MAXIMUM OF 10
 C
 C LIMIT*****MAXIMUM NUMBER OF TIMES TO PERFORM THE TRAJECTORY CALCULATION
 C FOR ONE PARTICLE
 C
 C THE FLUID IS ASSUMED TO BE FRICTIONLESS AND THE FLOW FIELD IS GOVERNED
 C BY POTENTIAL FLOW EQUATIONS. THE FLUID FLOW MODEL COVERS THREE DIFFERENT
 C SITUATIONS. 1) TWO DIMENSIONAL FLOW BETWEEN PARALLEL PLATES
 C 2) AXISYMMETRIC FLOW IN A CIRCULAR TUBE
 C 3) LINE SINK WITH ARBITRARY ORIENTATION TO THE ONCOMING FLOW.
 C THE USER CAN CHOOSE ANY OF THE ABOVE OPTION WITH PROPER VALUE OF AN
 C INTEGER PARAMETER 'NDIM'
 C NDIM =0 TWO DIMENSIONAL CASE
 C NDIM =1 AXISYMMETRIC CASE
 C NDIM =2 LINE SINK
 C
 C P*****PARTICLE RADIUS IN MICRONS (DIMENSION 'IST')
 C
 C PF*****MEASURED FRACTION OF VARIOUS PARTICLE SIZES (DIMENSION 'IST')
 C
 C PL*****LINEAR DIMENSION OF THE SAMPLING HEAD
 C
 C QC*****ELECTROSTATIC CHARGE ON THE SAMPLER HEAD.
 C
 C RI*****INITIAL RADIAL POSITION OF THE PARTICLE
 C
 C RT*****RADIUS OF THE TUBE(SAMPLING) OR CHARACTERISTIC DIMENSION OF
 C THE SAMPLER.
 C
 C STK*****STOKE'S NUMBER OF THE PARTICLE
 C
 C R*****RADIAL COORDINATE(DIMENSION 'JM')
 C
 C RE*****REYNOLD'S NUMBER BASED ON THE RADIUS
 C
 C TA*****RELAXATION TIME OF THE PARTICLES (DIMENSION IST)
 C
 C W*****THE SAMPLER WALL THICKNESS(INPUT). USED ONLY WITH
 C NDIM OPTION OF 0 OR 1
 C
 C UZ*****VELOCITY OF FLUID IN AXIAL DIRECTION(ARRAY OF IMXJM)
 C
 C UR*****VELOCITY OF FLUID IN TRANSVERSE DIRECTION(ARRAY OF IMXJM)
 C
 C U *****SAMPLING VELOCITY RATIO (INPUT)
 C
 C Z*****AXIAL COORDINATE (DIMENSION IM)
 C
 C ZI*****INITIAL AXIAL POSITION OF THE PARTICLE

ZLIP*****LIP DEPTH OF THE SAMPLER

ZMAX*****MAXIMUM AXIAL DISTANCE UPTO WHICH THE TRAJECTORY SHOULD BE
(CONTINUED (USUALLY EQUAL TO 0.))

TRAJEC DATA INPUT

CARD 1: INT FORMAT(I4)
 PRINTING INTERVAL

CARD 2: IE, IW, IS FORMAT(3I4)
 IE=0/1 ELECTROSTATIC EFFECT NOT INCLUDED/INCLUDED
 IW=1/-1 UPPER/LOWER WALL
 IS=0/1 SEDIMENTATION EFFECT NOT INCLUDED/INCLUDED

CARD 3: U, W, ANG FORMAT(3F10.4)
 U--VELOCITY RATIO, SAMPLING VEL/FREE STREAM VEL
 W--WALL THICKNESS OF THE SAMPLER
 ANG--TAPERING ANGLE IN DEGREES OF SAMPLER WALL

CARD 4: NDIM FORMAT(I4)
 FLOW FIELD OPTION
 =0 TWO DIMENSIONAL FLOW BETWEEN PARALLEL PLATES
 =1 AXISYMMETRICAL FLOW FOR CIRCULAR TUBE
 =2 FLOW FIELD WITH LINE SINK
 OPTIONS 0&1 REQUIRE THE FLOW FIELD TO BE DETERMINED BY THE PROGRAM
 'FLOWFI'

CARD 5: IDIM FORMAT(I4) OMIT IF NDIM=0 OR 1
 =0 TWO DIMENSIONAL LINE SINK
 AXISYMMETRICAL LINE SINK

CARD 6: JGR, JGR0 FORMAT(2I4)
 JGR--NUMBER OF GRID POINTS PER UNIT
 RADIAL DISTANCE, =1./GRID SPACING IN RAD, DIR+1
 JGR0--RADIAL GRID POINT AT WHICH OUTER EDGE OF THE WALL IS LOCATED
 JGR0=JGR IF NDIM=2 OR W=0. FOR NDIM=0,1 JGR&JGR0 ARE CALCULATED
 BY THE PROGRAM FLOWFI

CARD 7: IBW, IBW0 FORMAT(2I4)
 IBW--AXIAL GRID POINT AT WHICH INNER EDGE OF SAMPLER WALL IS LOCATED
 IBW0--AXIAL GRID POINT AT WHICH OUTER EDGE OF SAMPLER WALL IS

C LOCATED. $IBW0=IHW$ IF $NDIM=2$ OR $W=0$ OR $ANG=90$. FOR $NDIM=0$ OR 1 ,
 C IHW AND $IBW0$ ARE CALCULATED BY 'FLOWFI'
 C
 C CARD 8: JM, JM FORMAT(2I4)
 C IM --MAXIMUM NUMBER OF POINTS IN AXIAL DIRECTION <101
 C JM --MAXIMUM NUMBER OF POINTS IN RADIAL DIRECTION, <61
 C FOR $NDIM=2$ IM, JM ARE INPUT BY THE USER.
 C FOR $NDIM=0,1$ IM, JM ARE OUTPUT BY FLOWFI.
 C
 C CARD 9: $ISINK$ FORMAT(I4) OMIT IF $NDIM, NE.2$
 C =0 UNIFORM SINK STRENGTH DISTRIBUTION,
 C =1 TRIANGULAR SINK STRENGTH DISTRIBUTION.
 C
 C CARD 10: $F, ALPHA$ FORMAT(2F10.4) OMIT IF $NDIM, NE.2$
 C F --FRACTION OF DIAMETER OVER WHICH THE LINE SINK IS DISTRIBUTED
 C USUALLY $F=0.01$
 C $ALPHA$ --ORIENTATION ANGLE OF SAMPLER
 C
 C CARD 11: ---11+ IM/B $Z(I)$ FORMAT(8F10.4)
 C AXIAL COORDINATES OF GRID POINTS, FOR $NDIM=0,1$ $Z(I)$ IS CALCULATED
 C BY 'FLOWFI'. FOR $NDIM=2$ INPUT BY USER. THERE WILL BE
 C IM/B DATA CARDS.
 C
 C CARDS 11+ IM/B --11+ $IM/B+JM/B=N(SAY)$ $R(I)$ FORMAT(8F10.4)
 C RADIAL COORDINATES OF GRID POINTS, FOR $NDIM=0,1$ $R(I)$ IS CALCULATED
 C BY 'FLOWFI'. FOR $NDIM=2$ INPUT BY USER. THERE WILL BE
 C JM/B DATA CARDS.
 C
 C CARD N -- $N+IM*JM/B=M(SAY)$ $UZ(I,J)$ FORMAT(8F10.4) OMIT IF $NDIM=2$
 C UZ --AXIAL COMPONENT OF VELOCITY, FOR $NDIM=0$ OR 1 CALCULATED BY
 C 'FLOWFI'
 C
 C CARDS M -- $M+IM*JM/B=MM(SAY)$ $UR(I,J)$ FORMAT(8F10.4) OMIT IF $NDIM=2$
 C UR -- RADIAL COMPONENT OF VELOCITY, FOR $NDIM=0,1$ CALCULATED BY FLOWFI
 C
 C CARD ($MM+1$) LIM, DTI, ZI, RI, DR FORMAT(I5,4F15.6)
 C LIM --# OF TIMES TREJECTORY CALCULATION HAS TO BE DONE
 C DTI --TIME INCREMENT FOR EACH STEP (0.1)
 C ZI --INITIAL AXIAL POSITION OF THE PARTICLE.
 C RI --INITIAL RADIAL POSITION OF PARTICLE= $SQRT(U)$
 C DR -- RADIAL INCREMENT (0.2)
 C
 C CARD($MM+2$) $UINF, RE$ FORMAT(2F15.6)
 C $UINF$ --FREE STREAM VELOCITY USER INPUT
 C RE -- REYNOLD'S NUMBER BASED ON TUBE WIDTH
 C
 C CARD($MM+3$): $ZLIP$ FORMAT(F15.6)
 C $ZLIP$ --LIP DEPTH OF SAMPLER.
 C
 C CARD($MM+4$): QP, QC, PL FORMAT(3F10.4) OMIT IF $IE=0$
 C QP --ELECTROSTATIC CHARGE ON THE PARTICLE
 C QC --ELECTROSTATIC CHARGE ON THE SAMPLER.
 C PL --LINEAR DIMENSION OF THE SAMPLER.
 C
 C CARD($MM+5$): IST FORMAT(I4)
 C # OF SIZE INTERVALS IN THE SIZE DISTRIBUTION <10
 C
 C CARDS($MM+6$)--($MM+6+IST$) P, TA, PF FORMAT(3F15.8)


```

4 FORMAT(15,4F15.6)
5 FORMAT(2F15.6)
  READ(5,1) IST
  CALL BIAS(IST,ST,P,TA,PF,ICA,UINF,RE)
  ALPH=ALPHA/PI*180.
  WRITE(6,30)
30 FORMAT(//25X,'FLOW FIELD BOUNDARY'///)
  IF(NDIM.EQ.0) WRITE(6,31)
  IF(NDIM.EQ.1) WRITE(6,32)
  IF(NDIM.EQ.2) WRITE(6,33) ALPH,ISINK,F,IDIM
31 FORMAT(1H,10X,'FLOW FIELD FOR TWO PARALLEL PLATES',//,10X,
  1'TWO DEMENSIONAL CASE'//)
32 FORMAT(1H,10X,'FLOW FIELD FOR CIRCULAR TUBE',//,10X,
  1'AXIALLY SYMMETRIC CASE'//)
33 FORMAT(1H,9X,'FLOW FIELD WITH A LINE SINK',//,10X,
  1'ORIENTATION ANGLE ALPHA=',F10.6,'DEGREES TO THE FLOW',//,
  210X,'SINK DISTRIBUTION PARAMETER ISINK=',I4,//,
  310X,'SINK DISTRIBUTED OVER',F10.6,'OF THE PROBE DIAMETER',//,
  410X,'IDIM=',I4,//)
34 FORMAT(//,1H,25X,'WALL PARAMETER IW=',I4//)
  WRITE(6,39) ZLIP
39 FORMAT( 1H,10X,'ZLIP=',F15.6//)
  WRITE(6,35) IS,IE,ITS
35 FORMAT(1H,9X,'SEDIMENTATION PARAMETER=',I4,//,
  110X,'ELECTROSTATIC FIELD PARAMETER=',I4,//,
  110X,'SEDIMENTATION TRAJECTORY PARA ITS=',I4,//)
  WRITE(6,36)
36 FORMAT(1H,'RADIUS',3X,'FRACTION',/,1H,'MICRON')
  DO 37 I=1,IST
37 WRITE(6,2) P(I),PF(I)
  LIMIT=20
  CAT=1.05
  EPPS=1E-3
  EPP=10.*EPPS
  ZI0=Z1
  DT1=DTI
  DT2=5.*DT1
  DT3=DT1/10.
  DT3=DT1/5.
  DT4=DT3/2.
  IF(LIMIT.LT.1)STOP
  IWP=1
  IF(NDIM.EQ.2.AND.ALPHA.LT.1.57) IWP=2
  FWP=IWP
  YIJP=0.
  YLU=0.
  DO 24 II=1,IST
  IF(II.NE.1) DR=0.1
  STK=ST(II)
  TAU=TA(II)
  PP=P(II)
  ESP=3.*UP*UC/4./PI/PP**3/UINF**2*10.**12
  G=981.
  IF(IS.LT.1) GO TO 6
  VS=TAU*G
  GO TO 17
6 VS=0.
17 RT=RE*.1467/UINF
  FR=UINF**2/RT/G
  NR=PP*10**(-4)/RT

```

```

VS=VS/UINF
ZI=ZIO
WRITE(6,2)ZI,PP,HE,UINF,STK,FR,RT
DO 38 I1=1,IWP
I1=1
IF(I1,EN,2) I1=-1
FYW=I1
WRITE(6,34) I1
K=0
IF(I1,EW,1,AND,I1,EW,1) RO=RI
IF(I1,EW,1,AND,I1,NF,1) RO=YUP
IF(I1,EW,2,AND,I1,EW,1) RO=YUP-1.5
IF(I1,EW,2,AND,I1,NE,1) RO=YLO
RCA=0.
RES=0.
FII=0.
DO 20 I=1,LIM
IC=0
KODE=0
J=0
IHAL=0
IDIV=0
DT=DT3
DT=DT2
DT=DT1
IF(STK.LT.,.05) DT=DT3
IF(K.EQ.2) FII=1.
IF(K.EQ.1) FII=-1.
IF(K.EQ.4) FII=ABS(FII)/2.
IF(K.EQ.3) FII=-ABS(FII)/2.
RO=RO+DR*FII*FIW
IF(NDIM.NE.2,AND,RO.LT.0.) STOP
RO=RO
T=0.
ICAT=0
ZI=ZIO
ZII=ZI*SIN(ALPHA)-RO*COS(ALPHA)
R0=ZI*COS(ALPHA)+RO*SIN(ALPHA)
ZI=ZII
CALL OUTP(ZI,RO,KODE)
IC=1
CALL INTERP(RO,ZI,UX,UY,DUX,DUY)
VZ=UX
VR=UY
14 CALL FCT(RO,ZI,DVZ,DVR,UX,UY,VZ,VR,DUX,DUY)
DUX=DUX
DUY=DUY
DVZ=DVZ
DVR=DVR
IF(IDIV,EW,1)DT=DT1
IF(IDIV,EW,2)DT=DT3
IF(IDIV,EW,3)DT=DT4
IF(STK.LT.,.50,AND,ZI.GE.,ZCU) DT=DT4
0 M=1
C PREDICT NEW POSITION
9 IF(STK.LT.,.1) GO TO 42
V7P=VZ+DVZ*DT
VRP=VR+DVR*DT
GO TO 43
42 V7P=UX/(1.+STK*DUX)

```

```

VRP=UY/(1.+STK*DUY)
43 ZP=ZI+VZP*DT
RP=RO+VRP*DT
RAT=RP/RO
IF(ICAT.EQ.1) GO TO 10
IF(RAT.GT.CAT)DT=DT/2.
IF(DT.LE.1E-3) ICAT=1
IF(RAT.GT.CAT)GO TO 9
C CORRECT THE PREDICTED POSITION
10 CALL FCI(RP,ZP,CVZ,CVR,UXC,UYC,VZP,VRP,CUX,CUY)
VZL=VZ+(DVZ+CVZ)/2.*DT
VR=VR+(DVR+CVR)/2.*DT
IF(STK.LT..1)VZC=UX/2./((1.+STK*DUX)+UXC/2./((1.+STK*CUX)
IF(STK.LT..1)VRC=UY/2./((1.+STK*DUY)+UYC/2./((1.+STK*CUY)
ZC=ZI+VZC*DT
RC=RO+VRC*DT
C ITERATE FOR CONVERGENCE
IF(M.EQ.1) GO TO 11
IF(ABS(ZC1-ZC).LE.EPPS.AND.ABS(RC1-RC).LE.EPPS)GO TO 12
11 M=M+1
IF(M.GT.LIMIT) IDIV=IDIV+1
IF(IHAL.NE.0.AND.M.LE.LIMIT) GO TO 7
IF(IDIV.GT.3) GO TO 13
IF(M.GT.LIMIT) GO TO 14
7 ZP=ZC
RP=RC
VZP=VZC
VRP=VRC
RC1=RC
ZC1=ZC
GO TO 10
13 DT=DT/2.
IHAL=IHAL+1
IF(IHAL.GE.5)WRITE(6,5)ZI,RO,ZC,ZP,RP,RC,CVZ,CVR
IF(IHAL.GE.5)STOP
DVZ=DVZO
DVR=DVRO
DUX=DUXO
DUY=DUYO
GO TO 8
12 KODE=0
T=T+DT
CALL OUTP(ZC,RC,KODE)
IF(KODE.EQ.1) WRITE(6,15)
15 FORMAT(/5X,'CAPTURED')
IF(KODE.NE.1) GO TO 21
KCASE=0
IF(K.EQ.0) K=2
IF(K.EQ.1.OR.K.EQ.3) K=4
GO TO 23
21 CONTINUE
ZI=ZC
RO=RC
VZ=VZC
VR=VRC
IF(NDIM.NE.2.AND.RO.LT.0.) STOP
IHAL=0
IF(ALPHA.EQ.0.AND.RO.GE.1.) GO TO 41
IF(ZI.LT.ZMAX) GO TO 14
41 WRITE(6,27) T,ZI,RC

```

```

WRITE(6,18)
18 FORMAT(/5X,'ESCAPED')
27 FORMAT(1H,3(F15.6,10X))
   IF(K.EQ.0) K=1
   IF(K.EQ.2.OR.K.EQ.4) K=3
   RES=R00
23 RQ=R00
   IF(ABS(RCA-RES).LT.EPP) GO TO 25
20 CONTINUE
25 IF(IIW.EQ.1) YUP=RCA/2.+RES/2.
   IF(IIW.EQ.2) YLO=RCA/2.+RES/2.
   WRITE(6,40) CAT,ICAT
40 FORMAT(/,1H,10X,'MAX. POSITION RATIO=',F15.6,/,10X,
1'VALUE OF ICAT IS',I4,/)
38 CONTINUE
   EFF=((YUP-YLO)/FWP)**2/U
   IF(NDIM.NE.1.AND.IDIM.EQ.0) EFF=((YUP-YLO)/FWP)/U
   EFF=EFF+VS*COS(ALPHA)/U
   WRITE(6,26) U,EFF,STK,YUP,YLO
26 FORMAT(/5X,'VAL. RATIO=',F10.6,/5X,'CONC. RATIO=',F10.6,
1/5X,'STOKES NUMBER=',F10.6,/5X,'CRITICAL GRD.',F10.6,5X,F10.6)
   PF(II)=PF(II)/EFF
24 CONTINUE
   CALL BIAS(IST,ST,P,IA,FF,ICA,UNF,RE)
   STOP
   END
#FOR,I FCT
SUBROUTINE FCT(R0,Z0,DVZ,DVR,UX,UY,VX,VY,DUX,DUY)
COMMON/AAA/STK,FR
COMMON/BAT/NDIM,ISINK,F,ALPHA,U,IDIM
COMMON/SAR/IS,IE,OP,OC,IW,PL,ESP,ITS
FTW=I*W
CALL INTERP(R0,Z0,UX,UY,DUX,DUY)
IF(STK.LT..1) GO TO 2
DVZ=(UX-VX)/STK
DVR=(UY-VY)/STK
IF(IS.EQ.0) GO TO 1
DVZ=DVZ+COS(ALPHA)/FR*FTW
DVR=DVR-SIN(ALPHA)/FR*FTW
1 IF(IE.EQ.0) GO TO 2
FUN=SQRT((R0-1.)**2+70**2)
S=(R0-1.)/FUN
C=Z0/FUN
FUN=SQRT((R0-1.)**2+(PL-Z0)**2)
SS=(R0-1.)/FUN
CC=(PL-Z0)/FUN
FX=ESP/(R0-1.)*(S-SS)
FY=ESP/(R0-1.)*(CC-C)
DVZ=DVZ+FX
DVR=DVR+FY
2 RETURN
END
#FOR,I INTERP
SUBROUTINE INTERP(R0,Z0,UX,UY,DUX,DUY)
COMMON/AAA/R(61),Z(101)
COMMON/BAT/NDIM,ISINK,F,ALPHA,U,IDIM
COMMON/ABB/UZ(101,61),UR(101,61)
COMMON/ABC/IM,JM,JGR,JGRO,IBW,IHW0
IF(NDIM.EQ.2) CALL SINVEL(R0,Z0,UX,UY,DUX,DUY)
IF(NDIM.EQ.2) RETURN

```

```

DO1 I=1,IM
IF(ZO.GE.Z(I) .AND.ZO.LT.Z(I+1))GO TO 2
1 CONTINUE
2 IF(I.EQ.IM) I=I-1
DO 3 J=1,JM
IF(RO.GE.R(J) .AND.RO.LT.R(J+1))GO TO 4
3 CONTINUE
4 CONTINUE
UXL=(UZ(I+1,J)-UZ(I,J))/(Z(I+1)-Z(I))*(ZO-Z(I))
UYL=(UR(I+1,J)-UR(I,J))/(Z(I+1)-Z(I))*(ZO-Z(I))
UXU=(UZ(I+1,J+1)-UZ(I,J+1))/(Z(I+1)-Z(I))*(ZO-Z(I))
UYU=(UR(I+1,J+1)-UR(I,J+1))/(Z(I+1)-Z(I))*(ZO-Z(I))
UYL=UYL+UR(I,J)
UXU=UXU+UZ(I,J+1)
UYU=UYL+UR(I,J+1)
UXL=UXL+UZ(I,J)
UX=(UXU-UXL)/(R(J+1)-R(J))*(RO-R(J))
UY=(UYU-UYL)/(R(J+1)-R(J))*(RO-R(J))
DUY=(UYU-UYL)/(R(J+1)-R(J))
DUX=UZ(I+1,J)-UZ(I,J)+(UZ(I+1,J+1)-UZ(I,J+1)+UZ(I,J+1)+UZ(I,J))
1*(RO-R(J))/(R(J+1)-R(J))
DUX=DUX/(Z(I+1)-Z(I))
UX=UX+UXL
UY=UY+UYL
RETURN
END

```

*FOR,I SINVEL

```

SUBROUTINE SINVEL(RO,ZO,UX,UY,DUX,DUY)
COMMON/HAT/NDIM,ISINK,F,ALPHA,U,IDIM
COMMON/SAR/IS,IE,OP,OC,IW,PL,ESP,ITS
COMMON/ACH/T,IC,INT,ILP,ZLIP
FUN(X,Y)=SQRT(X**2+Y**2)
THIL(X,Y)=(X**2-Y**2)/(X**2+Y**2)
ARA(X,Y,Z)=ALOG((X**2+Y**2)/(Z**2+Y**2))
ACH(X,Y)=1./(X**2+Y**2)
RFAL M
C=COS(ALPHA)
S=SIN(ALPHA)
M=(U-S)/4./F
IF(ISINK.EQ.1) M=(S-U)/2./F**2
PJ=3.141596
THETA=PI-2.*ATAN(ZLIP)
M=M*PI/THETA
X=RO+F
Y=-ZO
XF=X-F
XFF=XF-F
IF(IDIM.EQ.0) GO TO 1
IF(ISINK.FQ.0) GO TO 13
IF(ABS(Y).LE..01) GO TO 10
A=FUN(X,Y)
B=FUN(XF,Y)
D=FUN(XFF,Y)
M=B+XF
E=XFF+D
G=X+A
UII3=-X/2./A+XF/B-XFF/2./D+ALOG(H/G)+ALOG(F/E)+
1Y**2/2.*(2./H/B-1./G/A-1./E/D)
UIR=X**2/2./Y/A-XF**2/Y/B+XFF**2/2./Y/D-Y/2.*(2./B-1./A-1./D)
UIR=UIR+A/2./Y-B/Y+D/2./Y

```

```

DIY=2./H-1./A-1./D
LUX=-X**2/A+2.*XF**2/H-XFF**2/D
DUX=DUX*M/Y**2
LIY=DIY*M
LIZ=UIZ*M
LUK=UUK*M
GO TO 11
10 IF(X.GE.0..AND.X.LE.(2.*F)) GO TO 12
UUR=0.
UIZ=M*ALOG(XF**2/X/XFF)
GO TO 11
12 UIZ=0.
LUK=0.
GO TO 11
13 A=FUN(X,Y)
M=FUN(XFF,Y)
IF(A.LE..01) A=.01
IF(M.LE..01) M=.01
UIZ=M*(1./A-1./H)
LUK=-M*(X/A/Y-(XF)/B/Y)
DIY=M*(-X/A**3+XF/H**3)
DUX=-M*(-X/A**3-X/A/Y**2+XFF/H**3+XFF/B/Y**2)
GO TO 11
1 M=4.*(S-U)/2./F**2/PI
IF(ISINK.EU.0) M=(U-S)/PI/F
M=M*PI/THETA
IF(ISINK.FU.0) GO TO 2
A=THIL(X,Y)
B=THIL(XF,Y)
L=THIL(XFF,Y)
E=ARA(X,Y,XF)
G=ARA(XF,Y,XFF)
H=ACH(X,Y)
P=ACH(XF,Y)
Q=ACH(XFF,Y)
AA=ATAN(Y/X)
AR=ATAN(Y/XF)
AC=ATAN(Y/XFF)
UIZ=X/2.*A-Y*AA-XF*R+2.*Y*AR+XFF/2.*D-Y*AC+X/2.*E-XFF/2.*G+Y**2
1*X*(H-P)-Y**2*XFF*(P-Q)
LUK=Y/2.*A-X*AA-Y*H+2.*XF*AR+Y/2.*D-XFF*AC-Y/2.*E+Y/2.*G-Y*X*
1(X*H-XF*P)+Y*XFF*(XF*P-XFF*Q)
DIY=E/2.-G/2.
DUX=-E/2.+G/2.
IF(ABS(KU).LE.F) UIZ=0.
IF(ABS(RU).LE.F) UUK=-F**2/2./Y
UIZ=UIZ*M
LUK=LUK*M
DIY=DIY*M
DUX=DUX*M
GO TO 11
2 A=ARA(X,Y,XFF)
B=ATAN(Y/X)
D=ATAN(Y/XFF)
G=ACH(X,Y)
H=ACH(XF,Y)
LIZ=-M*A
LUK=M*(H-D)
DIY=-M*(X*G-XFF*M)
DUX=M*(X*G-XFF*M)

```

```

11 CONTINUE
    UX=UUR+S
    UY=UUZ+C
    RETURN
    END
#FOR,I BIAS
    SUBROUTINE BIAS(IST,ST,P,TA,PF,ICA,UINF,RE)
    DIMENSION ST(IST),P(IST),TA(IST),PF(IST)
    TPF=0.
    IF(ICA.EQ.1) GO TO 1
    DO 2 I=1,IST
    READ(5,3) P(I),TA(I),PF(I)
    ST(I)=UINF**2*TA(I)/RE/.1467
2 CONTINUE
    ST(1)=.008
    ST(2)=.040
    ST(3)=.105
    ST(4)=.404
    ST(5)=1.744
    ST(6)=5.224
3 FORMAT(3F15.8)
    ICA=1
    RETURN
1 DO 4 I=1,IST
    TPF=TPF+PF(I)
4 CONTINUE
    DO 5 I=1,IST
    PF(I)=PF(I)/TPF
5 CONTINUE
    WRITE(6,36)
36 FORMAT(1H,35X,'ACTUAL DISTRIBUTION',//,
15X,'RADIUS',11X,'FRACTION',/5X,'MICRON'/)
    DO 6 I=1,IST
    WRITE(6,3) P(I),PF(I)
6 CONTINUE
    RETURN
    END
#FOR,I OUTP
    SUBROUTINE OUTP(ZP,RP,KODE)
    COMMON/ABA/R(61),Z(101)
    COMMON/ABC/IM,JM,JGR,JGRO,IBW,IRWO
    COMMON/ACB/T,IC,K,ILP,ZLIP
    COMMON/BAT/NDIM,ISINK,F,ALPHA,U,IDIM
    IF(IC.EQ.0) WRITE(6,7) T,ZP,RP
    PP=ABS(RP)
    N=N+1
    IF(N.FG,K)WRITE(6,7) T,ZP,RP
    IF(N.EQ,K) N=0
7 FORMAT(1H,3(F15.6,10X))
    IF(NDIM.EQ.2) GO TO 8
    DO 1 I=1,IM
    IF(ZP.GE.Z(I).AND.ZP.LT.Z(I+1)) GO TO 2
1 CONTINUE
2 IF(I=ILP)3,4,4
8 IF(ZP=ZLIP)3,4,4
4 DO5 J=1,JM
    IF(PP.GE.R(J).AND.PP.LT.R(J+1)) GO TO 6
5 CONTINUE
6 IF(J.GE.JGR.AND.J.LE.JGRO)KODE=2
    IF(J.LT.JGR) KODE=1

```

```
IF (KODE.NE.0) WRITE(6,7)T,ZP,RP  
3 RETURN  
END
```

**

Appendix E. Computer Program System - User Manual

The computer program system consists of two separate programs. Program 'FLOWFI' solves for the flow field and program 'TRAJEC' computes the particle trajectories in the specified flow region. Since the model uses the stream function equation only when the sampling head faces the stream, program 'FLOWFI' has to be run only with this option. For angular orientations the flow field is approximated by a line sink/source in a uniform stream and the flow field is incorporated in the 'TRAJEC' program. User instructions for both programs follow.

The fluid flow model covers various inlet geometries:

- Parallel plate inlet facing the stream
- Circular tube inlet facing the stream
- Slit inlet with arbitrary orientation to the stream

The user can choose any of the above options with proper value of an integer parameter 'NDIM'.

- NDIM = 0 Parallel plate inlet
- NDIM = 1 Circular tube
- NDIM = 2 Arbitrary orientation - slit

For options 0 or 1, it is necessary to obtain the flow field data from program 'FLOWFI' to do the trajectory calculations. However, for option 2 the flow field is incorporated in the program 'TRAJEC' and the use of 'FLOWFI' is not required. Various inlet geometries and physical conditions are simulated by proper selection of parameters U, W, ANG, NDIM, ZLIP, ALPHA. Figure 37 shows the physical meaning of these parameters.

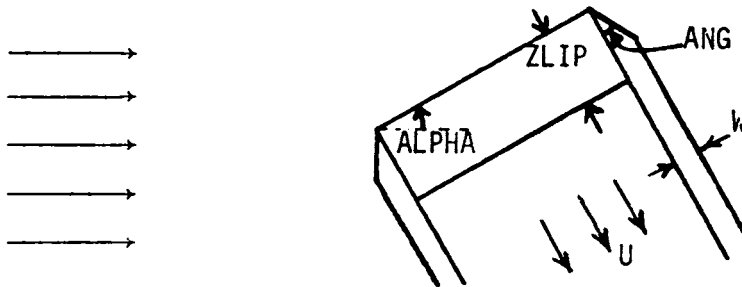


Figure 37. Parameter description for inlet geometry and orientation.

The 'FLOWFI' program input data and their description follows. The recommended values for some non-physical variables are also given.

'FLOWFI' DATA INPUT

CARD 1: NDIM,IPUNCH FORMAT()

NDIM.....FLOW FIELD OPTION PARAMETER
=0 TWO DIMENSIONAL CASE
=1 AXISYMMETRIC CASE
=2 LINE SINK

IPUNCH.....CONTROL PARAMETER FOR GETTING PUNCHED OUTPUT OF
PSI,UZ,UR,Z,R,ERC
=0 NO PUNCHED OUTPUT DESIRED.
=1 PUNCHED OUTPUT DESIRED.

CARD 2: ISINK,ALPHA,F FORMAT(I5,2F10.4) OMIT IF NDIM.NE.2

ISINK.....SINK DISTRIBUTION PARAMETER
=0 LINE SINK OF UNIFORM STRENGTH.
=1 LINE SINK OF TRIANGULAR STRENGTH DISTRIBUTION.

ALPHA.....ANGULAR ORIENTATION OF THE FACE PLANE OF SAMPLER HEAD.
=90 DEGREES WHEN SAMPLER FACES THE STREAM
=0 DEGREES WHEN STREAM IS TANGENTIAL TO THE HEAD.

F.....FRACTION OF THE PROBE DIAMETER OVER WHICH
THE SINK IS ASSUMED TO BE DISTRIBUTED.
RECOMMENDED VALUE IS 0.01.

CARD 3: ITERMA,RELAX FORMAT(I5,F10.4)

ITERMA.....MAXIMUM ALLOWABLE ITERATIONS FOR FLOW FIELD
TO CONVERGE

RELAX.....RELAXATION PARAMETER USED IN THE PROCEDURE OF
SUCCESSIVE OVER RELAXATION(SOR)
VALUES BETWEEN 1.0 AND 2.0.

CARD 4: ZM,ZMA,RO,U,W,ANG FORMAT(6F10.4)

ZM.....UPSTREAM FLOW FIELD BOUNDARY.LE.=5.

ZMA.....DOWNSTREAM FLOW FIELD BOUNDARY

RO.....FLOW FIELD BOUNDARY IN THE RADIAL OR TRANSVERSE
DIRECTION. RO.GE.5.

U.....ANISOKINETIC VELOCITY RATIO.

W.....SAMPLER WALL THICKNESS
WHEN NDIM.EQ.2 W=0.

ANG.....TAPERING ANGLE OF SAMPLER WALL
=0 IF W=0, OR NDIM.EQ.2

CARD 5: IGZ,JGR FORMAT(2I5)

IGZ.....GRID POINTS PER UNIT LENGTH IN AXIAL DIRECTION
= 1./GRID SIZE +1 Recommended value 6 or greater

JGR.....GRID POINTS PER UNIT LENGTH IN RADIAL DIRECTION
=1./RADIAL GRID SIZE +1 Recommended value 6 or greater

Program 'TRAJEC' solves for the limiting particle trajectory and calculates the true distribution of particle size from the measured distribution.

Program 'TRAJEC' starts the trajectory calculation at position ZI,RI input by the user. ZI is the upstream distance at which the particle is moving with the stream and is usually at least 5 radii from the sampling head. RI is the radial position to start the process to find RC, the radial position of limiting trajectory at ZI. If the trajectory of the particle starting at position RI enters the probe, then the next trajectory is started from a position $RI = RI + DR$, where DR is a preselected radial increment. If the trajectory from RI escapes the sampler, then the new RI is given by $RI - DR$. This process continues until the trajectories from successive radial positions alternate (i.e., one gets captured and another escapes). This process is repeated with successive halving of DR until the radial positions RES (at which the particle escapes) and RCA (at which the particle gets captured) are within a preselected tolerance EPP.

To calculate the trajectory accurately, it is necessary that the time or space step is not very large. This is accomplished by taking the ratio RAT of predicted radial position RP to initial radial position RD. If the ratio RAT is greater than a prespecified value CAT then the time/space step is halved and recalculation starts. The value of CAT used in the program is 1.05. Even with a step size that satisfies the ratio test, if the iterative convergence fails within LIMIT iteration than the step size is halved and the calculation procedure is restarted. The origin of the coordinate system lies at the center of the sampling head. The Z axis is along the centerline and R axis along the face plane. The efficiency calculation is performed for IST number of particles.

Subroutine BIAS calculates the actual size distribution from the measured size distribution. It uses the efficiency calculated by the subroutine INER. The Stokes number of a given particle K is also calculated by BIAS. The measured fraction PF, particle size P, relaxation time TAU are input to the subroutine BIAS. The maximum number of particle intervals that can be used is 10.

The input data and their description follows. The recommended values for non-physical variables are also given.

TRAJEC DATA INPUT

))
))

CARD 1: INT FORMAT(I4)
 PRINTING INTERVAL

CARD 2: IE, IW, IS FORMAT(3I4)
 IE=0/1 ELECTROSTATIC EFFECT NOT INCLUDED/INCLUDED
 IW=1/-1 UPPER/LOWER WALL
 IS=0/1 SEDIMENTATION EFFECT NOT INCLUDED/INCLUDED

CARD 3: U, W, ANG FORMAT(3F10,4)
 U--VELOCITY RATIO, SAMPLING VEL/FREE STREAM VEL
 W--WALL THICKNESS OF THE SAMPLER
 ANG--TAPERING ANGLE IN DEGREES OF SAMPLER WALL

CARD 4: NDIM FORMAT(I4)
 FLOW FIELD OPTION
 =0 TWO DIMENSIONAL FLOW BETWEEN PARALLEL PLATES
 =1 AXISYMMETRICAL FLOW FOR CIRCULAR TUBE
 =2 FLOW FIELD WITH LINE SINK
 OPTIONS 0&1 REQUIRE THE FLOW FIELD TO BE DETERMINED BY THE PROGRAM
 'FLOWFI'

CARD 5: IDIM FORMAT(I4) OMIT IF NDIM=0 OR 1
 =0 TWO DIMENSIONAL LINE SINK
 AXISYMMETRICAL LINE SINK

CARD 6: JGR, JGR0 FORMAT(2I4)
 JGR--NUMBER OF GRID POINTS PER UNIT
 RADIAL DISTANCE, =1./GRID SPACING IN RAD. DIR+1
 JGR0--RADIAL GRID POINT AT WHICH OUTER EDGE OF THE WALL IS LOCATED
 JGR0=JGR IF NDIM=2 OR W=0. FOR NDIM=0,1 JGR&JGR0 ARE CALCULATED
 BY THE PROGRAM FLOWFI

CARD 7: IHW, IHW0 FORMAT(2I4)
 IHW--AXIAL GRID POINT AT WHICH INNER EDGE OF SAMPLER WALL IS LOCATED
 IHW0--AXIAL GRID POINT AT WHICH OUTER EDGE OF SAMPLER WALL IS
 LOCATED. IHW0=IHW IF NDIM=2 OR W=0 OR ANG=90. FOR NDIM=0 OR 1,
 IHW AND IHW0 ARE CALCULATED BY 'FLOWFI'

CARD 8: IM, JM FORMAT(2I4)
 IM--MAXIMUM NUMBER OF POINTS IN AXIAL DIRECTION <101
 JM--MAXIMUM NUMBER OF POINTS IN RADIAL DIRECTION.<61
 FOR NDIM=2 IM, JM ARE INPUT BY THE USER.
 FOR NDIM=0,1 IM, JM ARE OUTPUT BY FLOWFI.

CARD 9: ISINK FORMAT(I4) OMIT IF NDIM.NE.2
 =0 UNIFORM SINK STRENGTH DISTRIBUTION.
 =1 TRIANGULAR SINK STRENGTH DISTRIBUTION.

CARD 10: F, ALPHA FORMAT(2F10,4) OMIT IF NDIM.NE.2
 F--FRACTION OF DIAMETER OVER WHICH THE LINE SINK IS DISTRIBUTED
 USUALLY F=0.01
 ALPHA--ORIENTATION ANGLE OF SAMPLER

CARD 11:---11+IM/H Z(I) FORMAT(8F10.4)
AXIAL COORDINATES OF GRID POINTS. FOR NDIM=0,1 Z(I) IS CALCULATED
BY 'FLOWFI'. FOR NDIM=2 INPUT BY USER. THERE WILL BE
IM/H DATA CARDS.

CARDS 11+IM/H--11+IM/H+JM/H=N(SAY) R(I) FORMAT(8F10.4)
RADIAL COORDINATES OF GRID POINTS. FOR NDIM=0,1 R(I) IS CALCULATED
BY 'FLOWFI'. FOR NDIM=2 INPUT BY USER. THERE WILL BE
JM/H DATA CARDS.

CARD N--N+IM+JM/H =M(SAY) UZ(I,J) FORMAT(8F10.4) OMIT IF NDIM=2
UZ--AXIAL COMPONENT OF VELOCITY. FOR NDIM=0 OR 1 CALCULATED BY
'FLOWFI'

CARDSM--M+IM+JM/H=MP(SAY) UR(I,J) FORMAT(8F10.4) OMIT IF NDIM=2
UR--RADIAL COMPONENT OF VELOCITY. FOR NDIM=0,1 CALCULATED BY FLOWFI

CARD (MM+1) LIM,DTI,ZI,RI,DR FORMAT(I5.4F15.6)
LIM--# OF TIMES TRAJECTORY CALCULATION HAS TO BE DONE
DTI--TIME INCREMENT FOR EACH STEP (0.1)
ZI--INITIAL AXIAL POSITION OF THE PARTICLE.
RI--INITIAL RADIAL POSITION OF PARTICLE=SQRT(U)
DR--RADIAL INCREMENT (0.2)

CARD(MM+2) UINF,RE FORMAT(2F15.6)
UINF--FREE STREAM VELOCITY USER INPUT
RE--REYNOLD'S NUMBER BASED ON TUBE WIDTH

CARD(MM+3): ZLIP FORMAT(F15.6)
ZLIP--LIP DEPTH OF SAMPLER.

CARD(MM+4): QP,QC,PL FORMAT(3F10.4) OMIT IF IE=0
QP--ELECTROSTATIC CHARGE ON THE PARTICLE
QC--ELECTROSTATIC CHARGE ON THE SAMPLER.
PL--LINEAR DIMENSION OF THE SAMPLER.

CARD(MM+5): IST FORMAT(I4)
OF SIZE INTERVALS IN THE SIZE DISTRIBUTION <10

CARDS(MM+6)--(MM+6+IST) P,TA,PF FORMAT(3F15.8)

P--PARTICLE RADIUS IN MICRONS
TA--RELAXATION TIME OF THE PARTICLE IN SEC
PF--MEASURED FRACTION OF PARTICLES
THERE WILL BE 'IST' DATA CARDS.

))
))

For NDIM options of 0 or 1, the data cards 3 through 'MM' are punched out in the same order by program 'FLOWFI'. However, for NDIM=2, the user has to calculate the axial and radial coordinates as shown below.

The flow region of interest is given by upstream boundary (ZM), downstream boundary (ZMA) and radial boundary (RO). Assuming the face of the sampler is located at the origin, then

$$IM = \frac{-ZM + ZMA}{\Delta Z} + 1$$

$$IBW = \frac{-ZM}{\Delta Z} + 1$$

$$JM = \frac{RO}{\Delta R} + 1$$

$$JGR = \frac{1}{\Delta R} + 1$$

where ΔZ , ΔR are the grid sizes in axial and radial direction. Coordinates of the grid points are

$$Z(I) = ZM + \Delta Z * (J-1) \quad \text{for } I = 1, IM$$

$$R(J) = \Delta R * (J-1) \quad \text{for } J = 1, JM$$

For typical values of $ZM=-5$, $ZMA=5$, $RO=5$ and $\Delta Z=\Delta R=0.2$, $IM=51$, $IBW=26$, $JM=26$ and $JGR=6$.

The axial and radial velocity data cards are omitted for option NDIM=2.

EXAMPLE PROBLEM

LET US ASSUME A CIRCULAR TUBE OF 0.93 CM RADIUS AND A WALL THICKNESS OF 0.09 CM IS SAMPLING FROM A STREAM AT A VELOCITY OF 300CM/SEC. THE WIND SPEED IS 200CM/SEC. THE SAMPLER FACES THE STREAM. THE MEASURED PARTICLE SIZE DISTRIBUTION IS GIVEN BELOW.

RADIUS(MICRONS)	FRACTION
3.5	0.1
7.5	0.24
12.5	0.23
20.5	0.32
51.0	0.06

CALCULATE THE TRUE PARTICLE SIZE DISTRIBUTION.

FOR THE ABOVE PROBLEM THE INDIM! OPTION OF 1 HAS TO BE USED.

THE VELOCITY RATIO $U=300/200=1.5$

THE WALL THICKNESS $w=0.09/0.92=0.1$

SINCE NO CHAMFER ANGLE IS GIVEN THE TAPERING ANGLE $\angle ANG1=90$.

FOR THE INDIM! OPTION OF 1 THE RESULTS FROM PROGRAM 'FLOWFI' ARE REFERRED TO FOR PROGRAM 'TRAJECT'. THE INPUT DATA FOR PROGRAM 'FLOWFI' IS AS FOLLOWS (REFER TO DATA INPUT DESCRIPTION FOR EXPLANATION AND FORMAT)

CARD 1	1	1					
CARD 2	40	1.5					
CARD 3	-5.	5.	5.	1.5	0.1	90.	
CARD 4	6	6					
CARD 5	1						
CARD 6	2						(STREAM FUNCTION VALUE FOR LOCUS)

THE OUTPUT FROM PROGRAM 'FLOWFI' FOLLOWS.

THE PUNCHED OUTPUT RESULTING FROM THE PROGRAM 'FLOWFI' IS A PART OF THE INPUT DATA TO THE PROGRAM 'TRAJECT'. THE INPUT DATA IS AS FOLLOWS. (REFER TO DATA INPUT DESCRIPTION FOR EXPLANATION AND FORMAT)

```

CARD 1      50
CARD 2      0  1  0
CARD 3      PUNCHED OUTPUT FROM FLOWFI
  \
  \
  \
  \
  \
CARD N      LAST CARD OF THE PUNCHED OUTPUT.
CARD N+1    20  0.1  -5.  1.224  0.2
CARD N+2    200.  1200.
CARD N+3    0.
CARD N+4    5
CARD N+5    3.5  3.7 E-05  0.1
CARD N+6    7.6  1.85E-04  0.28
CARD N+7    12.5  4.86 E-04  0.23
CARD N+8    26.5  2.147 E-03  0.32
CARD N+9    51.0  8.07 E-03  0.06

```

DUE TO THE LENGTH OF THE COMPLETE OUTPUT LISTING, THE TRAJECTORIES FOR ONE PARTICLE AND THE CORRECTED DISTRIBUTION ARE PROVIDED.

SAMPLING BIAS DETERMINATION

TRAJECTORY CALCULATION

VEL.RATIO= 1.500000
 WALL THICKNESS= .100000
 TAPERING ANG= 90.000000DEG

FLOW FIELD BOUNDARY

FLOW FIELD FOR CIRCULAR TUBE
 AXIALLY SYMMETRIC CASE

ZLIP= .000000

SEDIMENTATION PARAMETER= 0

ELECTROSTATIC FIELD PARAMETER= 0

SEDIMENTATION TRAJECTORY PARAMETER= 0

RADIUS(MICRONS)	FRACTION
5.5	0.1
7.5	0.28
12.5	0.23
20.5	0.32
51.0	0.06

WALL PARAMETER IN= 1

T	Z	R
.000000	-4.999998	1.224754
.980000	-4.019999	1.224754
1.980000	-3.019830	1.224403
2.979999	-2.017794	1.220267
3.979998	-1.008228	1.198568
4.489997	-.489925	1.163534
4.989997	-.016487	1.103450
5.009997	.001048	1.101434
5.009997	.001048	1.101434

ESCAPED

.000000	-4.999998	1.024754
.940000	-4.059999	1.024754
1.940000	-3.059878	1.024508
2.939999	-2.057465	1.020901
3.939998	-1.043345	.999490
4.469997	-.491433	.956265
4.889997	.000842	.844296

CAPTURED

.000000	-4.999998	1.124754
.140000	-4.859998	1.124754
1.140000	-3.859999	1.124753
2.140000	-2.859684	1.124218
3.139999	-1.856431	1.118748
4.069998	-.913105	1.093251
4.569997	-.398799	1.045445
4.929997	.013838	.909776

CAPTURED

.000000	-4.999998	1.174754
.260000	-4.739998	1.174754
1.260000	-3.739999	1.174747
2.259999	-2.739573	1.173951
3.259998	-1.735871	1.167162
4.129998	-.853696	1.140491
4.629997	-.344664	1.092050
4.949997	.001965	.991580

CAPTURED

.000000	-4.999998	1.199754
.340000	-4.659998	1.199754
1.340000	-3.659995	1.199737
2.339999	-2.659484	1.198730
3.339998	-1.655435	1.190942
4.169998	-.813938	1.163512
4.669997	-.307929	1.114391
4.989997	.007781	1.052651
4.989997	.007781	1.052651

ESCAPED

.000000	-4.999998	1.187254
.340000	-4.659998	1.187254
1.340000	-3.659995	1.187238
2.339999	-2.659475	1.186239
3.339998	-1.655329	1.178451
4.169998	-.813385	1.150797
4.669997	-.306744	1.100462
4.969997	.006864	1.021694
4.969997	.006864	1.021694

ESCAPED

.000000	-4.999998	1.181004
---------	-----------	----------

.380000
1.380000
2.379999
3.379998
4.189998
4.689997
4.959997
4.959997

-4.619998
-3.619992
-2.619412
-1.614929
-.792677
-.286671
.005292
.005292

1.181004
1.180984
1.179879
1.171548
1.143184
1.090367
1.006424
1.006424

ESCAPED

MAX. POSITION RATIO= 1.500000
VALUE OF ICAT IS= 0

VAL. RATIO= 1.500000
CUNC. RATIO= .924918
STOKES NUMBER= .008000
CRITICAL ORD.= 1.177870 .000000

CORRECTED SIZE DISTRIBUTION

RADIUS(MICRONS)	FRACTION
3.5	0.093
7.5	0.261
12.5	0.223
26.5	0.340
51.0	0.070

GLOSSARY

A_i	Aspiration coefficient due to inertia
B	Non-dimensional function (Equation 8)
C	Measured concentration ($\#/cm^3$)
C_0	Actual concentration ($\#/cm^3$)
D	Length of line sink (cm)
d	Diameter of particle
E	Efficiency of capture
f	Fraction of diameter with line sink
F	Rate of suction of sample (cm^3/sec)
F_e	External force ($gm \cdot cm/sec^2$)
Fr	Froude number (V_{st}/L)
f_i	Fraction of i^{th} particle group
g	Acceleration due to gravity (cm/sec^2)
H	Half width of channel (cm)
I	Grid point along Z direction
J	Grid point along y or r direction
K	Stoke's number (U_{jt}/L)
L	Characteristic length (cm)
m	Sink/Source strength
n	Number of particle groups
Pe	Peclet number (U_{jL}/E)
Q_p	Electrostatic charge on particle (statcoulums)
Q_c	Electrostatic charge on collector (statcoulums)
R	Radius of the tube
R_0	Radial boundary of flow field
r	Cylindrical coordinate
Sc	Schmidt number
t	Time scale

u	Suction velocity of sample
U_I	Free stream velocity
\bar{U}	Flow velocity vector
U_x, U_y	Flow velocity along $x + y$ direction
U_γ, U_z	Flow velocity along $\gamma + z$ direction
\bar{v}	Particle velocity vector
V_s	Terminal settling velocity of particle
W	Width of sampler wall
x, y, z	Cartesian coordinates
$\Delta y, \Delta z, \Delta \gamma$	Grid size intervals in y, z, γ directions
ψ	Stream function
ψ_c	Stream function at center line
α	Orientation of sampler face plane to the direction of flow
τ	Relaxation time of particles
η	Efficiency of sampling

DEPARTMENT OF HEALTH AND HUMAN SERVICES
PUBLIC HEALTH SERVICE
CENTERS FOR DISEASE CONTROL
NATIONAL INSTITUTE FOR OCCUPATIONAL SAFETY AND HEALTH
ROBERT A. TAFT LABORATORIES
4676 COLUMBIA PARKWAY, CINCINNATI, OHIO 45226

OFFICIAL BUSINESS
PENALTY FOR PRIVATE USE, \$300

Third Class Mail



POSTAGE AND FEES PAID
U.S. DEPARTMENT OF HHS
HHS 396